UNIVERSITY OF CATANIA

ELECTRIC ELECTRONICS AND COMPUTER ENGINEERING DEPARTMENT

PhD COURSE: SYSTEMS, ENERGY, COMPUTER AND TELECOMUNICATIONS ENGINEERING – XXXII Cycle (2016-2019)

PhD THESIS

Modeling, Software Simulation and Preliminary Test of a Biomass Pyrolysis Pilot Plant

---

Candidate:
Antonio Agrifoglio

Supervisor:
Prof. Eng. Alberto Fichera

Co-Supervisor:
Prof. Eng. Antonio Gagliano

Academic Year 2018-2019

Index

Nomenclature

GHG	=	Green House Gasses
RES	=	Renewable Energy Source
HHV	=	High Heating Value
M	=	Moisture
VM	=	Volatile Matter
FC	=	Fixed Carbon
Cell	=	Cellulose
Hemicell or HC	=	Hemicellulose
Lig or L	=	Lignin
T_{max}	=	Maximum Temperature
HR	=	Heating Rate
Rt	=	Residence Time
Φ	=	Particle Size/Diameter
FBR	=	Fixed Bed Reactor
BFBR	=	Bubbling Fluidized Bed Reactor
CFBR	=	Circulating Fluidized Bed Reactor
RCR	=	Rotating Cone Reactor
TGA	=	Thermogravimetric Analysis
LVG	=	Levoglucosan
DTG	=	Derivative Thermogravimetric
Ea	=	Activation Energy
k_0	=	Pre-exponential Factor
T	=	Temperature
PM	=	Molecular Weight

P	=	Pressure
P	=	Density
C_p	=	Heat Capacity
LHV	=	Low Heating Value
H	=	Efficiency
h_v	=	Heat of Vaporization
CHP	=	Combined Heat and Power
P	=	Power
el (subscript)	=	Electric
th (subscript)	=	Thermal
m (subscript)	=	Mechanical
w (subscript)	=	Water
cw (subscript)	=	Cooling Water
syn (subscript)	=	Syngas or Pyrogas
ex (subscript)	=	Exhaust
g (subscript)	=	Gas
pg (subscript)	=	Produced Gas
PFR	=	Plug Flow Reactor
CSTR	=	Continuous Stirred Tank Reactor
%wt	=	Weight Percent
%mol	=	Mole Percent
Daf	=	Dry Ash Free
BIOM	=	Biomass
Λ	=	Excess Air Coefficient
A/F	=	Air/Fuel
LCOE	=	Levelized Cost of Electricity
O&M	=	Operation & Maintenance

Abstract

This study has the aim to develop a simulation model able to predict the production of a biomass pyrolysis plant, which allows to define right working parameters for optimizing the process. Moreover, an analysis regarding an energy recovery line has been performed to maximize the valorization of products and reduce the utilization of external energy sources.

Biomass is a general name that includes a great number of organic substances with very different composition as well as physical and chemical properties; for this reason, in the library of the simulation software there is not a standard material suitable for this kind of processes. Nevertheless, there is the possibility to create non-conventional components starting from known characteristics, so a solid "biomass" determined by values derived from previous experimentation and literature researches has been defined.

The scheme of thermo-chemical process used in this work is based on layout of a pyrolysis pilot plant located in Sicily, fed by 30 kg/h of olive pits and agricultural residues and worked between 600 °C and 800°C. In accordance to plant feedstock specification, fraction of C, O_2 and H used to model the biomass has been chosen crossing standard ligno-cellulosic composition and average values of ultimate analysis of these considered materials.

The decomposition of organic matter is idealized as a two-stage process: firstly, in the reactor, it is decomposed in a residual solid fraction (char) and a gaseous mixture. Then, this mixture is directed in the cooling section in which condensable part is divided from permanent gas generating the pyro-oil.

To reproduce the degradation of biomass and the resulting evolution of chemical species, a new mathematical model, based on operative temperature (considered in a range between 500°C and 900°C) and kinetic of reaction involved during the process, was developed. Kinetic parameters are obtained performing all the reactions of decomposition of cellulose, hemicellulose and lignin.

The conversion process is simulated by a R-yield reactor supported by a calculator block set with the proposed model calculated for each component involved in considered reactions.

Permanent gas fraction was firstly characterized and then used to feed a micro-CHP system in order to produce electrical power and a thermal power. This latter is recirculated toward the pyrolysis plant to support drying or conversion process.

Simulations were developed at 600°C and 800°C and thus the obtained results were compared to highlight:

- Yield of each compound and differences during each section of the process;
- Characteristics, composition and energetic content of pyro-gas;

- Efficiency of micro-CHP system in terms of both electric and thermal power and respectively possibility to support the main process.

1) Current and Future Energy Scenarios

Continuous and increasing issues related to utilization of fossil fuels led to an increasing interest and studies about alternative, renewable and cleaner energy source able to limit air pollution as well as climatic and environmental problems.

Moreover, source as oil, coal and natural gas are non-renewable resources that will run out in a relatively short period.

This scenario prompted Europe to realize energy and environmental strategies to improve the use of green energy source, limits GHG emissions and develop technology for CO_2 capture.

Use of alternative source is also necessary to face the increasing request of energy due to the current continuous industrialization and civilization. Due to the multiple patterns to convert the raw material in energy, biomass is one of the most interesting green-source among the ones currently investigated.

European commission has already planned different long-time strategy to gradually face this issue, in order to reduce the use of fossil fuel and the emission of pollutant in atmosphere and mitigate climatic changes during the years.

After the first period of Kyoto Protocol (2008-2012) and in accordance with guidelines of the second period of Kyoto Protocol (2013-2020), the three main time-steps programmed by EU States are:[1]

- 2020 Climate & Energy Package;
- 2030 Climate And Energy Policy Framework;
- 2050 Low-Carbon Economy & Energy Strategy[2].

Furthermore, in accordance with results stipulated the XXI Conference of Parties (COP21) in Paris the 12th of December 2015, UN States commit to reduce, as soon as possible, CO_2, holding average global warming below 2°C above pre-industrial levels[3]. For this reason, it was developed the "*Emission Treading System"* (*ETS*), based on a cap for some GHG that will be reduced year by year in order to decrease quantity of total emission[4].

1.1. 2020 Climate & Energy Package

The 20/20/20 project was set by the EU leaders in 2007 and enacted in 2009. Its main aims, which are also the headline targets of the Europe 2020 strategy for smart, sustainable and inclusive growth[5], are the following: [6]

- 20% cut in greenhouse gas emissions (from 1990 levels);
- 20% of EU energy from renewables;
- 20% improvement in energy efficiency;
- ETS fixed a reduction of emission of 23% (of 2005 levels);
- Transport sector of EU Country must reach a 10% from renewable source.

Moreover, EU states commited to support research in energy, environment, sustainable bioeconomy and many other sectors, allocating approximately 80 billion of founding with the program *Horizon 2020*, between 2014 and 2020[7].

These investments are necessary from the economical point of view, because, to reach the target, development in several technological fields are needed. In these context, a possible solution may be the increasing the use of nuclear energy, able to produce clean energy and to avoid an excessive rise of price related to CO_2 emission and production. However, European policies limited the use of nuclear energy and, in this scenario, a fundamental roles for energy and climate goals becomes an increasing use of renewables in the energetic framework and the developed and integration of CCS (Carbon Capture System) to support the fossil fuel[8].

1.2. 2030 Climate And Energy Policy Framework

In October 2014 the UE States decided the guidelines to follow after reaching the goals of 2020 plan[9]. Indeed, the targets of this program is a further improvement of the previous three points:

- 40% cut in greenhouse gas emissions (from 1990 levels);
- 27% of EU energy from renewables;
- 27% (or30%) improvement in energy efficiency;
- ETS fixed a reduction of emission of 45% (of 2005 levels) [10].

The last trend to 2030 shows an increase of price of fossil fuel, a reduction of CO_2 emission due to new technology for carbon absorption and an improvement in renewable source, especially for production of electricity coming from green source as renewables and biomass[11].

According to data detected in 2015, around the 40% of the emissions are related to building sector. More than 30% of energy was consumed for space heating reason and the ≈50% of buildings were equipped with old and inefficient fossil fuel-based boilers. Moreover, The most utilized source in this sectors are the natural gas (≈34%) and petroleum (≈15). Within 2030 it is expected that these old heating systems will be replaced by more efficient and low-emission systems, fed by renewable source as geothermal, solar thermal and biomasses.
In the industrial sector, ≈30% of emission are difficult to reduce because are associated to non-energy related reason, as chemical reaction. Instead, regarding the energy-related emission, the reduction in the last years of its environmental impact is strictly connected to an increasing in energy efficiency, to the utilization of biomass as main feedstock and to the reduction of CO_2 and GHG emission.
However, the conversion to renewable heating and cooling system and the utilization of green energy sources, is slower than the one in buildings sector and the fossil fuel utilization is expected to be phased out in the period between 2030 and 2050.[12]

1.3. 2050 Low-Carbon Economy & Energy Strategy

European main target for low carbon economy are:

- Reducing of 80-95% from 1990 levels the GHG emissions, setting as intermediate step a reduction of 60% levels within 2040;
- A radical improvement of transport sector, breaking its dependence from oil and cutting CO_2 emission of 60% from 1990 levels.

To obtain these results, long-term investment in R&D sector for construction of new power plant, use of RES, development of carbon captures systems and modernization of current buildings and structure are needed. However, the high risks due to the uncertain and slow development of new technologies and the unclear and not-well defined guidelines for the scenario after the 2020 discourage funding in this field[13].
In a 2016 report, European Commission starting to develop a solid program for 2050 based on the interconnection of 10 models (fig.1). Moreover these models combine technical, economical and engineering prevision, building a complete framework based on a heavy connection among different sectors[14].

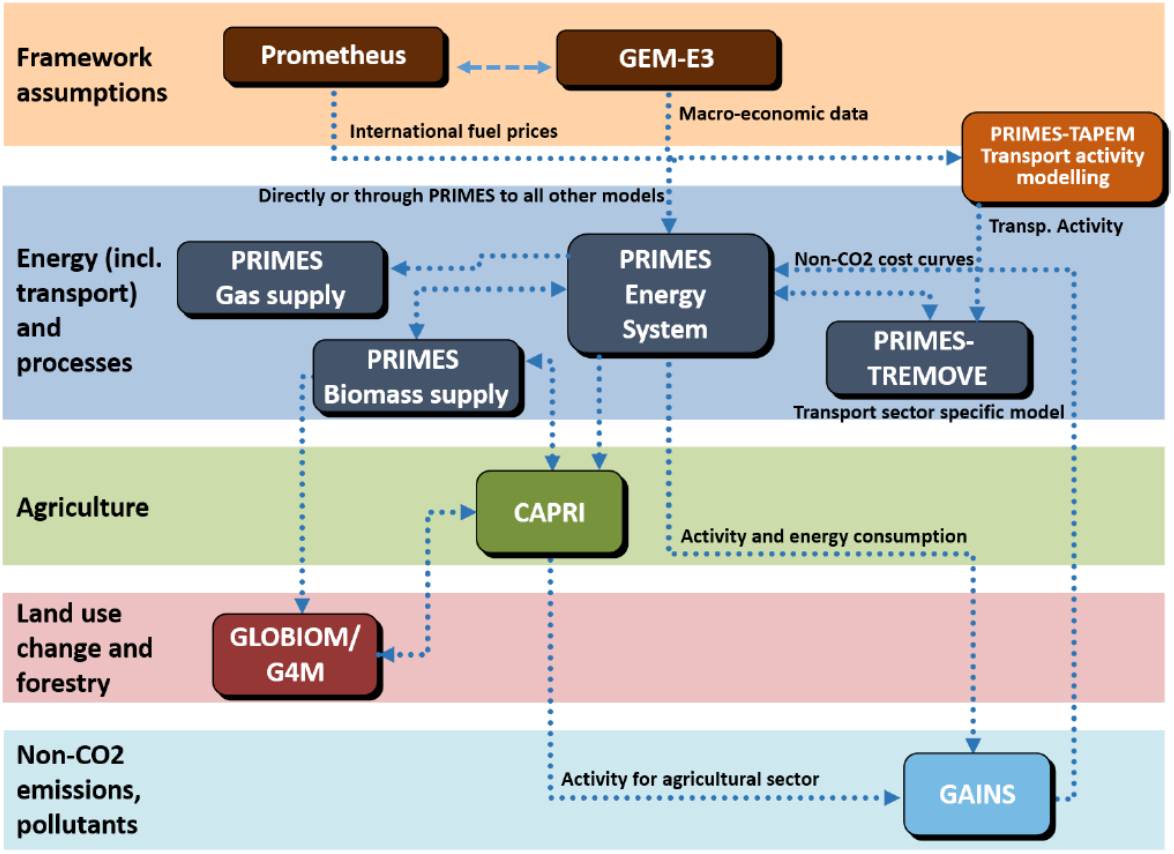

Fig. 1 – Modeling Suite for EU References Scenario 2016 [9]

Road to 2050 could have consequences regarding evolution of some jobs and employment rate. During those years, engineering and construction sector can benefit of large-scale investment necessary to enhance energy efficiency in structures and buildings. Development in carbon absorption technology and use of RES can advantage employment in technological, software and energy sectors, whereas increasing use of bio-fuel, biomaterial, biomass and other green source can advantage the agricultural sector.

Transport sector might radically change too. Restriction in carbon emission entail use of clean source as electricity, solar energy, biofuels, reducing demand in sector connected with use, extraction and manufacturing of fossil fuels[15].

2) Literature Investigation

2.1 Biomass

According to the European Energy and Environmental scenario mentioned in the previous chapter, nowadays biomass is considered one possible source able to limit fossil fuel and obtain clean green-energy from renewable. [16]

Van Krevelen diagram shows that these materials are mainly made up of C, H and O with a higher H/C and O/C ratio than solid fossil-fuel. These characteristics affect the HHV that is inversely proportional to the O/C ratio of a fuel. [17]

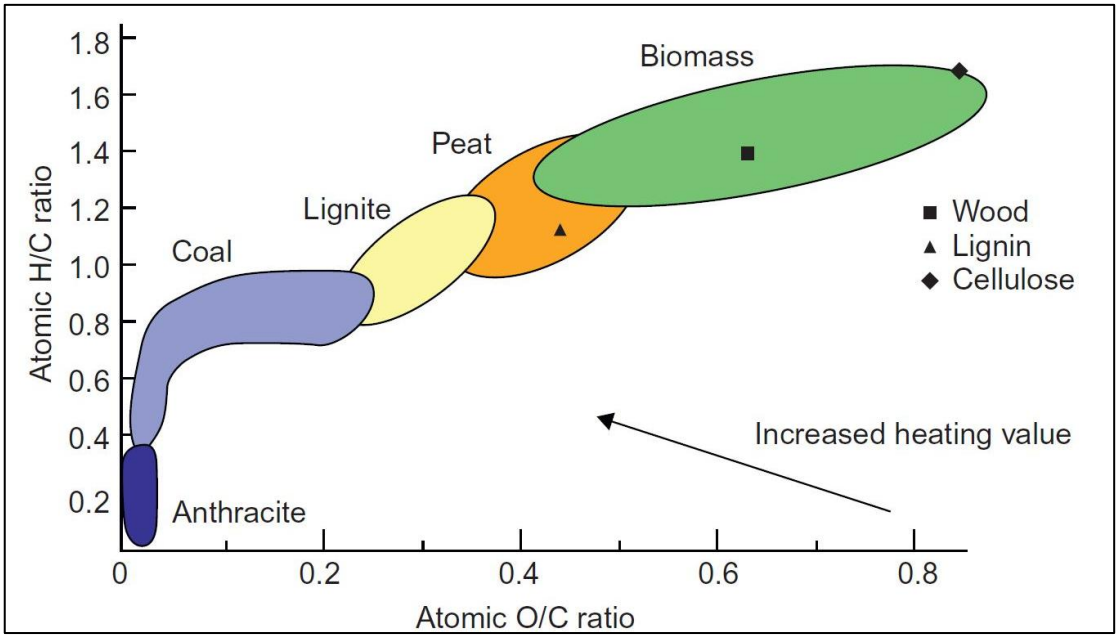

Fig.2 – Van Krevelen Diagram for many fuels

To classify these materials, the scheme proposed by Vassilev, in which biomass are divided in six groups based on their origin can be used [18]:

1. Woody: Coniferous, soft or hard form of wood species, bark, pellets, briquettes, sawdust, bark, chips, foliage and similar materials;
2. Herbaceous/agricultural: grasses, flower, straw, rice, oil, corn, residue of fruit, shell, grains, husk, pulps, cake, bagasse;
3. Aquatic: marine freshwater, algae, microalgae macroalgae, lake weed, water hyacinth;
4. Animal/human wastes: bone, meat, poultry litter, manures;

5. Contaminated/industrial wastes (semi-biomass): MSW, refuse-derived fuels, sewage sludge, hospital, tannery or paperboard wastes;
6. Biomass mixture: blends from above varieties;

First attempts of biomass exploitation to produce energy collided with problems related to competition between alimentary and energetic purpose for primary alimentary feedstock and the excessive stress of soil caused by its intensive use. For this reason, studies turned to utilization of inedible feedstock or organic waste derived from agricultural industries and processes. [19]

Agricultural biomass has not a fixed composition and depend on many variables such as environmental factors. Nevertheless, it is possible to find some prevalent characteristics in their composition: all of them are made up from cellulose, hemicelluloses and lignin and their elementary components are mainly carbon, hydrogen and oxygen.

However, to determine biomass structures is extremely important to maximize their exploitation. To properly defined a given feedstock, some preliminary analysis are necessary.

2.1.1 Ultimate Analysis

Ultimate Analyses is used to identify the elements that are present in the biomass, measured in wt%. Usually, Carbon, Hydrogen, Nitrogen and Sulfur are analyzed instead Oxygen is calculated as difference. Tab.1 shows the range of these species usually present in agricultural biomass composition.[20]

Element	**Symbol**	**Wt %**
Carbon	C	45÷50
Hydrogen	H	5.5÷7
Oxygen	O	40÷50
Nitrogen	N	<0.5
Sulfur	S	<0.2

Tab.1 – Typical Elementary composition of biomass

2.1.2 Proximate analysis

Proximate analyses of test allows to identify other type of property that can influence the biomass degradation process:[21]

Moisture (M): is one of the characteristics that mostly affect the pyrolysis process. It represents quantity of water, calculated as wt%, referred to db or daf material. Moisture removal preliminary treatment often can be really onerous from an energetic point of view.

Volatile Matter (VM): condensable and un-condensable vapor released during the heating up of feedstock. To determine it, feedstock will be heated in a controlled environment with standard temperature and heating rate.

Ash: Inert solid residue, resulting from the thermal decomposition. They are mainly composed from silicon, iron, aluminum and calcium but also little percentages of titanium, sodium and potassium can be found.

Fixed Carbon (FC): is the quantity of solid carbon present in the char after pyrolysis and de-volatilization processes. Usually it is calculated by difference according to the relation (1):

$$FC = 1 - M - VM - ASH \quad (1)$$

2.1.3 Biochemical composition

Biomass' structure is mainly composed by cellulose, hemicellulose and lignin. [22-23-24]

- **Cellulose (Cell)** $(C_6H_{10}O_5)_n$: polysaccharide in which long chain of D-glucose are connected each other by β-glicosidic bonds. The degree of polymerization, represented by the "*n*" in the formula, represent the number of glucose groups. Because of its crystalline structure, it has a great resistance to acid and alkalis. This component, during high temperature conversion, is the main responsible of volatile materials;
- **Hemi-cellulose (HC)** $(C_5H_8O_4)_n$: polysaccharide made up of chains that contain residues of D-xylose, D-mannose, D-glucose and D-galactose connected each others. It has an irregular, amorphous structure that results in a low mechanical resistance;
- **Lignin (Lig)**: Organic polymer made up by phenyl-propane units and its derivate randomly linked each other. It has a 3-Dimensional complex structure that conferring an high resistance to microorganism and a great mechanical strength and protection;
- **Starch** $(C_6H_{10}O_5)_n$: polysaccharide made up of D-glucose units connected by α-glicosidic bonds;
- **Proteins**: macromolecular compounds in which amino-acids have a high degree of polymerization.

2.1.4 Thermo-gravimetric Analysis

It can be used as alternative to ultimate and proximate analysis because less expensive. It is carried out monitoring continuously thermal history of considered material in controlled and inert atmosphere. The tests could be carried out in isothermal or in non-isothermal condition. This latter is the most common case and the heating rate can be programmmed from a fraction to hundreds °C/min, instead fournace can reach temperature up to 1000 or 1600°C.[25] Resulting curve can be showed in integral (TG) or differential (DTG) form and describes the mass loss occurred during the process. Furthermore, from these curves can e obtained some information about the composition of biomass in terms of cellulose, hemicellulose and lignin. [26]

For this reason, it is often used as preliminary investigation about the thermal degradation of materials.

2.2 Thermo-chemical conversion process

Conversion of biomass can be performed through physic-chemical, bio-chemical or thermo-chemical processes.[27]

In the last category, the most important conversion routs, showed in fig.3, are direct combustion, pyrolysis, gasification and direct liquefaction.[28]

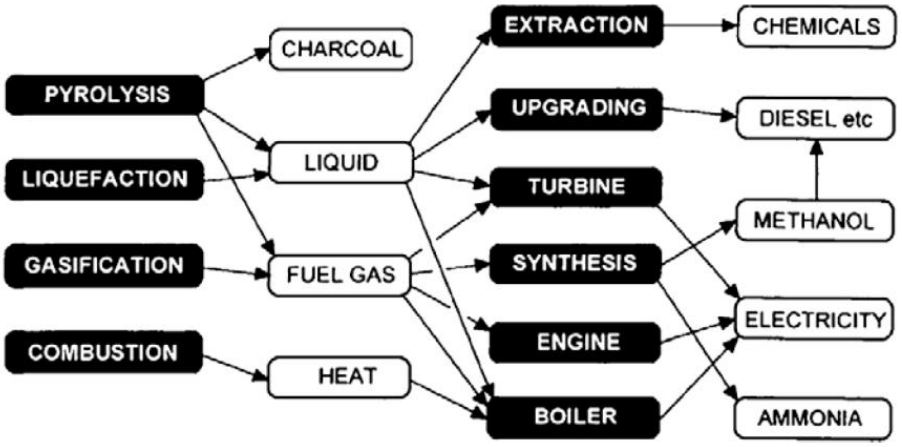

Fig.3 – Thermo-chemical conversion and corresponding products [28]

During these conversion processes, many chemical reactions occur to decompose the starting feedstock. Among these, pyrolysis will be the process examined in this thesis and will be discussed in details in the next paragraph.

2.3 Pyrolysis

Pyrolysis can be described as the breaking of chemical bonds using just the thermal energy; it causes the fracture of large particles into smaller ones.

The analytical pyrolysis observe and study the behavior of molecules during the degradation and/or the characteristics of the resulting smaller particles. To perform the analysis, some conditions are required:

- It is necessary to assemble a system able to heating small samples;
- the process and its conditions must be controlled and reproducible;
- the system must be interfaced to an instrument capable to analyze the products.

Moreover, some tools, as gas-chromatography (GC), a mass-spectometry (MS) or a Fourier-transform infrared (FT-IR), often support the process. [29]

This process takes place at high temperatures and in an inert or oxygen-deficient atmosphere. It can be also a preliminary stage of other thermo-chemical processes as combustion and gasification. Pyrolysis usually occurs in three stages depending on the reached temperature. During the first stage, or pre-pyrolysis, some chemical bound begins to break and there is an initial weight loss due to the release of small amount of water, CO and CO_2. The real pyrolysis takes place at temperature over 200-250°C and at this stage the massive biomass decomposition and weight loss occur. During the last step the char devolatilization continues due to the cleavage of C-H and C-O bonds.

During all the thermal degradation processes, there are many concurrent reactions with a complicated chemical kinetic that decompose organic matrix in char, several gas and also higher hydrocarbons (firstly contained in primary gas phase). The main reactions that take place during this process are: [30]

- Boudouard reaction – $C + CO_2 \rightarrow 2CO$
- Water gas shift – $C + H_2O \rightarrow CO + H_2$
- Methanation – $C + 2H_2 \rightarrow CH_4$
- Steam reforming – $CH_4 + H_20 \rightarrow CO + 3H_2$

Furthermore, after some refineries steps, usually including cyclone (to remove residual solid powder from gas) and a gas cooling/washing section (composed by scrubber, washing tower and filter), final pyrolysis-derived products can be classified in three main groups:

1) A porous, **solid** fraction named **char**, separated just after the reactor and mainly made up of **carbon**;

2) A **liquid** fraction named **bio-oil** or **pyro-oil**, derived from condensation of gas during the cleaning gas stages and made up of more component such as **tar**, **water** and **heavy hydrocarbons**;

3) A permanent **gaseous** fraction mainly made up of **CO**, **CO_2**, **H_2**, **CH_4**, **C_xH_y**.

Moreover, pyrolysis is one of the most investigated process because it allows to obtain not only thermal and electrical energy, but also chemicals and biofuels, as a result of processing of these primary products. [31]

The conversion process occurred in the reactor is controlled by some main parameters :

- **Maximum temperature (T_{max})** reached during conversion process;
- **Heating rate**, that is the progressive increase of process temperature until Tmax is reached, so it is the ratio between time and temperature;
- **Residence time** of materials at T_{max} temperature inside the reactor;
- **Residence time of gaseous species** before cooling and cleaning stage.

Usually, to control the parameter in the reactor, a flow on inert gas (as nitrogen) can be insufflated during the process. On the other hand, this gas can be insufflated before the process, just to guarantee an inert atmosphere inside the reactor, and the flow can be stopped during the pyrolysis and re-started if it is necessary for correcting some values. Different settings of these parameters allows obtain various kind of pyrolysis processes, resultings in a different distribution in product yield and different composition of final compounds, as showed in **Table 2**. [32-33-34-35].

Type	**Operative Parameters**			**Product Yield [%]**		
	T_{max} [°C]	HR [°C/sec]	rt [s]	Char	Oil	Gas
Slow	350 – 400	< 1	1,500 – 2,000	25 – 35	20 – 50	25 – 50
Intermediate	400 – 500	5 – 50	10 – 600	25 – 40	35 –50	20 – 30
Fast	500 – 750	100 – 500	< 2	15 – 20	55 –70	10 – 25
Flash[35]	750 – 1,000	500 – 1,000	< 1	15-20	10 – 20	65 – 75

Tab.2 – Operative Parameters and Production Yield of Pyrolysis Processes

2.4 Current pyrolysis plant in literature

A literature research about pyrolysis of many lignocellulosic materials was carried out to obtain preliminary data to evaluate the reliability of first simulations. Investigated plants are

fed with biomass composed by percentage of Carbon, Hydrogen and Oxygen (fig.4) similar to the ones used to create feedstock employed during simulations. [36-37-38-39-40-41-42-43-44-45] Detailed characteristics of biomasses, processes and products of considered plants are showed in Appendix A.

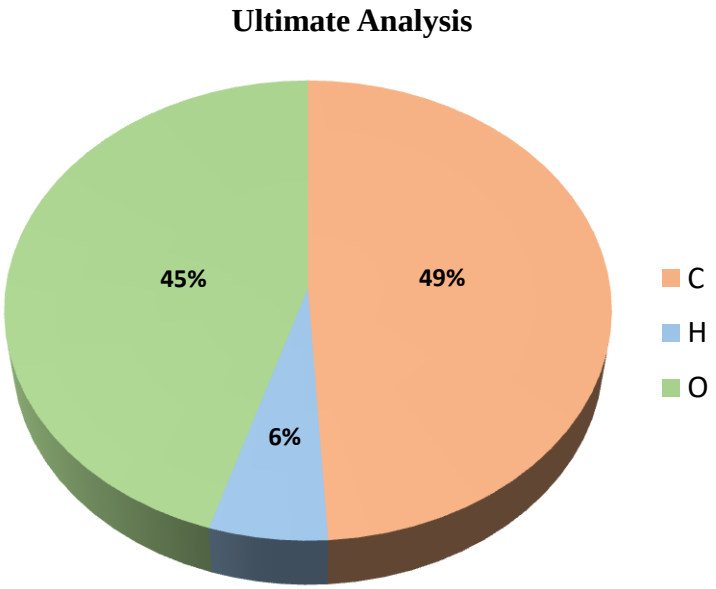

Fig.4 – Average components distribution of investigated biomass

Among considered studies, five works were deeper analyzed:

1) the first case examines the pyrolysis of the esparto by Debdoubi et al. [36]. The process was carried out in a fixed bed reactor powered by an electric furnace and it was controlled and monitored by a thermocouple. Argon gas-flow was used to purge the atmosphere. After reactor, a condenser, filled with ice, collect the outlet volatile material. Here part of this material was collected and condensed by ice producing water and tar and the non-condensable one was removed as pyrolysis gas. Solid product was removed at the end of the cycle, after cooling the reactor.

2) Other biomass considered is the olive stones from work of Blanco Lopez et al. [37]. In this experimentation was used a Gray-King type furnace suitable for biomass pyrolysis and a microbalance for TG/DTG studies. After the reaction, products were examined by a gas chromatography. Analysis of TG/DTG curve shows three relevant futures:
    1. Up to 200°C weight loss is due to release of moisture by biomass sample;

2. The greatest weight loss takes place between 200 and 400°C because hemicellulose decomposition (first step) and cellulose thermal degradation (second one).
3. Above 400 °C there is weight loss because of the slow lignin decomposition, which continues to highest temperatures

3) Next considered study is treated by Sánchez et al. [42] and compares products obtained from pyrolysis of two agricultural residues, rape and sunflowers, equally treated during the test. Reactor was made up of a quarts tube heated by an electrical furnace. Sample consists of 30g of raw material loaded into the front of pyrolyzer. A flow-rate of 200 mL/min of Helium was injected for 60 minutes for totally removing air from system.

4) Tsai et al. [43] study fast pyrolysis using rise husk as feedstock. Pyrolysis was carried out in a fixed bed horizontally tubular reactor, heated by high frequency generator. During experiments, temperatures were controlled and monitored by k-type thermocouple located above the bed, in the middle of tubular reactor. During reaction, a controlled and regulated nitrogen flow-rate was injected into reactor at room temperature and air pressure.

5) Last study case is referred to the work of Mohammed et al. [44] about Napier Grass pyrolysis. Reaction occurs in a stainless tubular fixed bed reactor heated electrically. During the experiments, temperature measurements were taken through a k-type thermocouple connected to a computer in order to control and monitor the reactor temperature.

However, the most important parameter considered during the selection of literature works is temperature. The range taken into account is between 450°C and 700°C. Nevertheless, the other operative conditions, as HR, kind of reactor or particle size Φ, can change among plants.

Temperature is the factor that most affect the distribution of products. Low temperature pyrolysis (300-400°C) produces a low quantity of gas. Moreover, percentages of oil and char depend from operative condition and characteristics of materials[46]. Usually, operating round 500-550°C, there is an equilibrium of the three products. However, an high heating rate and a rapid cooling of gaseous product can result in an ideal condition to produce an high quantity of liquid, minimizing the permanent gas. A further increasing of operative temperature takes to a rapid increasing of un-condensable product that, above the 700°C, is able to reach percentages in weight over 65%.

Other characteristic influenced by temperature is the gas composition. Till 550°C its made up of ~60÷65% of CO2, ~30÷35% of CO and just a little percentages of CH4 (4÷6%), ~1% of H2 and other compound in lower percentages. Over 600°C, there is a drop of Carbon Dioxide percentage and a rapid increase of Hydrogen and Methane, instead carbon monoxide is still stable around 30%.

2.5 State of Art of Pyrolysis Technologies

Although first researches concerning fast pyrolysis started in 1875 and the applicability of this process to lignocellulosic materials has been studied since the early 20th century, there were note significant results before the period of 1980.

Because of the necessity to find new solution to produce energy from green source, the number of research in this topic rapidly accelerate during the past decade, reaching more than 700 paper per year in 2016 (fig.5).

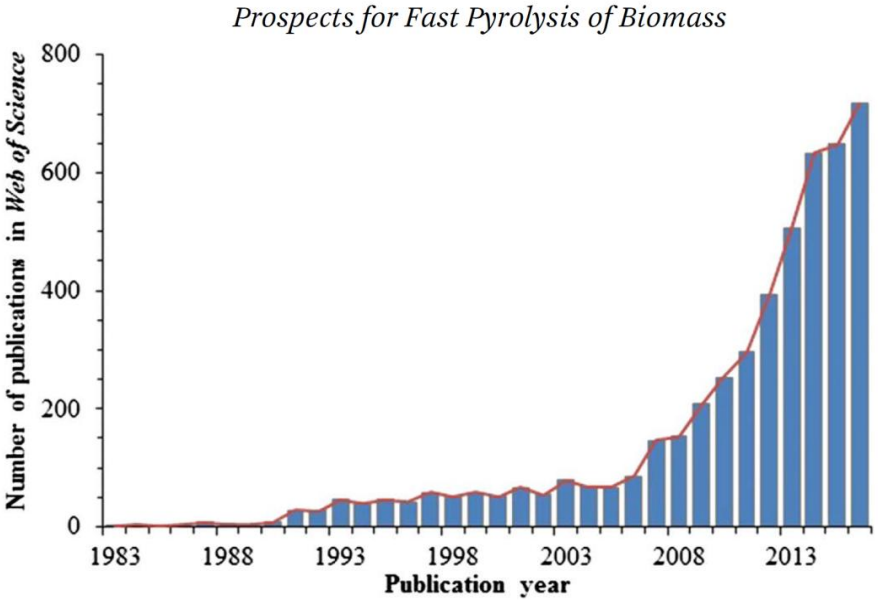

Fig.5 – Trend of scientific research regarding fast pyrolysis between 1983 – 2016 [47]

In considered period, many features were investigated to implement the process, increasing conversion efficiency, developing self-powered system or reducing waste materials maximizing the utilization of all produced fractions. Nevertheless, the growing interest and research in this topic obtained significant results just in little/demonstration scale and has not yet translated in significant success and progress in commercial scale plant. [47]

The main technologies developed to exploit energy from biomass feedstock are resumed in tab.3 and are deeply discussed in the next paragraphs.

Technol.	Φ [mm]	Liq %	Carrier Gas	r.t. [sec]	Scale	Other characteristics
Ablative	≤ 20	60 – 75	✓	Short	Small – Medium	Presence of solid recycle stream
FBR	1 – 2	≈ 60	✓	N.D.	Large	Contact between liquid-solid phases
BFBR	2 – 3	≈ 70	✓	≤ 2	Large	Self-cleaning
CFBR	1 – 2	65 – 75	✓	≤ 1	Large	Presence of second combustor
Screw	N.D.	55 – 65	✗	Very long	Medium	Mobile technology
RCR	≤ 10	60 – 70	Low Quantitity	≤ 0.5	Medium – Large	Spiral direction of particles
Vacuum	≤ 5	35 – 55	✗	short	Large	High bio-oil quality

Tab.3 – Developed pyrolysis technologies

2.5.1 Ablative Pyrolysis

The pioneer of ablative pyrolsysis was the CNRS of Nancy (France) during the ’80s, with investigations about the correlation among pressure, particles movement and temperature[48]. But the technology was developed during the ’90s and further improved in the 2000s.

During the early ’90, the National Renewable Energy Laboratory (NREL) (in that years called SERI) of Boulder (Colorado)[49] projected the first vortex ablative reactor, in which biomass were accelerated at supersonic velocity through a carrier gas (vapor or nitrogen) before entering in the reactor. This velocity caused high tangential forces in the hot cylinder. Centrifugal forces, due to high velocities, forced the biomass particles against the hot (625°C) wall of tubular reactor, producing melting of them with an effect similar to the one of melting butter against frying pan. This method causes a heat exchange unidirectional between surfaces, so, to optimize it, an increasing of contact layer is needed. A liquid film formed because of the pressure between the two surfaces lubricates the contact between

biomass and reactor. Vapors formed from this film were rejected from reactor through carrier gas, obtaining short vapor residence time.

One of the main advantages of this technology is the possibility to use big particles size (at least 20 mm). However, particles could escape from reactor even if they are too big (and so not completely pyrolyzed)[50]. For this reason the incorporation of a solids recycle stream near the output was necessary[51]. Thanks to this loop, big particles were re-circulated in the reactor, instead of the ones that were small enough to go out from reactor just when become re-entrained with vapor and gas.

Thanks to good removal efficiency and a good heating supplied to the system, this process was able to obtain a liquid yields of 60-65% from dry feedstock.

In 1989 NREL, in cooperation with Interchem Industries Inc (USA) tried to use this technology to produce alternative fuels, but, because of some problems related to vortex[52] pyrolysis process, in 1997 interrupted the project. The main difficulties[53] were:

- Erosion due to the high entering particles velocity during transition from linear to angular momentum;
- During recycle of particles , wear phenomena occurred, especially when inert material was inserted in the reactor with feedstock.
- Doubt about the possibility to supply and maintain throughout all the reactor length high velocity necessary to obtain high and constant pressure of particles against the reactor walls to guarantee a good heat transfer between surfaces.

Nevertheless, after some development, this configuration was able to produce a liquids yields around 75% and an oil product lighter than other fast pyrolysis process[54]. The problems were due to high velocity of particles. Furthermore, also with this configuration, is not possible to put thermocouples to check the temperature of reaction.

Peacocke and Bridgwater, from Aston University, had an important role for developing of these technologies. They started in 1994[55] with a small scale (2.5kg/h) prototype of rotating blade reactor for ablative pyrolysis in which biomass was pressed mechanically against reactor wall, avoiding the use of carrier gas. Oil yields collected with this methods was around 70-80%, however the mechanism presented the difficulty of heating up rotating disk and the impossibility to put thermocouples to measure temperature of reaction.

2.5.2 Fixed Bed Reactor (FBR)

In the FBR, the gas flow injected in the reactor passes through the biomass particles to promote the conversion. A better contact and interaction between the phases involved arises

in a better process results, so the main principle of FBR is to promote an intimate contact between fluid phase and stationary phase (feedstock particles).

Dimension and design used for this type of process are various and depend on dimension and aim on the entire pyrolysis system. During the design and dimension step it is important to consider that the reactor must be able to work on the specific feedstock. Moreover, the residence time must be based on desired product: i.e., if the main goal of the plant is the pyro-oil production, a very short residence time is needed (often for fast pyrolysis is less than 2 sec).[56]

Before starting the process it is important to consider the feedstock particle size. According to literature studies, bigger particles have a higher temperature gradient and it takes them longer to get warm. It takes also to a slight decreasing in liquid and gas fraction and an increasing in char production.

This technology often utilize a cylindrical shape, but in literature it is possible to find other ones as the U-shape[57]. Because of the high temperature and the high corrosive properties of liquid produced from pyrolysis, the main material used for the reactors are the stainless steel or quartz.

The tube can also be covered by GC-sheet to increase corrosion resistance. [58]

In the reactor, a gas carrier, usually nitrogen but it is possible to use other gas as argon, is injected to create and maintain the inert environment. Moreover, in some plants, this gas can be used also to regulate parameters such as temperature and pressure during the process. To check and control this flow, a flow meter must be inserted in the system.

The sweeping gas flow rate influences the production yield: a correct flow rate can minimize secondary reaction, including thermal cracking, repolymerization and recondensation. Moreover, removes products from the hottest zone, maximizing liquid fraction. On the other hand, an excessive rapid flow rate can cause an increasing in gaseous product due to a non-sufficient cooling or to an expulsion of pyrolysis vapor too much rapid that does not allow the condensation process.[59]

Other parameter that can influence the distribution of product is the cooling velocity of gas product: a really fast cooling is able to maximize oil production.

Moreover, decrease of temperature and increase of pressure cause respectively a slowdown and a restriction in movement of gas particles, so a decreasing of gas kinetic energy, and promote condensation process.

Condenser are often used also for pretreatment, instead of more expensive equipment as burners or absorbers, to reduce quantity of vapor before treatment. The system works with small particle size (at least 1-2 mm) and liquid yield obtained can be around 50-60% .[60]

2.5.3 Bubbling Fluidized Bed Reactor (BFBR)

In BFB an hot gas is pumped through the reactor and sand is used as inert solid bed material to speed up the heating of biomass. When inlet gas reaches the minimum fluidization velocity, suspended solid particles behave like a fluid. This behavior implicates an excellent mixing, an uniform temperature control and an high heat transfer that support the pyrolysis process. An important characteristic of BFBR is the self cleaning[61], which means that char particles are carried out from the reactor with product gas and vapor and separated downstream through cyclones.[62] But to obtain this result, it is important to choose accurately the right range of particle size. Oversize particles might not be entrained out of reactor. Moreover char has a lower density than the one of fluidized media, so it will float on the surface of the bed. This can cause a vapor cracking catalyst and affect liquid production. For this reason it is very important that a rapid separation of char occurs.[63] On the other hand, fines can be entrained before pyrolysis reaction occurs and compromise the process.

Although this process is well understood and relatively easy to scale-up, there are some constraint that must be taken into account for larger/commercial scale plants.

Usually, condition to maximize liquid yield are 500-550°C, 0.5-2 sec of gas residence time and particle size is are between 2 and 3 mm[64] (also to obtain a good heating rate), but all of that values can vary depending on biomass feedstock and dimension of plant. Indeed, according to literature, bigger plants can operate at lower temperature and longer residence time. Moreover, part of produced gas and/or char can be burned and heat can be re-circulated to heat-up the pyrolyzer for the next cycle.[65] I.e. commercial plant of DynaMotive needs to integrate combustion of these products to supply the necessary heat, instead of pilot plant that is able to work just with natural gas.

University of Waterloo was the pioneer of this technology that today is considered well-known and very reliable.

Basing on their research, Union Fedrosa, in Spain,[66] built a pilot plant (now dismantled) of 200 kg/h. Others plants based on these studies are located in Ontario (Canada) and were projected by Dynamotive: the first in 2005 in West Lorne fed by 100 t/d of dry woodchips and the second in Guelph in 2007 fed by 200 t/d of wood west.

Other example of BFBR plants are in UK where Biomass Engineering Ltd are finalizing a pilot plant of 250 kg/h and in Finland, where Metso, in collaboration with UPM and VTT have projected a plant of 4MWth in Tampere.[67]

Moreover, University of Science and technology of China has planned to project a pilot plant of 3 t/d and a demonstration plant of 15 t/d fed by crops residue. These plants will operate between 470 and 550 °C, cold bio-oil product will be used to condense the hot gasses in the

reactor and non-condensable gas and char will be combusted to heat-up the pyrolysis chamber of reactor. Conversion rate of feedstock is estimated to be around 55%.[50]

2.5.4 Circulating Fluidized Bed Reactor (CFBR)

Circulated fluidized bed reactors (CFBR) are deeply investigated and utilized for fast pyrolysis because, thanks to their restricted residence time, allow oil yields between 65 and 75%.[68]

First configurations of this technology were equipped with just one reactor and char was separated and collected as a fine by-product powder. Instead, most recent configurations use a second combustor, that works at lower temperature, to burn this product in presences of sand[69]. The hot sand is re-circulated to the main reactor to supply the energy needed for the next cycles. This moving of great quantity of materials between the two reactors is quite onerous and complex from energetic and thermodynamic point of view. Moreover, it requires a strictly control of temperature in the recycle loop.

One of main characteristic of this process is the high gas velocity (higher than BFBR) that allows the entrainment of solid particles between riser, where the reaction occurs, and downer, where particles are re-circulated.[70] Furthermore, thanks to this velocity it is possible process a great amount of material and obtain very high percentages of liquid product. On the other hand, the oil will be more "dirty" than the other processes because of a substantial presence of carbon particles.[71] To avoid this inconvenient, should be useful to consider in the project the possibility of an appropriate char removing system as a filter.

Other difference between this technology and BFBR is the residence time of solid particles in the reactor, that is similar to gas or vapor residence time and is around 0.5 or 1 sec. So, to allow an uniform heat distribution inside the particles, CFBR required very small particle size (1-2 mm of diameter).[72] Bigger diameter will take to an incomplete pyrolysis of biggest particles and will reduce yield of oil.

Ensys applied extensively this technology under the name of Rapid Thermal Processing (RTP) and developed many large/industrial scale plant. First one starting to be operative in '96 and processed 36 t/d of material. Moreover, this group collaborated also with ENEL[73] and CRES to develop two plants respectively in Italy and Greece.[74] Most recent are the plants in Rhinealender (US) up to 40 t/d and operative since 2002 and the one in the R&D center of Renfrew (Canada) up to 100 t/d and operative since 2006. Its technology, using wood feedstock, produce approximately 75% of oil, 13% of char and 12% of gas.

2.5.5 Screw Reactor

Screw reactor are tubular and continuous reactor in which an endless screw is used to mix and transport through the reactor the solid biomass particles and to control residence time of feedstock. An inert gas is fed through an hopper to guarantee the inert environment in the reactor. Heating of feedstock changes according to the dimension of reactor: for small diameter, the tube could be heated through an external source; instead of, for the larger one, a solid heat carrier is fed to help the diffusion of heat in biomass particles.[75]

After conversion, produced vapors moves in a condensation system to produce the oil and the char is collected in a tank. If a solid carrier is used, it will be separated from char by a sort of sieve and re-circulated.

This technology has the advantage to be really compact. Moreover it can be used when feedstock is heterogeneous or difficult to handle.[76] Residence time are longer than the other processes and has a liquid yield lower than fluidized bed and an high yield of char.

A prerogative of this kind of reactor is that can be built as a portable equipment. It allows to work directly on the site of production of feedstock, reducing operative and transportation cost.[71] An example of this technology was used from Renewable Oil International, LLC (ROI) of Florence.[77]

Karlsruhe Institute of Technology (KIT) developed a Twin screw mixing reactor for fast pyrolysis in which carrier materials is used to heat up the biomass and is re-circulated after the process. This process is able to reach liquid yield between 53-66%, char yield between 14-22% and gas yield around 20%.[78]

The European Bioenergy Research Institute (EBRI) of Aston University developed the mobile PyroformerTM, a medium-pyrolysis with a screw reactor.

2.5.6 Rotating Cone Reactor (RCR)

In RCR technology feedstock and sand (used as hot carrier) are fed near the bottom part of the reactor. Centrifugal force transports biomass particles through the reactor wall with a spiral direction.[79] Moreover the elevated rout per minutes (around 360-390 rpm) allows a good mixing of the materials and a suitable heat transfer.[80] Thanks to these characteristics, a rapid heating of biomass and resulting pyrolysis conversion occur. Solid residence inside the reactor is ≈0.3 sec and, after reaction, gas residence time is ≈0.5 sec. Liquid yield obtained from dry feedstock is between 60-70%.[81]

Some disadvantages of RCR are an heat transfer less efficient than the one of FBR, the possibility of the erosion due to high velocity solid particles against risers part of the system. Moreover, there could be some troubles related to the scaling-up of these technologies,

because a larger reactor could have not enough heating surface to guarantee a suitable heating of feedstock. Nevertheless, in these years some characteristics are been imrpved: diameter of feedstock particles could be up to 10 mm and the overall efficiency of the system is increased considerably. Furthermore, RCR requires a quantity of carrier gas lower than the other pyrolysis systems.[82]

Pioneer of this system was the Twente University of Technology in the '90 and it was developed from Biomass Technology Group (BTG) in early 2000 with a pilot plant fed by 250 kg/h. In 2006 BTG designed a commercial plant, today decommissioned, fed by 2 t/h (1.7 effective) of palm residue in Malaysia with a oil yield between 60 and 70%. [83]

Moreover, in 2014 BTG-BTL started the construction of a plant of 5t/h fed in Hangelo, Netherland under the EMPYRO European Process. Plant should be able to produce between 20,000 and 25,000 t/y of pyrolysis oil, electricity, process steam, and aqueous organic acids.[84]

2.5.7 Vacuum Pyrolysis

First experimentation of Vacuum pyrolysis was carried out by Universty of Laval in Quebec (Canada) to produce liquid from biomass through a multiple furnaces to heat the feedstock. From 1988 to 2002 the process was developed from Pyrovac Industries that combined some aspects of both slow and fast pyrolysis and designed it as an horizontal moving bed. Indeed, this technology is not properly a fast process: it has a slow heat transfer to and through the feedstock and slow heating rate; on the other hand, this process works with a short vapor residence time in the hot zone, to avoid that secondary reactions occur, and it is able to produce 35-50% of liquid product.[85]

Compared to the others fast processes, the production rate of bio-oil is lower, because it is negatively influenced by the low internal heating rate, and contain an higher percentages of water (more than 25 % of total liquid production) but it produces a very high quality bio-oil.[86]

In 1999 Pyrovac group projected a commercial plant of 3.5t/h on Quebec. In early 2000 this plant was successfully tested also for crumb rubber but a problem that occurred in a condensing tower carried to the stop of the process and the closing of the entire plant in 2002.

In this process, a metal belt carries the biomass to the horizontal chamber that works in vacuum condition around 450-600 °C. Here the feedstock is indirectly heated by a mixture of molten salt, respectively heated by the non condensable fraction of pyrolysis products. Moreover, some patented mechanical agitators are needed to blend uniformly the feedstock on the belt and to limit, as much as possible, an external heat transfer. [67]

All this equipment make the process really complicated and expensive. Moreover, it needs a continuous maintenance and some specialized devices to work in vacuum condition (i.e. feeding and discharging), that make the investment and the costs even higher. Also, the process can produce some liquid effluent that could damages the vacuum pump. It is possible to avoid this problem trying to re-circulates it to the scrubbers.
Nevertheless, this process has also some advantages: [51]

- It does not require carrier gas to occur that minimizes production of aerosol;
- Easy condensation of liquid product;
- It is possible to use particles larger than the ones in the other process (till 2 or 5mm);
- High bio-oil quality with a very low presence of char in it because of slow gas velocity.

3) BIO4BIO Pyrolysis Plant

The aims of BIO4BIO project are the valorization of lignocellulosic material, the production of energy from this kind of biomass source and production of biofuel. To achieve these goals, a pyrolysis pilot-plant, showed in Figure 6, was built in Caltagirone (CT), Sicily.

Fig.6 – Macro of Pyrolysis Pilot-Plant [87]

This plant is in co-ownership with:

- Department of Electrical, Electronic and Computer Engineering (DIEEI) of University of Catania (ex-Department of Industrial Engineering DII);
- "Plastica Alfa s.r.l."
- "*Consiglio Nazionale delle Ricerche* (CNR)" of Catania

The goal of study is to set pyrolysis parameters able to maximize the production of pyrogas, which can be directly used to feed an electrical engine.

Further, bio-oil is a very interesting product from an energy point of view. Nevertheless, even if it cannot be directly used as gas, after some post-production refinery stage it can be used to produce bio-fuels and chemicals. [88]

Table 4 shows some characteristics and operative parameters provided for this plant:

Feedstock		Lignocellulosic Biomass
Size of	Particle	2-4 [mm]
	Pellet	5x10 [mm] or 5x20 [mm]
Flow Rate (daf)		30 [kg/h]

T_{max} of conversion	500-680 [°C]
Heating Rate	10-60 [°C/min]

Tab.4 – Provided Characteristics

3.1 Description of equipment

Residence time is strictly connected to heating rate and its value will be chosen through various tests.

The main characteristics of each part of the plant are described below in detail.

3.1.1 Loading section

A hopper and a cochlea (fig.7) are powered up by two electrical engines.

Cochlea is designed as a endless screw able to transport the feedstock in the reactor, thanks to its rotation.

Fig.7 – Hopper and cochlea

3.1.2 Reactor

The pyrolyzer is a cylindrical rotating drum reactor (fig.8) power up by an external electrical engine similar to the ones of loading section and heated up by resistors.

It is divided in a pre-heated zone (showed in fig.9 and drown with a reticular background in fig.19) in which materials reach temperature between 350-500°C and a real pyrolysis section able to work up to 850°C.

The residence time of feedstock in the reactor depends on rotation speed of drum.

During the conversion, temperature is monitored by three thermocouples located respectively at the end of pre-heated zone, in the middle of reactor and in the outlet section.

Moreover, the equipment is provided with pressure controllers which required to monitor the gas flow as well as for safety reason.

Fig.8 – Macro of pyrolyzer

Fig.9 – Pre-heated section

3.1.3 Heat Exchanger

The first heat exchanger (fig.10) is necessary to cool down the gasses before entering in the gas cleaning section because some equipment can be damage working at temperature too high (above 400°C).

On the other hand, temperature cannot decrease under the dew point of the products (around 350°C), to avoid premature condensation because tar present in the two-phase mixture can damage and/or clog some equipment.[89-90]

Definitely, gas should leave the heat exchanger between 400 and 350°C.

Cooling air is re-circulated by a pump to avoid a dilution with external air.

Fig.10 – Heat Exchanger

3.1.4 Cooling/Cleaning Gas System (fig.11)

Cyclone (fig.13) is used to separate solid coarse and the heaviest material from gaseous flow. This kind of particles sink on the bottom instead gas are directed through the Venturi scrubber (fig.12). This tool is able to work at medium-high temperature preserving a good removal efficiency of rough particles.

Gas mixture enter in a system made up of a Venturi scrubber and two washing towers (fig.14). During this step a sudden cooling by cold water (≈10°C) take to a formation of condensable fraction (tar and water) and its separation from permanent gas.

These equipments are also able to operate a further cleaning able to remove contaminant and particulate.

Fig.11 – Cleaning Gas Section

Fig.12 – Scrubber

Fig.13 – Cyclone

Fig.14 – Washing Tower

3.1.5 Hydraulic System

A *chiller* (fig.15) provides the water for two heat exchanger:

the first one (fig.17) is located at the end of gas washing section and cool down the cleaned permanent gas;

the second one (the plate heat exchanger showed in fig.16) is located near the washing towers and provides cool water to all the washing-gas section.

After these operations, hot water is re-directed to the chiller.

Fig.15 – Chiller

Fig.16 –Plate heat exchanger

Fig.17 – Heat Exchanger

3.1.6 Sand Filter and Gas Ramp

Sand filter (fig.18) is specifically designed for combustible gasses and for water vapor removal and works the last cleaning before the gas ramp.

For safety reason is designed to hold fine powder, residual of particulate or condensable and moisture.

Fig.18 – Filter

3.2 Description of conversion process

Figure 19, that shows the layout of the plant, is used as guideline to illustrate the entire process. Numbers used during the description of the conversion, are in accordance with the ones in **Figure 19** and identify each device.

First, feedstock is inserted in the reactor via a screw conveyor (2).

The conversion process, that takes place in a rotating reactor (3), is divided in two consecutive stages:

- Preheating of the material up to 300-500°C;
- Real pyrolysis, during which the biomass reaches temperatures up to 850 °C.

During the process, nitrogen can be insufflated inside the rotating reactor to create the inert atmosphere (the main features of pyrolysis process) or to correct any parameters (such as temperature or pressure) that does not meet the predicted values. During the reaction, the process temperature is controlled by three thermocouples located respectively at the beginning of reactor, at the end of preheating zone and at the end of reactor. Moreover, there are some pressure controller, located at the end of reactor, to check gas flow level and for safety reason.

Leaving the reactor, the output product is directed in an airtight tank (4). In this tank, solid residues (char) sink to the bottom by gravity, whereas gaseous fraction in suspended on the surface and moved to the cooling and washing processes.

A first cooling is carried out by an air heat exchanger (5), which allows the pyrogas to reach

a temperature between 350 and 400 ° C.

After the first cooling, the pyrogas is directed to the gas-washing section, made up of a cyclone (7), a scrubber (8) and two washing towers (9). Thee equipment are used to remove the small residual solid particles and to continue the cooling process, in order to allow the separation of condensable fraction, mainly composed of water and tar.

Coming out from washing towers, gaseous residual is directed in a water heat exchanger (10), where the temperature decreases up to 60°C. Cooled product passes (11) through a sand filter (12) to remove particulate and humidity. At the end, the final product arrives at the gas ramp (13) that has three outlets:

1. the first one for the gas-chromatograph, which allows the analysis of samples of the output product;
2. the second one directly connected to the engine;
3. the last one to send the gas out of the flashlight.

All the system is managed through an external PLC that monitors both temperature and pressure and the resistors used to heat up the reactor.

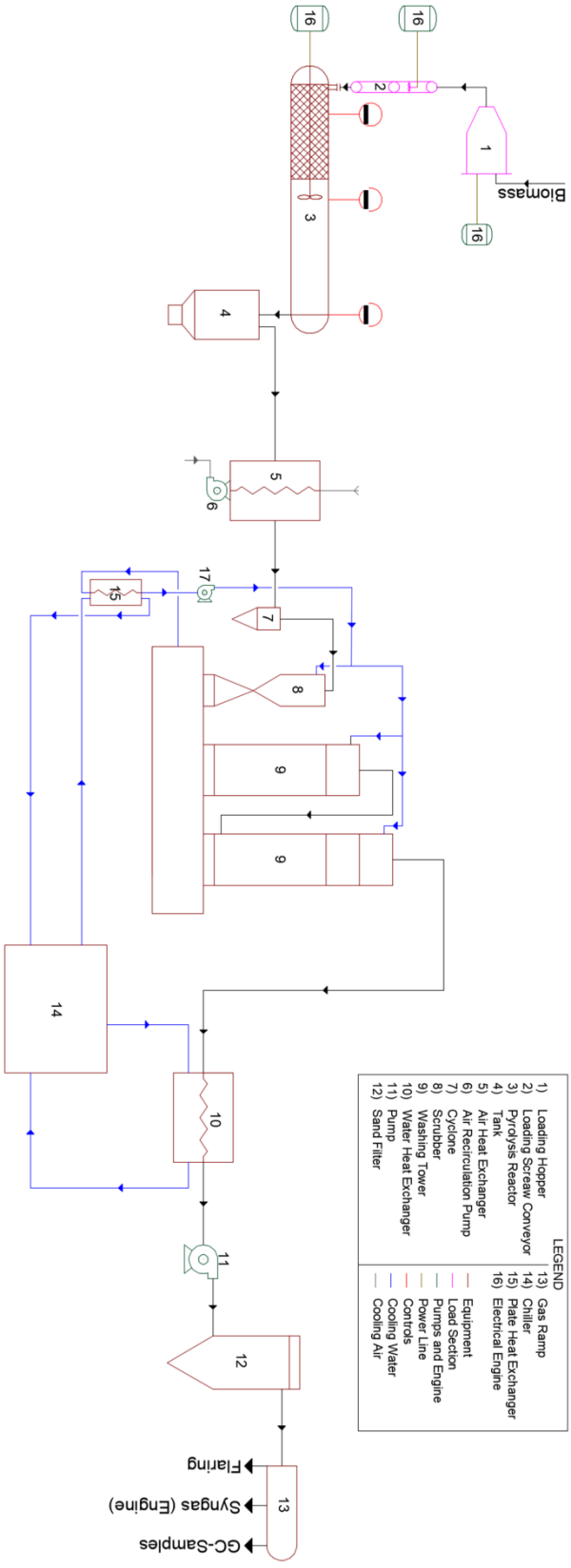

Fig. 19 – Plant Design

4) Methodology

4.1 Preliminary consideration about feedstock composition

In literature, many studies represent biomass degradation as the sum of decomposition of cellulose, hemicellulose and lignin.[91-92]

From TG-Analysis is possible to analyze the decomposition curve of these three constituents and examine the range of temperature in which begins the broken of the polymers chains.[93-94]

- Cellulose is made up by a crystalline structure, which is difficult to breake. TG-Analysis shows that its degradation process begins around 300°C, has a single mass loss peak that occurs between 340 and 360 °C and finishes below 400°C. Moreover, during the process are involved different chemical species as the LVG.
- Decomposition of Hemicellulose, analyzed by DTG curve, shows that it is easier to decompose than cellulose and the process occurs at lower temperature. Process begins around 200°C and the higher value of weight and mass loss occurs between 250-275°C.
- Degradation of lignin occurs in a very large range of temperature with a relatively low conversion rate, so probably it is the main responsible for the char production. It begins at lower temperature, compared to the others components, and the shape of the curve has not a clear maximum point but it looks like a continuous long tail that ended above the 900 °C.

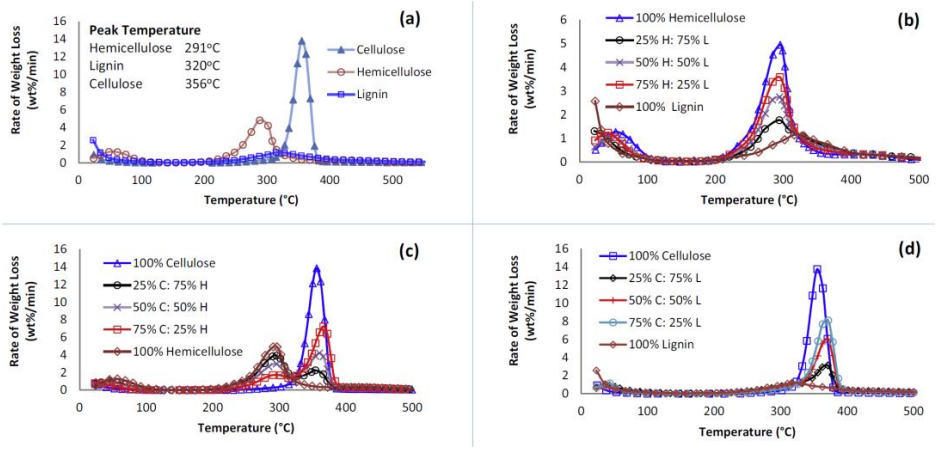

Fig.20 – DTG curve of C, HC and L and their interaction[94]

Instead, fig.21 represent DTG curve of untreated miscanthus biomass (a) and its change in absence of hemicelluloses (b), with a reduction of cellulose (c) and in absence of lignin (d). Analyzing these data, is possible to note:

- A first hump that corresponds to hemicellulose degradation;
- The maximum peak that corresponds to cellulose degradation;
- A long tail given by the behavior of lignin degradation.

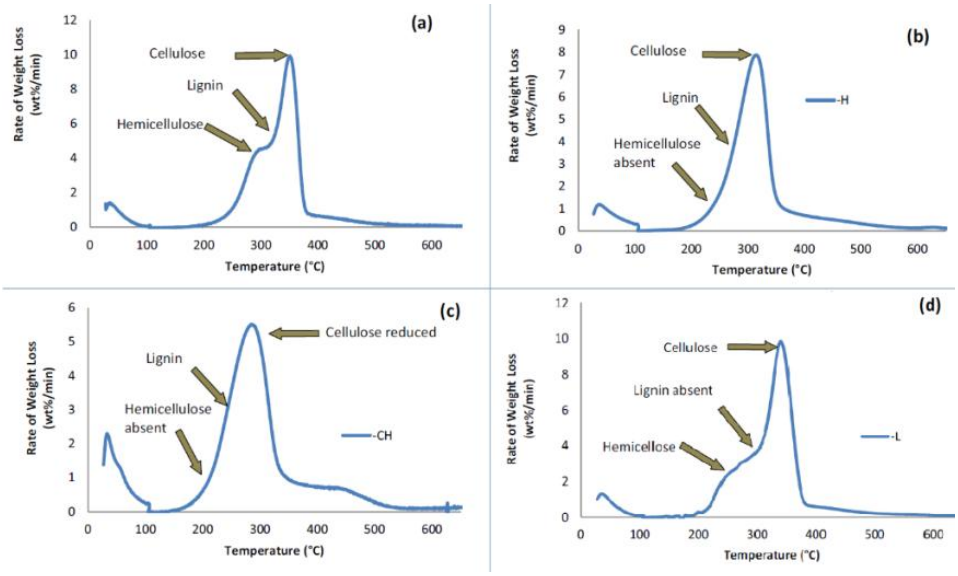

Fig.21 – Effect of C, HC and L on biomass DTG curve[94]

A comparison among the curves shows that biomass degradation behavior is strongly affected by its biochemical characterization.

For this reason, and because of the difficulty to work directly with a very complex compound as biomass that decomposes through many chemical reactions, authors decide to start implemented a simplified simulation for each component and then implement the one for the complete biomass.

4.2 Building of simulation feedstock

As mentioned above, biomass can be analyzed from an elemental (C, H and O) or from a biochemical (Cell, Hemicell, Lig) composition. To build a feedstock as similar as possible to real composition, these two characteristics are both considered and mixed.

In order to reach the final thesis goal, it is necessary to analyze the thermo-chemical decomposition of cellulose, hemicellulose and lignin, highlighting the intermediate compounds and the characteristics products derived from pyrolysis for each of these components.

4.2.1 Cellulose

Composition of cellulose was obtained according to different literature sources, instead the molecular structure was obtained using Ranzi et al. as reference source.[95] To verify the composition, a stoichiometric balance, based on a work of degradation of lignocellulosic material, was carried out. It composes ~41%wt of total biomass. Reactions due to the increasing of temperature carry to a separation of water and carbon from starting matrix and to a formation of an intermediate compound named "active cellulose".[96-97] By degradation of this latter, a characteristic compound derived from pyrolysis cellulose process, named Levoglucosan, is achieved. The non converted part is decomposed in a mixture of other components. The following schema resumes this process:

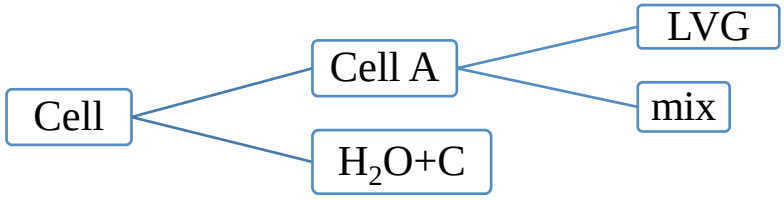

Fig.22 – Cellulose decomposition[95]

4.2.2 Hemicellulose

Composition of hemicellulose was obtained from different literature sources, while the molecular structure was obtained from Ranzi et al.[95]. To verify the composition, a stoichiometric balance, based on a work of degradation of lignocellulosic material, was carried out. It composes ~32%wt of total biomass. Reactions due to the increasing of temperature separate the main matrix in 0.4 of HC1 and 0.6 of HC2.[96-98] This latter is decomposed in a mixture of component instead HC1 has three different sub-reactions. One of them carries to a formation of a characteristic product derived from pyrolysis hemicellulose, named Xylosan.

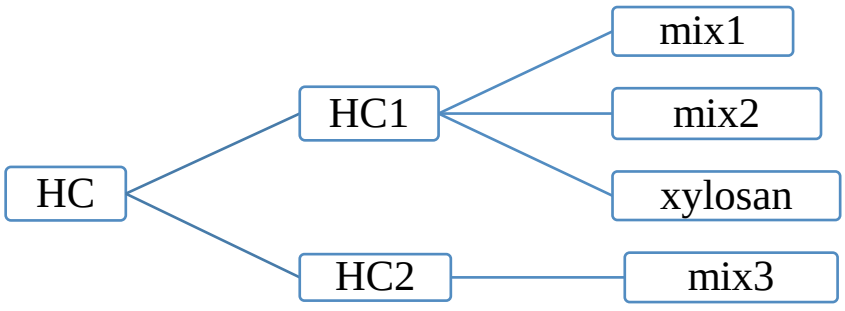

Fig.23 – Hemicellulose decomposition

4.2.3 Lignin

Lignin has a more complicated structure that needed more calculation. It composes ~27%wt of total biomass. Literature works consider lignin as made up by three different sub-lignin materials, each of them characterized from the dominance of an element: [95-96]

Lig-C – $C_{15}H_{14}O_4$ – 23%wt

Lig-H – $C_{22}H_{28}O_9$ – 39%wt

Lig-O – $C_{20}H_{22}O_{10}$ – 38%wt

Lig-C is decomposed in an intermediate component called Lig-CC and a mixture of common compounds. From Lig-CC a characteristic product derived from pyrolysis Lignin, named Coumaryl, is attained.

On the other hand, Lig-H and Lig-O create an intermediate component called Lig-OH. From Lig-OH, after some reactions, a characteristic product derived from pyrolysis lignin, named Sinapaldehyde, is obtained. However, pyrolysis of lignin is also responsible for production of an important compounds as Phenol.

The sum of these components was combined to obtain the composition of total lignin obtained.

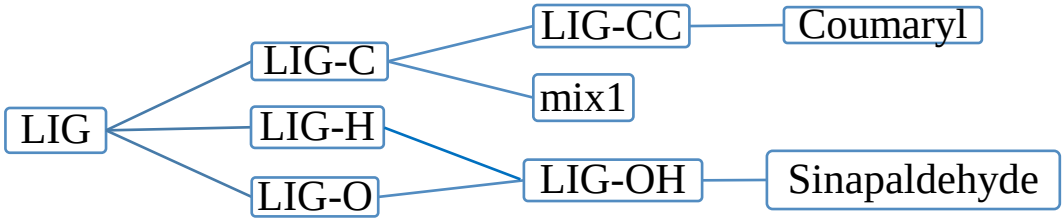

Fig.24 – Lignin decomposition

4.2.4 Conclusive Biomass

The product obtained mixing cellulose, hemicellulose and Lignin has not a weight percentages of these components comparable with the one of typical biomass expressed in the previous paragraphs. For this reason, the three main components need to be managed, finding coefficients able to satisfy this characteristic.

Regarding elemental composition, an average value of ultimate analysis of some olive pits compounds coming from previous works [99-100], online database[101] and literature source[37] and some value of H/C and O/C ratios were considered.

The two considered parts were combined: elemental composition was arranged to fit the lignocellulosic composition, obtaining the definitive biomass component.

Eventually, the right distribution of C, H and O, was again verified by the stoichiometric balance of the complete biomass decomposition extrapolated from literature [95-96].

Once that the definitive feedstock was obtained, other information such as H/C and O/C ratio and its calorific values were calculated.

Formula (2), which is appropriate for each kind of biomass[102], is used to calculate Higher Heating Value (HHV). For the calculation, [C], [H] and [O] derive from Ultimate Analysis of considered materials:

$$HHV_B = -0.763 + 0.301\,[C] + 0.525\,[H] + 0.064\,[O] \quad (2)$$

4.3 Modeling of decomposition process

Decomposition of biomass can be modeled basing on just primary or both on primary and secondary reactions. [103-104]

In the first case, feedstock is directly decomposed in solid, liquid and gaseous products. On the other hand, primary reactions produce some intermediate compounds that evolve in final products after secondary reactions. [105]

In this thesis, to model the degradation of biomass, a two steps process is proposed.

In the reactor, due to medium-high temperature, feedstock is firstly decomposed in a solid component, which is mainly composed by carbon, mostly because of the inert material and fixed carbon (char), and in a gaseous fraction that includes both condensable and un-condensable products. In the second stage, due to cooling and cleaning gas systems, condensable part is separated from permanent gas to obtain the liquid product, composed by water and final pyrolysis oil.

In accordance to this model, decomposition can be written as:

$$m_f = m_c + m_{g1} \quad (3)$$

and

$$m_{g1} = m_{g2} + m_l \quad (4)$$

so, definitively, mass balance of biomass decomposition can be resumed as:

$$m_f = m_c + m_l + m_{g2} \quad (5)$$

in which:

m_f = mass of inlet feedstock in the reactor;

m_c = mass of solid char product;

m_{g1} = mass of primary gas (condensable + un-condensable);

m_l = mass of liquid product;

m_{g2} = mass of un-condensable gas product;

This procedure is schematically represented in fig.25.

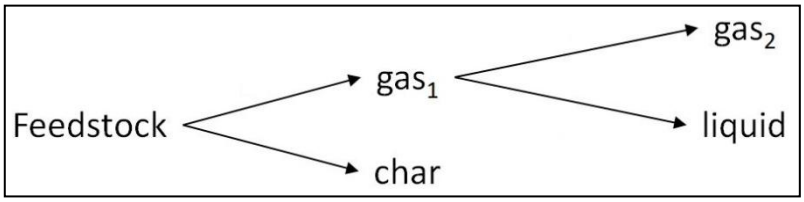

Fig. 25 – Biomass decomposition schema

4.3.1 Mathematical model

To describe the conversion process it is important to consider the percentage of the mass change of each compound involved during the reaction.
Usually this factor is acquired analyzing the curves resulting from experimental TGA analysis and it is described by the parameter α, expressed as:

$$\alpha = \frac{m_i - m}{m_i - m_f} \tag{6}$$

in which:

α = conversion rate;
m_i = initial mass;
m = current mass;
m_f = final mass;

The evolution of conversion rate of species involved in the pyrolysis (dα /dT) is expressed in formula 6 and depends on two factors:

- Heating rate (k), necessary to describe the kinetic of reaction;
- A polynomial function f(T), empirically obtained, used to correlate the trend of compound with the increasing of temperature during the simulation.

$$\frac{d\alpha}{dT} = k \cdot f(T) \tag{7}$$

4.3.2 Arrhenius equation

Pyrolysis is a thermo-chemical conversion based on many primary and secondary chemical reactions that occur during the heating of the feedstock, and in fact, temperature is the most influential parameter affecting yields and composition of final products.
Moreover, all the reactions, involved during the process, are governed by a kinetic law. For this reason, a necessary goal to implement an accurate simulation is to propose a model able to reproduce the kinetic of the chemical decomposition and that can take into account the factors that most affected the pyrolysis.

The law that describe the kinetic of any chemical reaction is mainly governed by Arrhenius equation (5):

$$k=k_0 \exp(-Ea/RT) \quad (8)$$

in which:

k = rate constant (describe the degree of decomposition);

k_0= pre-exponential factor;

Ea= activation Energy;

R = 8.314 [J/kmol] is the universal gas constant;

T= Absolute Temperature;

4.3.3 Polynomial Function f(T)

Through the determination of percentages of each species in a temperature range 773<T<1,173 K, was defined the function:

$$f(T) = a + bT + cT^2 \quad (9)$$

In which coefficients *a*, *b* and *c* were determined for each components by Microsoft® Excel Solver feature.

4.4 Gas Cleaning-Cooling Section

After the outlet section of reactor, char is separated by gravity, while the gaseous product is directed and treated in the cleaning-cooling section.

Equipment involved in this process are a cyclone, a Venturi Scrubber and some heat exchanger.

During this procedure, a strictly temperature control is necessary: in fact, an improper cooling can cause a premature condensation in the machinery parts that are inappropriate to work with liquid, resulting in a damage of them.

4.4.1 Cyclone

The main equipment used for removing coarse and suspended particulate matter is the cyclone.

The use of this technology is very common because is cheap, compact and is able to work at very high temperature with a good removal efficiency.[106]

Inlet particles are subjected to a centrifugal force that pulls them against the wall of the equipment. This contact reduces the speed of the particles that fall down and are collected in

a hopper located at the bottom. During the separation, the temperature should be higher than tar dew point to avoiding the condensation that can damage the equipment.

During a design of cyclone, it is necessary consider the following relation:[107]

$$N = \frac{1}{H}\left(L_b + \frac{L_c}{2}\right) \; ; \; d_p = \sqrt{\frac{9\mu W}{2\pi N v_i(\rho_p - \rho_g)}} \quad ; \quad \Delta t = \frac{\pi D N}{v_i} \quad ; \quad v_i = \frac{W}{\Delta t} \; ; \; v_t = \frac{(\rho_p - \rho_g) v_i d_p^2}{9\mu D}$$

In which:

N = number of revolution of gas in the equipment;

H = height of inlet section;

L_b = length of main body of cyclone;

L_c = Length of cyclone final cone section.

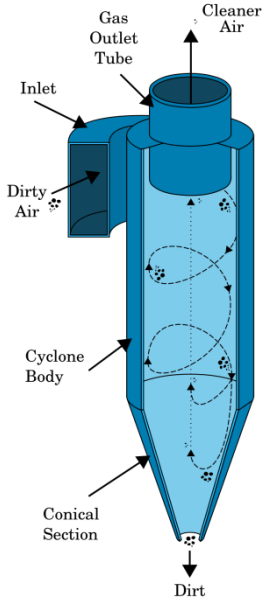

Fig.26 – Cyclone separator

4.4.2 Venturi Scrubber

Inlet gas crosses a convergent section, designed to increase its velocity and create a turbulent flow, and arrives in a throat. Simultaneously, little drops of nebulized liquid, able to absorb particles of tar and fines, are injected in the inlet section or just before the throat. The outlet section is a divergent tube design to reduce the fluids velocity, simplifying the dropping and collection of condensed fraction.[108]

This technology is more expensive than cyclone but is able to guarantee a very high removal efficiency due to an interaction between gas and liquid drop.

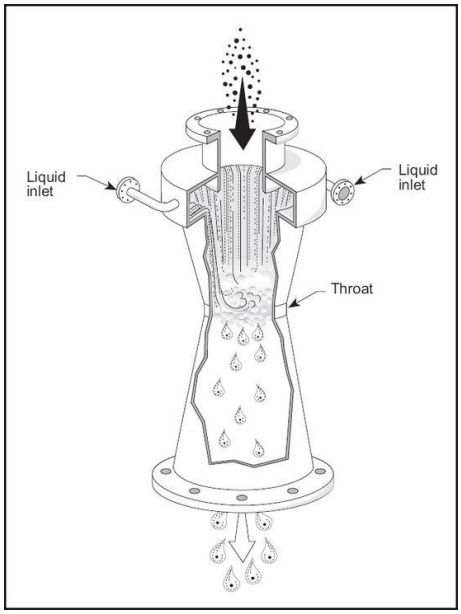

Fig.27 – Venturi Scrubber

Collection efficiency can be calculated by the Contact Power Theory, based on a series of experimental observation. According to its fundamental assumption, "when compared at the same power consumption, all scrubbers give substantially the same degree of collection of a given dispersed dust, regardless of the mechanism involved and regardless of whether the pressure drop is obtained by high gas flow rated or high water flow rates" (Lapple and Kamack, 1955).

The theory, analyzed and re-elaborated by Semrau, relates the total pressure loss (p_t) with the collection efficiency by the relation:[109]

$$\eta = 1 - e^{-\alpha p_t^{\beta}} \tag{10}$$

In which α and β are parameters depending on particles collected.

The total pressure loss is calculated as:

$$P_T = P_G + P_L \tag{11}$$

with:

$$P_G = (2.724 \times 10^{-4})\Delta p \text{ [kWh/1000m}^3\text{]} \tag{12}$$

is the power expended to move the gas into the system expressed in terms of scrubber pressure drop Δp [kPa];

$$P_L = 0.28 p_L (Q_L/Q_G) \text{ [kWh/1000m}^3\text{]} \tag{13}$$

is the power expended in the liquid stream, in which:

p_L = liquid inlet pressure;

Q_L = Liquid feed rate;

Q_G = Gas flow rate.

During the simulation, the quantity of water needed to cool down the gas condensing the liquid product is calculated by:

$$\dot{m}_w = (\dot{m}_g \cdot c_{p,g} \cdot \Delta T_g)/(c_{p,w} \cdot \Delta T_w) \quad (14)$$

with:

$\dot{m}_w$ = mass flow of water;

$\dot{m}_g$ = mass flow of gas mixture;

$c_{p,g}$ = specific heat of gas mixture;

$\Delta T_g = T_{i,g} - T_{f,g}$ = difference between initial and final gas mixture temperature;

$c_{p,w}$ = specific heat of water;

$\Delta T_w = T_{i,w} - T_{f,w}$ = difference between initial and final water temperature.

4.5 Characterization of products

Once formulated and verified the model, it is important to characterize all the products and understand their energetic possibility. Considering that the three final products are in different physical state and are very different also from a chemical point of view, it is necessary to use a different method for each one of them.

To assess the energetic potential of pyrolysis product, some characteristics of gas and oil were investigated. [110]

Starting from molar composition, it is possible to calculate some properties of the obtained gas.

Partial volume(V_a) is defined as the volume of one component of the gas mixture so to evaluate it, it is necessary to know the molar fraction of the compound and the total volume

$$V_a = X_a \cdot V_{tot} \quad (15)$$

It is possible to employ the same reasoning to calculate the partial pressure (P_a), defined as the pressure of the gas if the gas was in the same volume and temperature of the gas mixture

$$P_a = X_a \cdot P_{tot} \quad (16)$$

Where:

X_a is the molar fraction of the singular gas;

P_{tot} is the total gas mixture pressure;

V_{tot} is the total gas mixture volume

The gas density (ρ) is given by the following formula:

$$\rho = \frac{m}{V} = \frac{n \cdot PM}{V} \quad (17)$$

it may be deduced that:

$$\frac{\rho}{PM} = \frac{n}{V} \quad (18)$$

The ratio n/V is the molar concentration of a substance and it is also calculated through the ideal gas law:

$$PV = nRT \rightarrow \frac{P}{RT} = \frac{n}{V} \quad (19)$$

Equaling equation (18) and (19), is achieved:

$$\frac{\rho}{PM} = \frac{P}{RT} \quad (20)$$

which it is possible to isolate ρ:

$$\rho = \frac{P \cdot PM}{RT} \quad (21)$$

where:

P is pressure;

R is the universal molar gas constant and it is equivalent to $8.20575*10^{-5}$ J K^{-1} mol^{-1}

T is the temperature

To calculate the partial gas density (ρ_a), the molar fraction is necessarily included in the formula. So, instead of the total pressure, it is mandatory to utilize the Partial pressure (P_a):

$$\rho_a = \frac{P_a \cdot PM}{RT} \rightarrow \frac{P_{tot} \cdot X_a \cdot PM}{RT} \quad (22)$$

The total gas density will be defined by the sum of all the partial gas density of the single gas of the mixture:

$$\rho_{tot} = \rho_{P1} + \rho_{P2} + \cdots + \rho_{Pm} \rightarrow \frac{P_1 \cdot X_1 \cdot PM_1}{RT} + \frac{P_2 \cdot X_2 \cdot PM_2}{RT} + \cdots + \frac{P_m \cdot X_m \cdot PM_m}{RT} \rightarrow \frac{\sum_{i=1}^{m} P_{p_i} \cdot X_i \cdot PM_i}{RT} \quad (23)$$

Where *i* is the element of the gas mixture.

The Heat Capacity of each component (C_{pi}) is calculated by Nasa Polynomial Methods [111-112] expressed in formula (24):

$$\frac{c_{p,i}}{R} = a_1 + a_2 T + a_3 T^2 + a_4 T^3 + a_5 T^4 \quad (24)$$

In which R is the universal gas constant, coefficients $a_{1..5}$ are defined for each component and tabulated in literature and T represents the gas temperature.

The Heat Capacity of a total gas mixture ($C_{p,t}$) is obtained by the product of each $C_{p,i}$ times the mass fraction (y_i) of each component:

$$c_{p,t} = \sum_{i=1}^{n} c_{i,t} \cdot y_i \quad (25)$$

Moreover HHV of each gas component is calculated by formulas (26) and (27) [113], depends on the presence of oxygen particles in the structure.

$$HHV = 0.303\ (C) + 1.423\ (H) \quad (26)$$

$$HHV = 0.305\ (C) + 1.423\ (H) - 0.154\ (O) \quad (27)$$

The same procedure was used to calculate HHV of oil, expressed by Formula (28) [114]:

$$HHV = 0.352\ (C) + 0.944\ (H) - 0.105\ (O) \quad (28)$$

In these formulas, (C), (H) and (O) represent the percentages of the carbon, hydrogen and oxygen of pure compound.

Correlating these values with weight percentage composition of total gas mixture, Authors calculate the total HHV.

Eventually, correlation between HHV and LHV is expressed by formula (29) [30].

$$LHV = HHV - h_v \cdot ((9H/100) + (M/100)) \quad (29)$$

In which:

h_v is the heat of vaporization of water;

M is the moisture content of pyro-oil.

4.6 Recycling

According to technical specification of pilot-plant, line of produced gas can be directly connected to an engine to produce electrical energy. To maximize the energy content of pyrolysis products, a CHP system is planned.

This system is based on the utilization of an engine fed by pyrolysis-gas, able to recover thermal energy from cooling water and exhaust and connected to a electrical generator. The heat released during the combustion process is recovered by heat exchangers to sustain the drying and/or pyrolysis stages.

4.6.1 Air/Fuel ratio

The theoretical quantity of oxygen necessary for the complete combustion of a fuel (m_{O2})[115], expressed in [kg_{O2}/kg_{fuel}], is calculated as:

$$m_{O2} = Y_C \cdot \left[\frac{M_{O2}}{M_C}\right] + \frac{Y_H}{4} \cdot \left[\frac{M_{O2}}{M_H}\right] + Y_S \cdot \left[\frac{M_{O2}}{M_S}\right] - Y_O \quad (30)$$

in which:

M_i= molecular mass of compound i (with i = O_2 or CO_2), expressed in [kg_i/kmole];
M_j = molecular mass of element j (with j = C, H, S or O), expressed in [kg_i/kmole];
Y_j = mass fraction of element j (with j = C, H, S or O), expressed in [kg_j/kg_{fuel}].

From this data and knowing that percentage of oxygen in the air composition is around 21%, it is possible to calculate the stoichiometric air/fuel ratio (AFR_{stoich}), defined as the ratio between mass of air and the mass of fuel during the combustion process:

$$\frac{m_{O2}}{m_{air}} = 0.21 \rightarrow m_{air} = \frac{m_{O2}}{0,21} \cong 4.762 \cdot m_{O2} \quad (31)$$

The AFR_{stoich} is the minimum quantity of air necessary for the process but, to ensure the complete combustion and an high performance of the engine, is considered an excess air obtaining an actual air/fuel ratio (AFR) that is the one really considered during the process.
This procedure introduces the Air-fuel Equivalence Ratio (ER or λ) defined as:[116]

$$\lambda = \frac{\mathrm{AFR}}{\mathrm{AFR_{stoich}}} \rightarrow \mathrm{AFR} = \lambda \cdot \mathrm{AFR_{stoich}} \quad (32)$$

4.6.2 Thermal recovery

In accordance with specification of CHP system, the thermal energy content of cooling water of the engine and exhaust gas can be recovered by an heat exchanger and re-circulated.[117]
Thermal energy of exhaust (Q_{ex}) is calculated as:

$$Q_{ex} = m_{ex} \cdot c_{p,ex} \cdot \Delta T_{ex} \quad (33)$$

in which:
$m_{ex} = m_{air} + m_{syn}$ is the mass of the exhaust.
$\Delta T_{ex} = T_{i,ex} - T_{o,ex}$;

Thermal energy of cooling water (Q_{cw}) is calculated as:

$$Q_{cw} = m_{cw} \cdot c_{p,cw} \cdot \Delta T_{cw} \quad (34)$$

The values of m_{cw} and ΔT_{cw} are given by data sheet of the equipment.

4.6.3 Mechanical and Electrical Power

The mechanical power (P_m) generated by the system can be calculated as[118]:

$$P_m = Q_{syn} - Q_{cw} - Q_{ex} - Q_l \quad (35)$$

in which:

$Q_{syn} = m_{syn} \cdot LHV_{syn}$ is the heat generated by syngas combustion;

Q_l are the losses due to combustion chamber, mechanical friction and lubricate oil;

Considering the alternator efficiency (η_{gen}), the definitive electrical power (P_{el}) produced is:

$$P_{el} = P_m \cdot \eta_{\mathrm{gen}} \tag{36}$$

4.7 Features of Simulation Software

To implement a simulation of a chemical process, such as the decomposition of a certain chemical species, it is necessary to examine and analyze some specific software.

Their functioning is based on the interaction among compounds involved during the considered process and some unit block (linked each other) chosen to develop the simulation.

The required input to build the simulation are based on the specification of chemical species involved during the process and their physical and chemical characteristics.

Consequently, it is necessary to choose a suitable layout (and so the blocks) to implement the process.[119-120-121]

The specification of output, as mass-flow rate, temperature, pressure, etc.., are elaborated by analysis techniques, while calculation of mass and energy balances, thermodynamic equilibrium, rate equations are based on mathematical model or empirical correlations that can be:[122-123]

- Already included in the software;
- Developed by users in Fortran languages or Excel Sheet and read by a calculator block tool.

The latter option is directly linked to a specific block and works according to input and output variables defined from users before the calculation. The input variables are processed according to mathematical model developed by users in the Excel or Fortran file. Eventually, results are re-directed in the simulation software and showed as output variables.

The software used in this work to simulate the pyrolysis of lignocellulosic biomass are Chemcad and Aspen plus. Both of them work according to logic showed in fig.28.

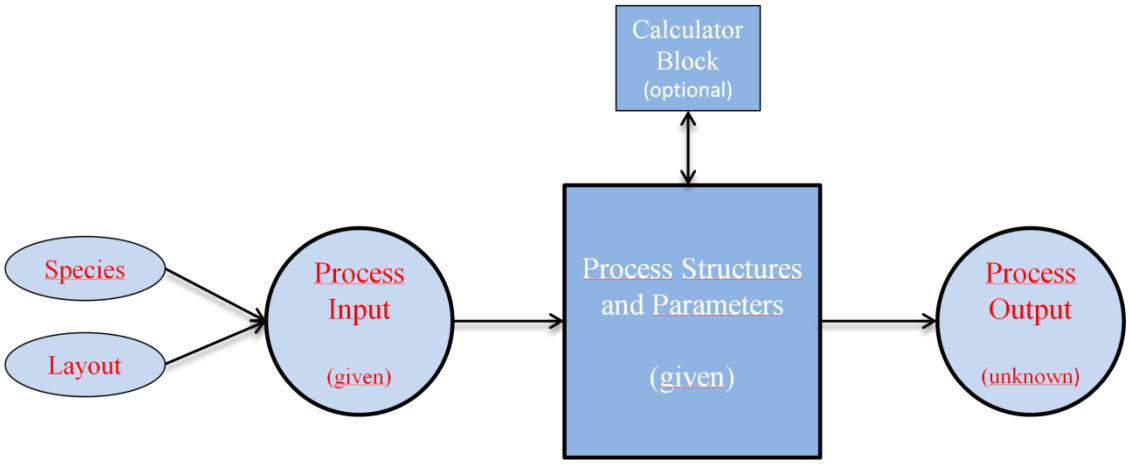

Fig.28 – Software Simulation Logic

The main problem is that a typical model able to simulate a wide range of biomass decomposition does not exist because of its variability on composition.[124-125] It is possible to overcome this issue by implementing an ideal model derived from experimental data or correlating the properties of the biomass with other data of gasification ones coal-kind. Moreover, both of software have the possibility to build an user-defined chemical species as *nonconvential-component*. Thanks to this tool, is possible to define the feedstock in accordance to its real composition and characteristics.[126]

In literature are developed many different way to simulate the thermo-chemical conversion by these softwares.

Benanti et al.[127] used a plug flow reactor set by kinetic parameter obtained from decomposition reactions of biomass to study the correlation between temperature and composition of final products obtained in a slow pyrolysis plant.

In the work of Fonseca et al.[128], fast pyrolysis is simulated by a Yield Reactor block able to evaluate a rigorous estimation of properties and heat capacity of products. Straw used as feedstock is built as a non-conventional solid based on experimental analysis.

The same process can be also simulated by two different reactor[129]: a Yield one, able to decompose the non-conventional fuel in conventional components, and a Gibbs one to simulate the decomposition reaction of obtained conventional components.

Also Adeniyi et al. [130] combined these two type of reactor to perform pyrolysis of Banana for bio-oil production. But in this case, the yield reactor is connected to a calculator block able to split the non-conventional component in pure component, instead the Gibbs one is utilized to calculate their chemical and phase equilibrium.

Moreover, simulation programs has many features that allow to perform these kind of processes. Usually the most utilized blocks are those showed in Tab.5:[127-1280-129-130-131-132-133-134-135-136]

Reactors		CHEMCAD	Aspen Plus
Stoich	Solve mass/energy balance for a single reaction. Requires specification of stoichiometry and extent of reaction or its conversion fraction. Can be specified also thermal model and key component. Kinetic of reaction is not required.	✓	✓
Gibbs	Estimates the extend of reaction based on free energy minimization. Need to specify P/T or P/H of the reactor. Reaction stoichiometry is not required.	✓	✓
Equil	Single/multiple reactions. Calculates equilibrium data or conversion for each reaction by solving stoichiometric chemical and phase equilibrium.	✓	✓
Kinetic	Accurate model using kinetic rate expression. During the input specification it is possible to choose between Plug Flow Reactor (PFR) or Continuous Stirred Tank Reactor (CSTR).	✓	✗
Plug	Rigorous model of PFR. A cooling stream around the reactor is optional. It is possible to model concurrent or countercurrent coolant streams. Need only the rate-based kinetic of reactions.	✗	✓
CSTR	Rigorous model of CSTR. Can be used when reaction kinetics are known and content of reactor has the same property of output.	✗	✓
Yield	Requires the specification of reaction yields for each component. Kinetic and stoichiometric are not necessary.	✗	✓

Tab.5 – Available Reactors

4.8 Economic Model

An economic analysis was conducted in order to evaluate the convenience of proposed technology.

It is based on a balance among capital costs, Operating costs and all the incomings earned from the obtained products. For the calculations, yearly working hours and estimated lifetime of the plant were assumed.

Payback time and revenues obtained during the lifetime period of the plant, were determined from this balance.

The Operating costs include the expenses for the personnel, the feedstock, all the O&M costs, the water treatment and the waste disposal. The electrical demand of the plant is completely supported by the CHP system, so these charges will be considered as avoided costs.

The revenues are obtained from the residual electrical energy sold to electrical grid, while the incomings from the sale of the produced pyrolysis oil and the revenues from the incentives for the high-efficiency CHP system (the White Certificate).

Moreover, another economic assessment of a plant can be determined by the Levelized Cost Of Electricity (LCOE), that represent the net present value of the unit-cost of electrical energy over the lifetime of a generating asset. This value is calculated as [137]:

$$LCOE = \frac{\sum_{t=1}^{n} \frac{C_t + O_t}{(1+r)^t}}{\sum_{t=1}^{n} \frac{E_t}{(1+r)^t}} \quad (37)$$

In which:

- t = considered year;
- n = plant lifetime;
- C_t = Capital Cost in year t;
- O_t = Operating Cost in year t;
- E_t = Electricity produced in year t;
- r = Discount rate;

5) CHEMCAD Simulations

First simulations were developed in Chemacad with the aim to have a preliminary prevision of the production of a pilot plant fed by olive-pits.

Feedstock properties and decomposition reactions are based on literature work,[127] instead the simulation layout is based on the pilot plant in Caltagirone. [87]

To implement the process, the first step was the definition of the chemical species involved in the decomposition.

A pseudo-component "Biomass", made up of carbon, hydrogen and oxygen and described in tab.6 and tab.7, was created as feedstock. The HHV of feedstock is calculated by [102]

$$\mathrm{HHV_B} = -0.763 + 0.301 \cdot 61.22 + 0.525 \cdot 6.16 + 0.064 \cdot 32.62 = 22.986 \left[\frac{\mathrm{MJ}}{\mathrm{kg}}\right] \quad (38)$$

Pyrolysis oil were simulated through n-propyl alcohol (C_3H_8O), a compound that has almost the same calorific value (≈29MJ/kg) instead char is considered as pure carbon-graphite.

Comp.	**Phormula**	**[C]**	**[H]**	**[O]**
Biomass	$C_{100}H_{120}O_{40}$	61.22%	6.16%	32.62%

Tab.6 – Feedstock Properties

Comp.	**PM**	***H/C***	***O/C***	***M %***	***HHV***
Biomass	1961.99	1.2	0.4	0.15	22.986

Tab.7 – Feedstock Properties

The layout of this simulation, is shown in fig.29. System is initially fed by 20 kg of feedstock that are directed into a dryer for the removal of moisture. The died feedstock is then directed to the pyrolysis reactor, the gas cooling and cleaning section, composed by a cyclone and a scrubber, and a two component separator. Moreover, two heat exchanger are used during the cycle to control the temperature of the process.

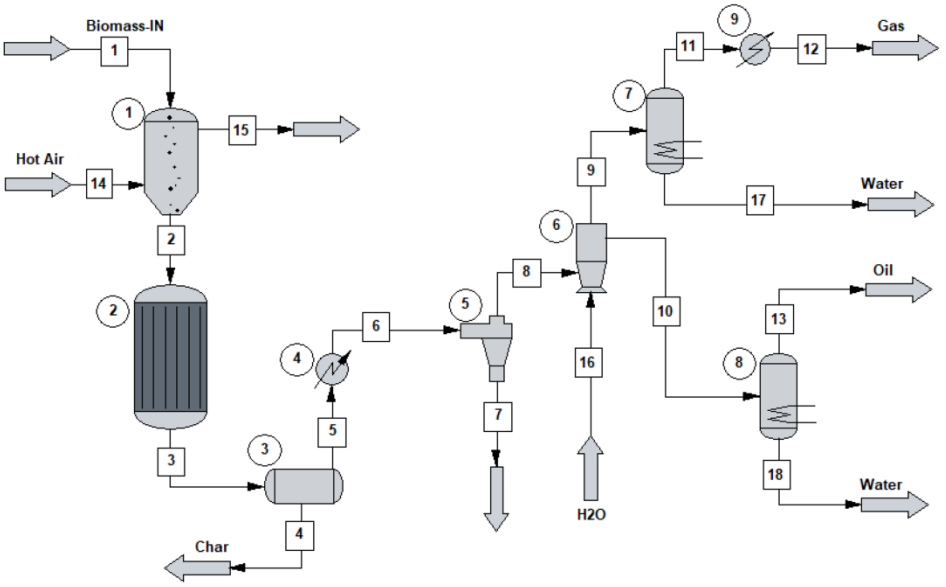

Fig.29 – Layout of first simulation

Conversion process is performed in a Kinetic-reactor, set on Plug-flow option, working at 500°C and fed by 17kg of daf biomass. The required input of this block [8] consists in the definition of the reactions 39 to 45 used to describes the degradation of biomass:

$$C_{100}H_{120}O_{40} \rightarrow 66.976C + 6.203C_3H_8O + 17.136H_2O + 9.734H_2 + 3.852CO + 6.404CO_2 + 4.159CH_4 \quad (39)$$

$$C + CO_2 \rightarrow 2CO \quad (40)$$

$$C + H_2O \rightarrow H_2 + CO \quad (41)$$

$$C + 2H_2 \rightarrow CH_4 \quad (42)$$

$$H_2O + CH_4 \rightarrow CO + 3H_2 \quad (43)$$

$$C_3H_8O \rightarrow 3C + H_2O + 3H_2 \quad (44)$$

$$6C_3H_8O + H_2O + 3H_2 \rightarrow CO + 3CO_2 + 14CH_4 \quad (45)$$

First one is a decomposition reaction that considers the most important species obtained from the degradation, the others are reactions commonly involved during the thermo-chemical conversion processes.

After the pyrolysis stage, char is separated by gravity, while the fluid fraction continue towards cooling and cleaning section, simulated by a cyclone and a scrubber, able to separate condensable product from permanent gas.

Quantity of water utilized by the scrubber is calculated as:

$$\dot{m}_w = \frac{\dot{m}_g \cdot c_{p,g} \cdot \Delta T_g}{c_{p,w} \cdot \Delta T_w} = \frac{10.01 \cdot 2.155 \cdot 270}{4.205 \cdot 70} = 19.8 \left[\frac{kg}{h}\right] \quad (46)$$

In which:

$\dot{m}_g$ = 10.01 [kg/h] is the mass flow of gas injected in the scrubbers;

$c_{p,g}$= 2.155 [kJ/kgK] is the specific heat of gas injected in the scrubbers;

$c_{p,w}$ = 4.205 [kJ/kgK] is the specific heat of water injected in the scrubbers;

$T_{i,w}$= 10 °C is the temperature of inlet water injected in the scrubbers;

$T_{i,g}$= 350°C is the inlet temperature of gas injected in the scrubbers;

$T_{f,g/w}$= 80°C is the final temperature of gas and water;

ΔT_g= 270°C (350-80) is the difference between initial and final temperature of the gas;

$\Delta T_{w,g}$= 70°C (80-10) is the difference between initial and final temperature of the water.

After this operation, two phase separators are used to isolate the gas and liquid products from processing water.

According to this layout the main products obtained at the end of the cycle are char, gas and oil, respectively in streams 4, 12 and 13.

Yield and compositions of the three final products are summarized in the Tab.8, and Fig.30 instead a comparison between these results and the production of literature plants [36-37-38-39-40-41-42-43-44-45] already described in paragraph 2.4 and in Appendix-A, is summarized in tab.9 and fig.31. This comparison shows an inappropriate distribution of product, stressed by an excessive production of char and an insufficient liquid production. Data obtained are the starting point that will be gradually improved with the next simulations.

Comp	T [°C]	CH_4	H_2O	CO_2	CO	C_3H_8O	H_2	C	**Tot [kg]**	**Yield [%]**
Char	500	0.00	0.00	0.00	0.00	0.00	0.00	6.95	**6.95**	**40.88**
Oil	75	0.00	2.20	0.00	0.00	2.30	0.00	0.00	**4.50**	**26.47**
Gas	65	0.58	0.48	2.44	0.93	0.95	0.17	0.00	**5.55**	**32.65**

Tab.8 – Product Composition and yield

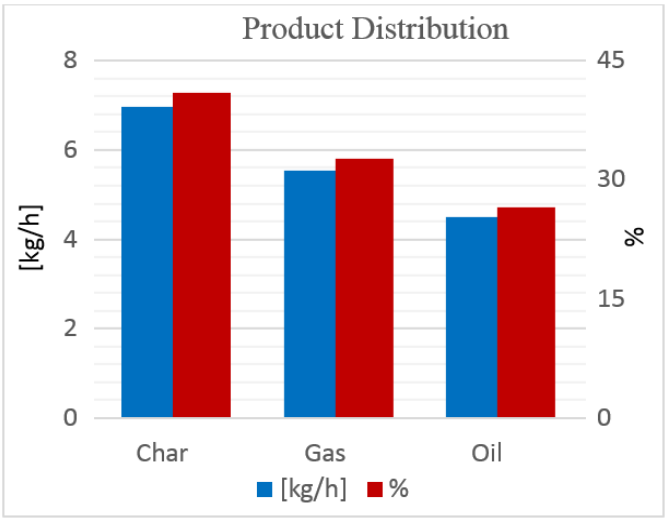

Fig.30– Diagram of obtained results

.Feedstock	Char	Liquid	Gas
Literature	29.81	41.36	26.26
Simulation	40.88	26.47	32.65

Tab.9 – Yields comparison

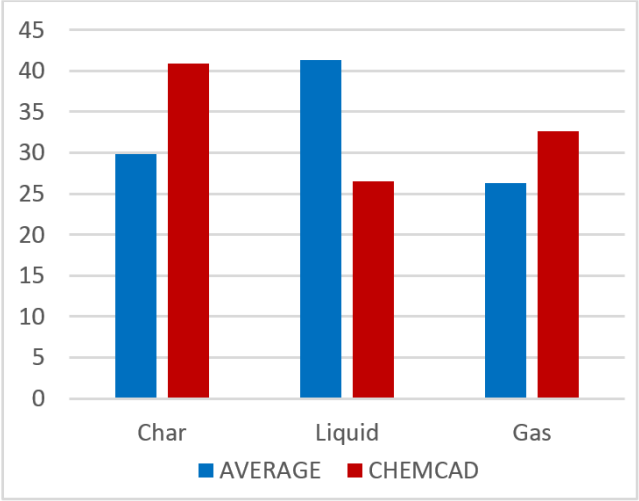

Fig.31– Yields comparison

Particularly, the procedure tried for this simulation shows two problems:

- Excessive out-put of carbonaceous product at the expense of the other two products;
- Low production of liquid obtained from gas condensation.

In spite of these obstacles, tools of CHEMCAD should be able to design an accurate pyrolysis model. K-Reactor, set-up with right parameters and reaction, should be able to deliver result very similar to the real ones.

5.1 Characterization of products

To evaluate the energetic potential of pyrolysis product, some characteristics of gas and oil were investigated.

Starting from molar composition of obtained gas, is possible to calculate the Heat Capacity (C_p) by Nasa Polynomial Methods [111] expressed in formula (47):

$$(c_p/R) = a_1 + a_2T + a_3T^2 + a_4T^3 + a_5T^4 \quad (47)$$

In which R is the universal gas constant, coefficients $a_{1..5}$ are tabulated in literature and defined for each component (see Appendix-B) and T represented the gas temperature.

Moreover, by formulas (48) and (49) [113], HHV of each gas component is calculated.

$$HHV = 0.303\,(C) + 1.423\,(H) \quad (48)$$

$$HHV = 0.305\,(C) + 1.423\,(H) - 0.154\,(O) \quad (49)$$

The same procedure was used to calculate HHV of oil, expressed by Formula (50) [102]:

$$HHV = 0.352\,(C) + 0.944\,(H) - 0.105\,(O) \quad (50)$$

In these formulas, (C), (H) and (O) represent the percentages of the carbon, hydrogen and oxygen of pure compound.

Correlating these values with weight percentage composition of total gas mixture, Authors calculate the total HHV.

Eventually, correlation between HHV and LHV is expressed by formula[30] (51).

$$LHV = HHV - h_v \cdot ((9H/100) + (M/100)) \quad (51)$$

In which:

h_v=2.26 MJ/kg is the heat of vaporization of water;

M is the moisture content of pyro-oil

Obtained results are summarized in tab.10:

Compound	**c_p [KJ/kg·K]**	**HHV [MJ/K]**	**LHV [MJ/K]**
Gas	1.69	16.35	14.32
Liquid	--	16.39	14.94

Tab.10 – Characterization of products

6) Preliminary Analysis by ASPEN Software

6.1 Simplified components simulation

Some preliminary simulations are developed for Cell, Hemicell and Lig components with the aim to understand and choose the best solution to recreate the decomposition process.
These are not pure compounds, so they are not included in Aspen Components Database; therefore, due to the tool of software to draw the molecular structure of new conventional solid, the components were created.[138] Figg.32 and 33 show respectively Cellulose and Hemicellulose molecules created in Aspen Plus. [139]

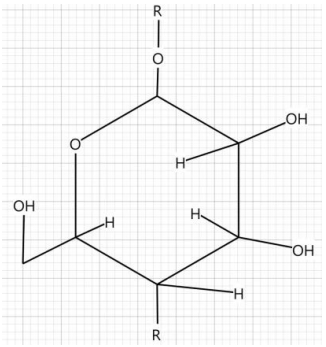

Fig.32 – Cellulose molecule

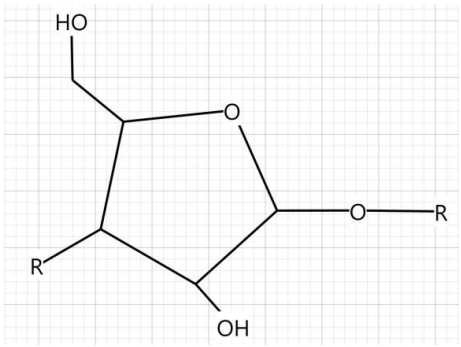

Fig.33 – Hemicellulose molecule

Because of the necessity to choose the most suitable block able to provide the right mechanism of decomposition, different type of reactors were tried.
The aim of this first part of the work is verifying the correct balance of the reaction. Since this is a strict constraint to implement the simulation, in this case a reactor is the only block used, whereas all the washing-gas and separation steps are omitted. In each simulation, a calculator block in Microsoft© Excel was used to implement the conversion process (fig.34).

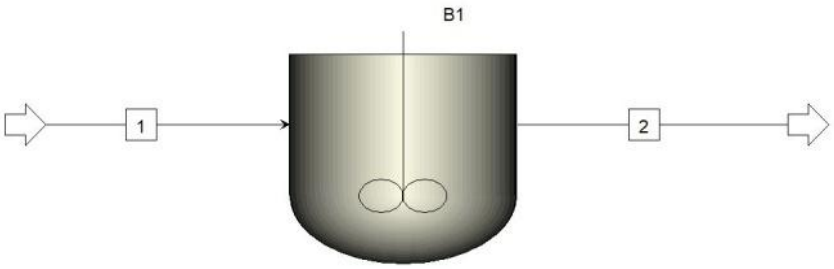

Fig.34 – Simplified layout to verify Cell, HC and Lig decomposition.

The reactions utilized to launch the reactor are:[140]

Reactant		Product
CELLULOSE DECOMPOSITION		
CELL	→	CELL-A
CELL-A	→	HAA + 0.2 Glyoxal + 0.2 C2H4O + 0.25 HMFU + 0.2 C3H6O + 0.22 CO2 + 0.16 CO + 0.1 CH4 + 0.01G{H2} + 0.83 H2O + 0.01 HCOOH + 0.61 Char
CELL-A	→	LVG
CELL	→	5 H2O + 6 Char
HEMICELLULOSE DECOMPOSITION		
HCE	→	0.4 HCE1 + 0.6 HCE2
HCE1	→	1.025 G{H2} + 0.025 H2O + 1.075 CO2 + 0.025 HCOOH + 1.1 CO + 0.3 CH2O + 0.125 C2H5OH + 0.25 G{CH3OH} + 0.625 CH4 + 0.25 C2H4 + 0.875 Char
HCE1	→	0.4 G{H2} + 0.25 H2O + 0.75 CO2 + 0.05 HCOOH + 0.7 CO + 0.15 G{CO} + 1.3 G{COH2} + 0.625G{CH4} + 0.375G{C2H4} + 0.675 Char
HCE1	→	XYLAN
HCE2	→	0.2 H2O + 0.425 CO2 + 0.55 G{CH4} + 0.275 G{C2H4} + 0.1 CH2O + 0.1 C2H5OH + 0.2 HAA + 0.025 HCOOH + 0.55 G{CO2} + 0.2 CO + G{COH2} + 0.325G{H2} + Char
LIGNIN DECOMPOSITION		
LIG-C	→	0.35 LIGCC + 0.1 COUMARYL + 0.08 PHENOL + 0.41 C2H4 + H2O + G{COH2} + 0.495 CH4 + 0.32 CO + 5.735 Char
LIG-H	→	LIGOH + C3H6O
LIG-O	→	LIGOH + CO2

LIG-CC	→	0.3 COUMARYL + 0.2 PHENOL + 0.35 HAA + 0.7 H2O + 0.65 G{CH4} + 0.6 G{C2H4} + G{COH2} + 0.4 G{CO} + 0.4 CO + 6.75 Char
LIG-OH	→	LIG + 0.15 G{H2} + 0.9 H2O + 0.5 CH3OH + 0.5 G{CH3OH} + 0.05 CO2 + 0.3 CO + G{CO} + 0.05 HCOOH + 0.6 G{COH2} + 0.45 G{CH4} + 0.2 G{C2H4} + 4.15 Char
LIG-OH	→	1.3 G{H2} + 1.5 H2O + 0.5 CO2 + 1.6 G{CO} + 3.9 G{COH2} + 1.45G{CH4} + 0.7 C2H4 + 10.15 Char
LIG	→	FE2MACR
LIG	→	0.95 H2O + 0.2 CH2O + 0.2 C2H4O + 0.4 CH3OH + CO + 0.2 C3H6O + 0.6 G・CH4・ + 0.65 G・C2H4・ + 0.05 HCOOH + 0.45 G{CO} + 0.5 G{COH2} + 5.5 Char
LIG	→	G・CH4・ + 0.5 G・C2H4・ + 0.4 G{H2} + 0.6 H2O + 0.4 CO + 0.4 CO2 + 0.2 G{CO} + 2 G{COH2} + 6 Char

Tab.11 – Scheme of reactions

Once the possibility to implement the reaction of the decomposition of Cell, Hemicell and Lig is confirmed, these processes have been combined to develop the simulation of the conclusive biomass. After this step, simulation with different type of reactor have been tested to find the final solution to implement this process.

6.2 Modeling of definitive feedstock

First of all, the three components need to be managed to obtain the correct mass percentage of biomass: starting from molecular weight of each component, coefficients are investigated to obtain the right weight distribution. [140]

Comp.	PM	Initial %wt	Coeff.	Final %wt
Cell	162.1424	11.5	8	31.40
Hemicell	132.1161	9.4	13	41.58
Lig	1116.112	79.1	1	27.02

Tab.12 – Correct distribution in final feedstock

In accordance with this distribution, feedstock composition and percentage of [C], [H] and [O] are calculated and compared with literature results:

Source	[C]	[H]	[O]
phyllis.nl #364	53.72	6.81	39.47
phyllis.nl #1327	50.4	6.43	43.17
phyllis.nl #1488	50.42	6.44	43.14
phyllis.nl #1824	46.59	6.04	47.37
phyllis.nl #1978	47.07	5.95	46.98
phyllis.nl #3494	51.12	6.27	42.61
Empirical data	51.3	5.94	42.06
Average	**50.1**	**6.3**	**43.6**

Tab.13 – Average of Literature Ultimate Analysis[101-118]

Comp	Coeff	[C]	[H]	[O]
Cell	8	48	80	40
Hemicell	13	65	104	52
Lig	1	57	63	23
Tot		170	247	115

Tab.14– Feedstock Composition

Comp	PM	Coeff	%wt
[C]	12.0107	170	49.43
[H]	1.0079	247	6.03
[O]	15.99	115	44.54

Tab.15 – Calculated Ultimate Analysis

Defined the Biomass structures and composition, its Higher Heating Value (HHV) can be calculated by Formula (52)[102] :

$$\mathrm{HHV_B} = -0.763 + 0.301 \cdot 49.43 + 0.525 \cdot 6.03 + 0.064 \cdot 44.54 = 20.13\ [\frac{\mathrm{MJ}}{\mathrm{kg}}] \quad (52)$$

Definitively, created feedstock has the characteristics resumed in tabb.16 and 17:

Comp.	Phormula	[C]	[H]	[O]	PM
Biomass	$C_{170}H_{247}O_{115}$	49.43	6.03	44.54	4130.76

Tab.16 – Biomass Characteristics

Comp.	H/C	O/C	Cell	HC	Lig	HHV
Biomass	1.453	0.67	31.40	41.58	26.02	20.13

Tab.17 – Biomass Characteristics

On the Aspen software packages many kind of reactors are available, diversifying each other depending on the treatment of inlet feedstock.
The kind of blocks investigated in this work are the *R-Stoich*, *R-CSTR* and *R-Yields* because they are the most utilized in literature to simulate the thermo-chemical conversion.

6.3 Continuous Stirred Tank Reactor (CSTR)

CSTR is able to work with multiple reactions and requires a knowledge of both stoichiometric coefficients and kinetic parameters for each of them. It was used to implement the first attempt but, because of some issues observed during the tests, the use of these blocks were shelved.
Eleven non conventional components have been defined in order to perform the reactions of decomposition already seen in tab.11.
Some of these have the same composition and structures:

- Cellulose and Active-Cellulose;
- Hemicellulose, Hemicellulose-1 and Hemicellulose-2;
- Lignin-C and Lignin-CC.

But, since the software is not able to read the same species in reactant and products, they have been created as different compounds. The ultimate analysis of this compounds are listed in tab.18.[141]

Compounds	Formula	H%	C%	O%	PM
CELL	$C_6H_{10}O_5$	44.446	6.216	49.338	162,1424
CELL-A					
HC	$C_5H_8O_4$	45.456	6.103	48.441	132,1161
HC-1					
HC-2					
LIG-C	$C_{15}H_{14}O_4$	69.757	5.464	24.779	258.274
LIG-CC					
LIG-H	$C_{22}H_{28}O_9$	60.542	6.466	32.992	436.459
LIG-O	$C_{20}H_{22}O_{10}$	56.872	5.25	37.878	422.389

LIG-OH	$C_{19}H_{22}O_8$	60.312	5.86	33.828	378.379
LIG	$C_{11}H_{12}O_4$	63.454	5.81	30.736	208.214

Tab.18 – Non conventional components

The layout of this simulation is showed in fig.35. Composition of initial feedstock (S1), showed in tab.19 was calculated in accordance with biomass specification.

The dryer (B1) is utilized for the removal of moisture, expelled in (S3), in order to obtain the daf materials (S2) to feed the reactor (B2).

Component		**wt%**		**Kg/h**	
CELL		31.4		9.421	30 **(daf Biomass)**
HC		41.58		12.473	
LIG	LIG-C	27.02	6.25	1.874	
	LIG-H		10.55	3.167	
	LIG-O		10.22	3.065	
H_2O		15		5.294	Moisture

Tab.19 –Feedstock Composition

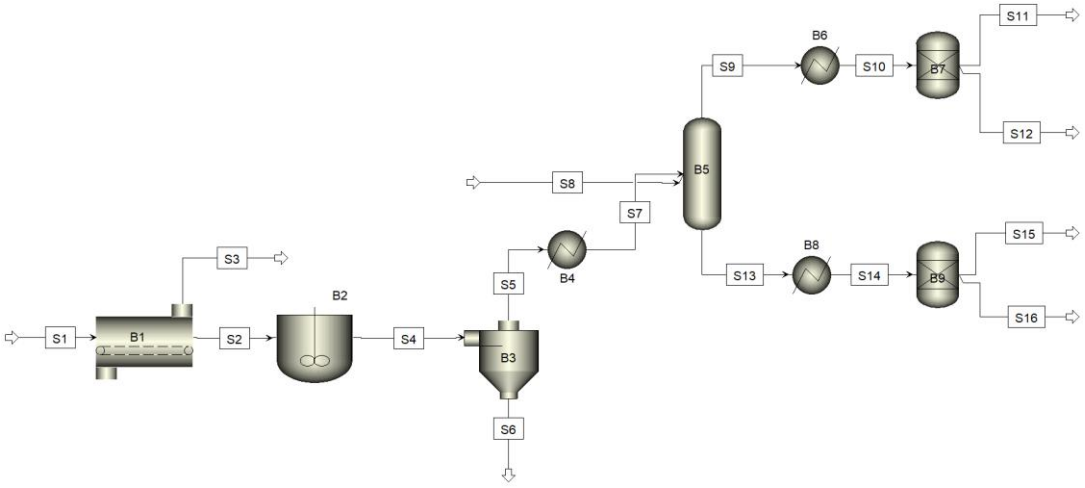

Fig.35 – Simulation Layout

The other non-conventional materials involved during the reactions and not specified yet during the process, can be directly defined in the reactor using the "component attribute" menu.

Reactions occurred in RCSTR can be defined by an Equilibrium balance or by their Kinetic, both calculated through a power-law.

During this simulation, all the reactions were defined by their kinetic, expressed as:[136]

$$k = T^n \cdot k_0 \cdot e^{-\frac{E}{RT}} \quad (53)$$

In which T is the temperature set in the reactor, so it is the same for each reaction, instead the exponent *"n"* is automatically set to 0 value by software.

After this block, char is removed by a cyclone (B3), while gas is firstly cooled due to an heat exchanger (B4) and then directed in the cleaning/washing section simulated by a distillation column (B5). Here, a water flow is injected from (S8) to decrease product temperature allowing separation between condensable product and permanent gas.

The two products leave this system (Gas in S9 and Liquid in S13) at ≈100°C so a further cooling, obtained by two heat exchanger (B6 and B8), is necessary to reach a final temperature around 65°C. Because the processing water is still mixed with them, after the cooling process, the two products are directed in two phase separator (B7 and B9), which is able to divide the desired fraction of water.

Simulation was firstly developed at 600°C and the reactions utilized to set the reactor are the same showed during the test of decomposition of CELL, HC and LIG. Kinetic parameters of the reaction 18 are showed in tab.20. Some pre-exponential factors (k_0) depend on temperature so both, k_0 law and its value at 600°C are showed, instead k is just showed at 600°C.[140]

Component	Reactions	k_0	k_0 – 600°C	Ea	k – 600°C
Cellulose	1	8E+13	8E+13	45000	1,626E+11
	2	1.00E+09	1.00E+09	30000	16045033
	3	4 · T	3.49E+03	10000	880,90496
	4	8.00E+07	8.00E+07	31000	1118429,5
Hemicellulose	5	1.00E+10	1.00E+10	31000	139803693
	6	3.00E+09	3.00E+09	32000	36544155
	7	0.15 · T	1.31E+02	8000	43,511523
	8	3 · T	2.62E+03	11000	575,66303
	9	1.00E+10	1.00E+10	33000	106138925
Lignin	10	4.00E+15	4.00E+15	48500	5,02E+12
	11	2.00E+13	2.00E+13	37500	1,142E+11

	12	1.00E+09	1.00E+09	2500	708671638
	13	5.00E+06	5.00E+06	31500	65249,571
	14	3.00E+08	3.00E+08	30000	4813510
	15	1.00E+02	1.00E+02	15000	12,666899
	16	8 · T	6.99E+03	12000	1337,5656
	17	1.20E+09	1.20E+09	30000	19254040
	18	0.25 · T	2.18E+02	8000	72,519205

Tab.20 – Kinetic parameters of decomposition reactions

After the reactor, the 4.3 %wt of char particles is entrained by gas and oversteps the cyclone. To calculate the amount of water ($\dot{m}_w$), injected in S8, it is necessary to find the $c_{p.g}$ of the gas mixture. Thanks to NASA method [111-142] all the $c_{p,n}$ of the 21 component of S7 flow has been calculated. Then, by the summation of each mass fraction (y_n) times $c_{p,n}$ of each species, value of $c_{p.g}$ is calculated. In the two values, subscript n indicates the considered compound.

$$c_{p,g} = \sum_{n=1}^{21} y_n \cdot c_{p,n} = 2.15 \ [\frac{kJ}{kg \cdot K}] \tag{54}$$

The water flow necessary to cool down the gas fraction allowing the separation is:

$$\dot{m}_w = \frac{\dot{m}_g \cdot c_{p.g} \cdot \Delta T_g}{c_{p.w} \cdot \Delta T_w} = \frac{23.8 \cdot 2.15 \cdot 250}{4.205 \cdot 75} = 40.68 \ [\frac{kg}{h}] \tag{55}$$

In which:

$\dot{m}_g$ = 23.8 [kg/h] is the mass flow of produced gas;

$c_{p.w}$ = 4.205 [kJ/kgK] is the specific heat of water injected in the scrubber;

$T_{i,w}$= 25 °C is the temperature of inlet water injected in the scrubber;

$T_{i,g}$= 350°C is the inlet temperature of gas injected in the scrubber;

$T_{f.g/w}$= 100°C is the final temperature of gas and water;

ΔT_g= 250°C (350-100) is the difference between initial and final temperature of gas;

ΔT_w= 75°C (100-25) is the difference between initial and final temperature of water;

Distribution of product obtained at the end of the cycle, are showed in fig.36:

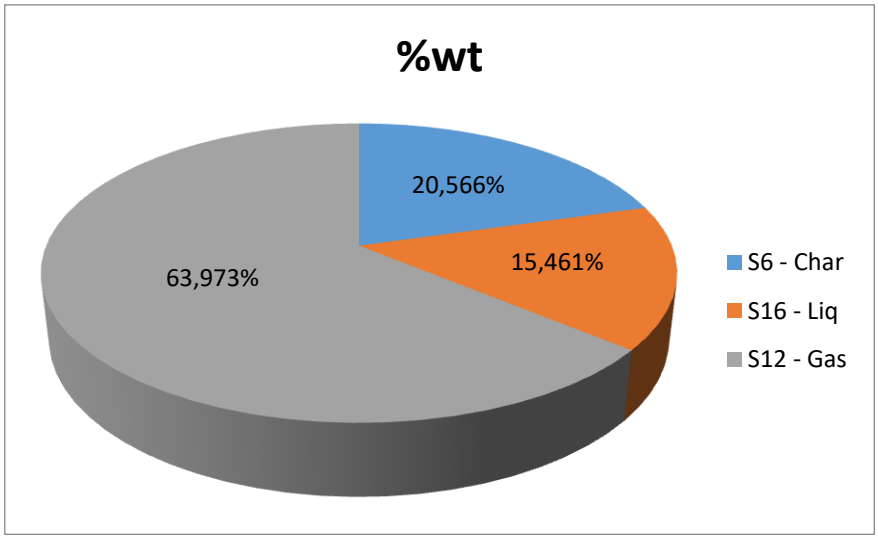

Fig.36 – Product Distribution

The chemical composition of each product is summarized in tab.21, tab.21 and tab.23:

Species	kmol/h	kg/h
Char	0,513684	6,169856
T [°C]	600	

Tab.21 – Char production (S6)

Species	kmol/h	%mol	kg/h	%wt
CO_2	7,77E-05	0,000653	0,00342	0,000737
HCOOH	0,000746	0,006262	0,034324	0,0074
HAA	0,04532	0,380518	2,721573	0,586753
H_2	7,07E-06	5,93E-05	1,42E-05	3,07E-06
CH_4	2,56E-05	0,000215	0,000411	8,87E-05
HMFU	0,004927	0,04137	0,621372	0,133964
LVG	3,19E-06	2,68E-05	0,000517	0,000111
C_2H_5OH	0,000916	0,007691	0,042199	0,009098
C_2H_4	2,38E-05	0,0002	0,000668	0,000144
Coumaryl	0,000144	0,001206	0,021565	0,004649
FE2MACR	1,06E-07	8,86E-07	2,2E-05	4,74E-06
Phenol	0,00018	0,001511	0,016938	0,003652

Xylosan	5,95E-07	4,99E-06	7,86E-05	1,69E-05
CH_3OH	0,001571	0,013187	5,03E-02	0,01085
CH_2O	0,000567	0,004761	0,017026	0,003671
C_3H_6O	0,001392	0,01169	0,080862	0,017433
C_2H_4O	0,000268	0,002246	0,011787	0,002541
Glyoxal	0,0005	0,0042	0,02903	0,006259
CO	8,03E-06	6,74E-05	0,000225	4,85E-05
Char	0,023081	0,193794	0,277224	0,059768
H_2O	0,039343	0,330337	7,09E-01	0,152808
Tot.	0,1191	1	4,638362	1

Tab.22 – Liquid production (S16)

Species	**kmol/h**	**%mol**	**kg/h**	**%wt**
CO_2	0,102529	0,077117	4,512282	0,235115
HCOOH	0,001469	0,001105	0,067599	0,003522
HAA	0,00114	0,000857	0,068438	0,003566
H_2	0,72664	0,546541	1,46482	0,076325
CH_4	0,117875	0,088659	1,891041	0,098534
HMFU	1,01E-09	7,57E-10	1,27E-07	6,62E-09
C_2H_5OH	0,004751	0,003574	0,218893	0,011406
C_2H_4	0,02859	0,021504	0,802067	0,041792
Coumaryl	1,95E-07	1,47E-07	2,93E-05	1,53E-06
FE2MACR	2,24E-13	1,69E-13	4,67E-11	2,43E-12
Phenol	9,94E-07	7,48E-07	9,36E-05	4,87E-06
CH_3OH	0,015528	0,011679	0,497539	0,025925
CH_2O	0,077401	0,058217	2,324057	0,121096
C_3H_6O	0,034494	0,025944	2,003395	0,104388
C_2H_4O	0,011151	0,008387	0,491222	0,025595
Glyoxal	0,008065	0,006066	0,468068	0,024389

CO	0,078151	0,058781	2,189044	0,114062
H_2O	0,121741	0,091567	2,193195	0,114278
Tot.	1,329526	1	19,19178	1
T [°C]	65			

Tab.23 – Gas production (S12)

Another test was developed at 800°C but product distribution and properties result were ver similar to this experiment.

This means that the process temperature does not significantly affect the kinetic of reactions and the formation and distribution of chemical species. As result, this kind of reactor was considerer unsuitable to simulate this kind of process.

6.4 Stoichiometric Simulation

Another test was developed with a block RStoich. It requires the knowledge of the stoichiometric of reaction, while kinetic parameter and other specifications are not needed.[136]

The developed process is similar to the one explained for the CSTR. The only differences are the choice of the reactor and the feedstock utilized in the system.

In this simulation cellulose, hemicellulose and lignin are just used to obtain a realistic material but they are not modeled and directly involved during the process. Instead, a non-conventional solid named “Biomass” was defined and modeled in accordance with the specification already explained in tabb.16 and 17 (paragraph 6.2) .

This solution takes to an arrangement of all the reactions, that have been combined in a single reaction of Biomass decomposition.

Consequently, the inlet stream (S1) is just fed by 30 kg of this material and 5 kg of water, that represents the 15% of moisture. The proposed layout is showed in fig.37.

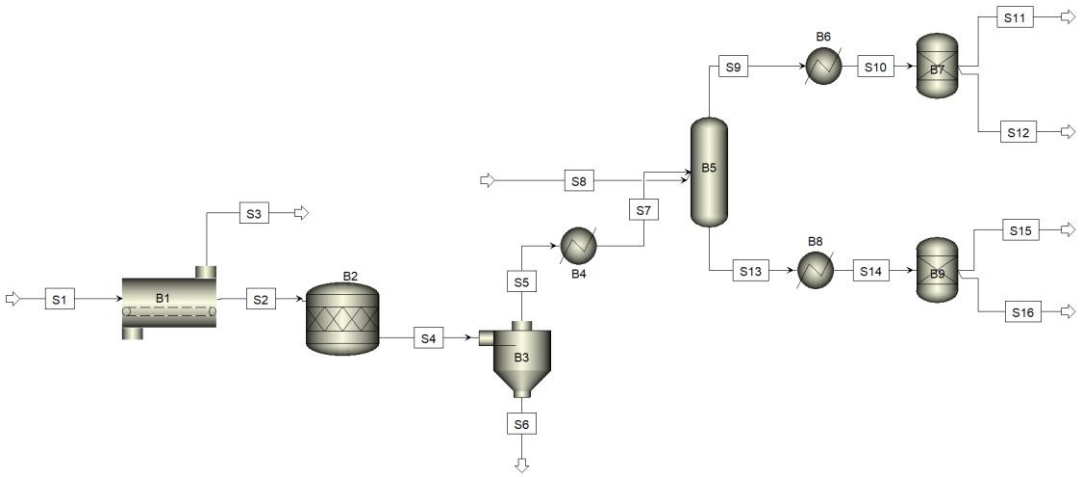

Fig.37 – RStoich Simulation Layout

Also this simulation was firstly performed with a reactor set at 600 °C.

After the moisture removal in (B1), the 30kg/h of daf feedstock are directed in the RStoich (B2). Reaction used to perform the biomass degradation is:

$$BIOM \rightarrow 12.1\ HAA + 2.05\ Glyoxal + 2.26\ C_2H_4O + 2.58\ HMFU + 3.06\ C_3H_6O + 13.27\ CO_2 + 8.98\ CO + 7.57\ CH_4 + 9.11\ H_2 + 17.41\ H_2O + 0.45\ HCOOH + 43.68\ Char + 0.001\ LVG + 13.64\ CH_2O + 1.06\ C_2H_5OH + 1.65\ CH_3OH + 3.18\ C_2H_4 + 0.001\ Xylosan + 0.4\ Coumaryl + 0.3\ Phenol + 0.65\ C_3H_4O_2 + 0.9\ FE2MACR + 0.2\ C_3H_6O_2 \quad (56)$$

After this block, ≈95.5%wt of char is removed by a cyclone, instead the remaining fraction isentrained by gas and directed towards the cleaning-gas system. Here, this mixture is firstly cooled through an heat exchanger and then directed in the cooling/washing section simulated by a distillation column. Here, a water flow ($\dot{m}_w$) is injected from (S8) to decrease the temperature of the mixture, allowing the condensable product separation from the permanent gas.

To calculate this value it is necessary to find the $c_{p.g}$ of the gas mixture. Thanks to NASA polynomial method all the 23 component of S7 flow has been calculated. [111-142] Then, by the summation of each mass fraction (y_n) times $c_{p,n}$ of each species, value of $c_{p.g}$ is calculated. In the two values, subscript n indicates the considered compound.

$$c_{p,g} = \sum_{n=1}^{23} y_n \cdot c_{p,n} = 1.298\ \left[\frac{kJ}{kg \cdot K}\right] \quad (57)$$

Once obtained this property, the quantity of water is calculated in accordance with mixture mass-flow and its properties,:

$$\dot{m}_w = \frac{\dot{m}_g \cdot c_{p.g} \cdot \Delta T_g}{c_{p.w} \cdot \Delta T_w} = \frac{25.75 \cdot 1.298 \cdot 250}{4.205 \cdot 75} = 27.3 \left[\frac{kg}{h}\right] \quad (58)$$

In which:

$\dot{m}_g$ = 25.75 [kg/h] is the mass flow of mixture;

$c_{p.w}$ = 4.205 [kJ/kgK] is the specific heat of water injected in the scrubber;

$T_{i.w}$= 25 °C is the temperature of inlet water injected in the scrubber;

$T_{i.g}$= 350 °C is the inlet temperature of gas injected in the scrubber;

$T_{f.g/w}$= 100 °C is the final temperature of gas and water;

ΔT_g= 250°C (350-100) is the difference between initial and final temperature of gas;

$\Delta T_{w.g}$= 75 °C (100-25) is the difference between initial and final temperature of water.

The product leaves this system at ≈100°C so a further cooling, obtained by two heat exchanger (B6 and B8), is necessary to reach a final temperature around 65°C.

Because processing water is still mixed with them, after the cooling the two products are directed in two phase separator (B7 and B9) able to divide the desired fraction of water.

Definitively, yields and characteristics of the three obtained products are resumed fig.38 and specified in tab.24, tab.25 and tab.26.

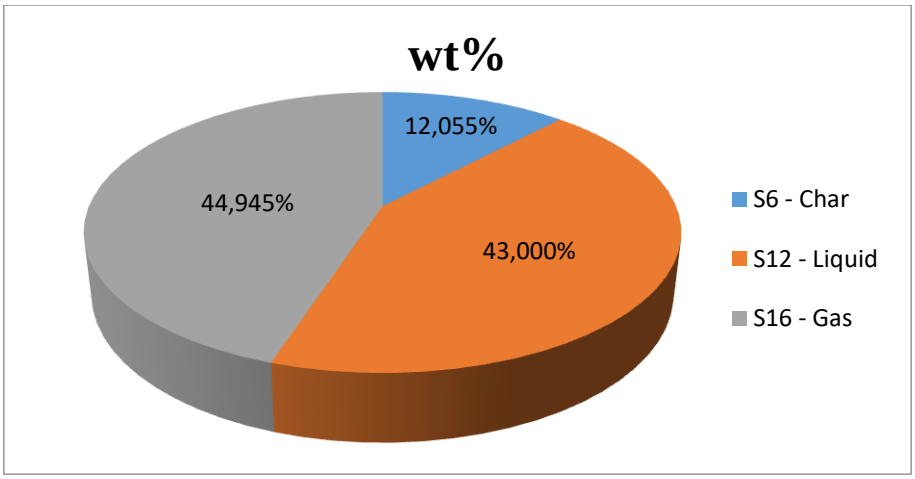

Fig.38 – Distribution of products

Compound	kmol/hr	mol%	kg/hr	wt%
Char	0.293876	1	3.529746	1
T	600	°C	873.15	K

Tab.24 – Characteristics of Char in Stream-6

Compound	kmol/hr	mol%	kg/hr	wt%
CO_2	0.093805	0.215282	4.128319	0.327887
HCOOH	0.000292	0.00067	0.013436	0.001067
HAA	8.62E-05	0.000198	0.005176	0.000411
CO	0.063792	0.146404	1.786846	0.141918
H_2	0.064742	0.148584	0.130512	0.010366
Glyoxal	0.008745	0.02007	0.50754	0.040311
CH_4	0.053738	0.12333	0.862111	0.068472
C_2H_4O	0.013203	0.030302	0.581648	0.046197
HMFU	1.91E-10	4.38E-10	2.41E-08	1.91E-09
C_3H_6O	0.015464	0.035489	0.898125	0.071333
CH_2O	0.091614	0.210256	2.75084	0.218482
C_2H_5OH	0.002026	0.004649	0.093327	0.007412
CH_3OH	0.005295	0.012152	0.169669	0.013476
C_2H_4	0.022492	0.051618	0.630976	0.050115
Coumaryl	1.34E-07	3.08E-07	2.01E-05	1.6E-06
Phenol	4.06E-07	9.33E-07	3.82E-05	3.04E-06
$C_3H_4O_2$	2.28E-05	5.23E-05	0.001644	0.000131
FE2MACR	6.35E-10	1.46E-09	1.32E-07	1.05E-08
$C_3H_6O_2$	0.000411	0.000944	0.030457	0.002419
Tot.	0.435729	1	12.59068	1
T	65	°C	338.15	K

Tab.25 – Characteristics of Gas in Stream-12

Compound	kmol/hr	mol%	kg/hr	wt%
CO_2	0.000543	0.002108	0.023914	0.001817
H_2O	0.083839	0.325207	1.510377	0.114769
HCOOH	0.002927	0.011355	0.134736	0.010238
Char	0.016616	0.064451	0.19957	0.015165

HAA	0.086096	0.333961	5.170261	0.392874
CO	5.43E-05	0.000211	0.001522	0.000116
H_2	5.51E-06	2.14E-05	1.11E-05	8.44E-07
Glyoxal	0.005889	0.022841	0.34175	0.025969
CH_4	9.50E-05	0.000368	0.001524	0.000116
C_2H_4O	0.002852	0.011062	0.125633	0.009547
HMFU	0.018292	0.070954	2.306847	0.175291
C_3H_6O	0.006278	0.024351	0.364608	0.027706
LVG	5.08E-06	1.97E-05	0.000824	6.26E-05
CH_2O	0.005359	0.020789	0.160924	0.012228
C_2H_5OH	0.005543	0.021501	0.255357	0.019404
CH_3OH	0.006424	0.024919	0.205839	0.015641
C_2H_4	0.000147	0.000569	0.004116	0.000313
Xylosan	3.74E-07	1.45E-06	4.94E-05	3.76E-06
Coumaryl	0.002843	0.011027	0.426939	0.032442
Phenol	0.00199	0.007718	0.187259	0.014229
$C_3H_4O_2$	0.004597	0.017832	0.331286	0.025173
FE2MACR	0.006397	0.024813	1.331909	0.101208
$C_3H_6O_2$	0.00101	0.003919	0.074849	0.005688
Tot.	0.257801	1	13.1601	1
T	65	°C	338.15	K

Tab.26 – Characteristics of Liquid in Stream-16

The second test was developed setting the reactor temperature at 800°C but product distribution and properties result almost the same. The only difference was a negligible fraction ($3.226 \bullet 10^{-3}$ [kg/h]) of char transferred from solid to liquid fraction.

This means that obtained results derived directly from stoichiometric coefficients of species involved in the reactions and they are not affect by other pyrolysis parameters, limiting the possibility for the user to manage the simulation.

Because of this issue, the use of this block was consider unsuitable to simulate this kind of process.

7) Conclusive Analysis

7.1 Yield Reactor

The conclusive simulation was developed by a Yield Reactor supported by a Calculator block.

It differs from the previously reactors because it does not require exact information about stoichiometry or kinetic. To use this equipment, users just need to specify the production yields of interested chemical species. Since this specification does not depend on the temperature of the process, the calculator block is employed because it is able to overcome this issue utilizing a distribution law defined by users for each compound. So, the matching of these two blocks provides a major possibility for the user to manage the formation of chemical species. Consequently their simultaneous utilization is employed to develop the definitive simulation of thermo-chemical conversion of biomass.[143]

Moreover, because the mixing gas flow leaving the reactor changes with temperature, a second calculator is used to set the amount of water needed in the scrubber for the condensation process.

Building and composition of feedstock and the first part of simulation (till the drying system) is the same as the one illustrated in stoichiometric simulation. So, non-conventional solid named “Biomass” is modeled in accordance with the specification already explained in tabb.16 and 17 (paragraph 6.2)

Furthermore, the layout, as presented in fig.39, is very similar to the previous ones, with the only exception for the type of Reactor and the presence of the two Calculator block:

- First one, named Reactor, directly linked to the R-Yield;
- Second one, named H_2O, connected to stream S8 and S7.

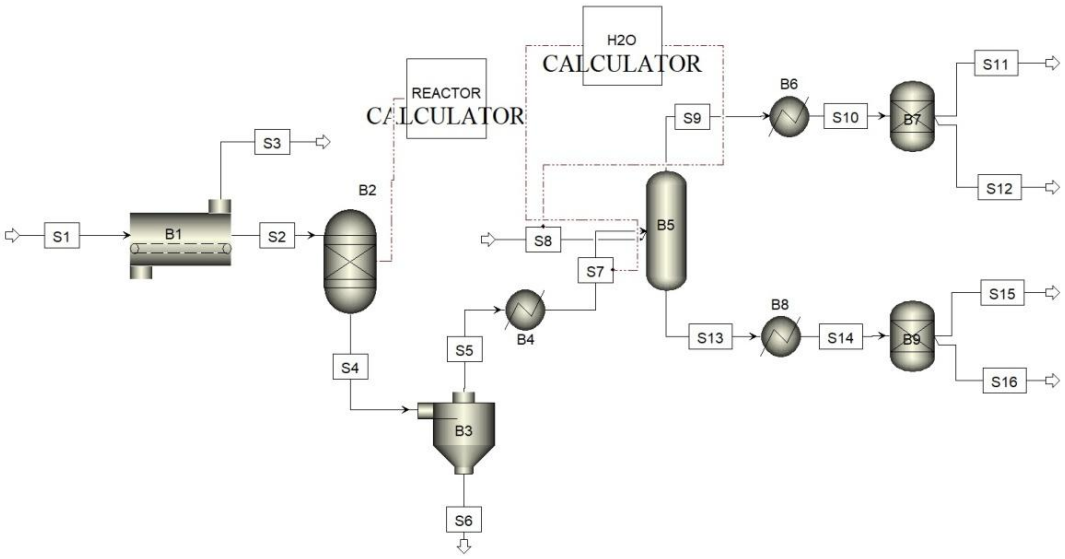

Fig.39 – Simulation Layout

Initial feedstock is made up of a 30 kg of biomass with 15% of moisture. Dryer (B1) is used to obtain the daf pre-heated material to feed the reactor.

The software processes the component that arrives in the reactor by the calculator. In this block one import variable and twenty-one export variables are defined, elaborated by a model specified by user in an excel sheet.

In this simulation the import variable is the process temperature sets during the specification of reactor operative condition, whereas export variables are all the chemical species involved during the thermo-chemical conversion.

The evolution of the compound during the conversion (m_x), in which x is the considered compound), is derived from empirical and literature[144-145-146-147-148] data used to develop this simulation and analyzed in a range of temperature between 500°C and 900°C. For this reason, available results and validation of model are considered reliable just in this range. The distribution law expressed in formula (59), is based on a combination between Arrhenius Equation and a Polynomial function of temperature.

$$m_x = k \cdot f(T) = \mathrm{k_0} \cdot \exp\left(-\frac{\mathrm{Ea}}{\mathrm{RT}}\right) \cdot a + bT + cT^2 \qquad (59)$$

Coefficients A, B and C (listed in tab.27) are obtained for each compound by a comparison among empirical and literature results.

Aspen-ID	**Compound**		**A_**	**B_**	**C_**
Glyco-01	$C_2H_4O_2$	HAA	7.12	- 0.01273	5.76E-06
Glyox-01	$C_2H_2O_2$	GLYOXAL	0.979	0.00115	- 1.62E-06

Aceta-01	C_2H_4O	ACETA	- 13.98	0.031	- 1.6E-05
5-hyd-01	$C_6H_6O_3$	HMFU	- 30.65	0.0688	- 3.7E-05
(+)-P-01	C_3H_6O	PROPILEN	1.61	- 0.00387	2.32E-06
Carbo-03	CO_2	C-DIOX	6.678	- 0.0105	4.84E-06
Carbo-02	CO	C-MON	- 14.48	0.03041	- 1.4E-05
Metha-01	CH_4	METHANE	5.204	- 0.0118	7.00E-06
Hydro-01	H_2	HYDROG	- 24.7	0.0482	- 2.1E-05
Water-01	H_20	WATER	10.86	- 0.01615	7.53E-06
Formi-01	CH_2O_2	FORMIC AC	- 45.05	0.107	- 5.8E-05
Carbo-01	C	CHAR	12.91	- 0.02248	1.02E-05
Levog-01	$C_6H_{10}O_5$	LVG	- 49191	109.97	- 0.05743
Forma-01	CH_2O	FORMALD	- 7.91	0.017824	- 9.44E-06
Ethan-01	C_2H_6O	ETHANOL	- 4.13613	0.007301	- 2.91E-06
Metha-02	CH_3OH	METHANOL	- 3.09	0.00718	- 3.87E-06
Ethyl-01	C_2H_4	ETHYLENE	4.14	- 0.01	6.03E-06
gluta-01	$C_5H_8O_4$	XYLOSAN	- 4345	8.31	- 0.00179
Ethyl-02	$C_9H_{10}O_2$	COUMARYL	- 27.89	0.0374	9.93E-06
Pheno-01	C_6H_6O	PHENOL	- 27.7	0.0273	3.83E-05
Benza-01	$C_{11}H_{12}O_4$	FE2MACR	90610	- 215.7	0.1285

Tab.27 – Coefficient for yield distribution

After the reactor, outlet products are directed in the cyclone (B3) where the gas-solid separation occurs. According to simulation results, cyclone efficiency slightly increases with temperature.

The quantity of water injected in scrubber by S8 depends on gas flow in S7 that in turn depends by the process temperature of the reactor. So, to guarantee the exactly quantity, water flow is defined as export variable of H_2O-calculator and it is obtained by an excel sheet according to relation:

$$\dot{m}_w = \frac{\dot{m}_g \cdot c_{p,g} \cdot (T_{fg} - T_{ig})}{c_{p,w} \cdot (T_{fw} - T_{iw})} \quad (60)$$

In which:

- $\dot{m}_g$ and $T_{i,g}$ are the gas flow and temperature of S7 and $T_{i,w}$ is the initial water temperature of S8. All of them are defined in calculator block as imported variables;
- $c_{p,g}$ is the specific heat of gas mixture in S7;

Moreover, the molar mass fraction of the 21 component of S7 flow has been added in the calculator block as imported variables in order to calculate $c_{p,g}$:

$$c_{p,g} = \sum_{n=1}^{21} y_n \cdot c_{p,n} \quad (61)$$

As in previous simulations, after the liquid-gas splitting, the processing water is still present in both of the flows and is separated at the end of the cycle by the two phase separators (B7 and B9).

Trend of char, liquid and gaseous fractions in relation to temperature are summarized in fig.40. Additionally, the evolution of each chemical species in the range 500 – 900°C, are summarized in figg.41,42,43 and 44.

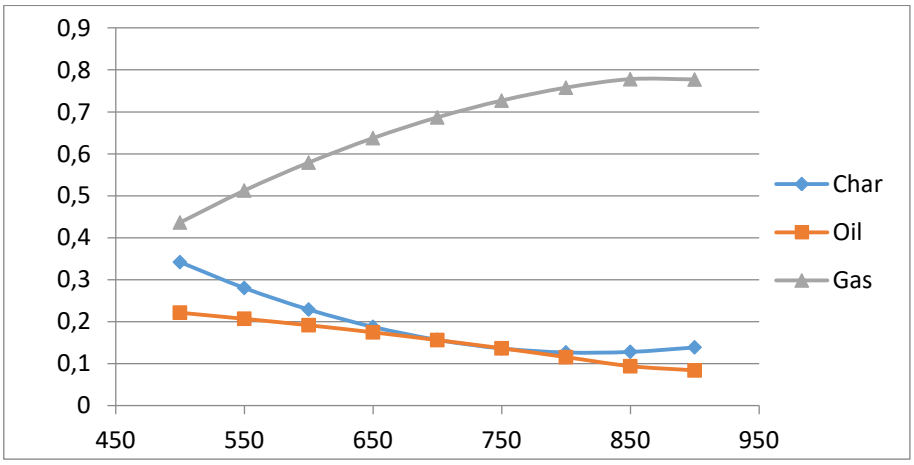

Fig.40 – Trend of Products

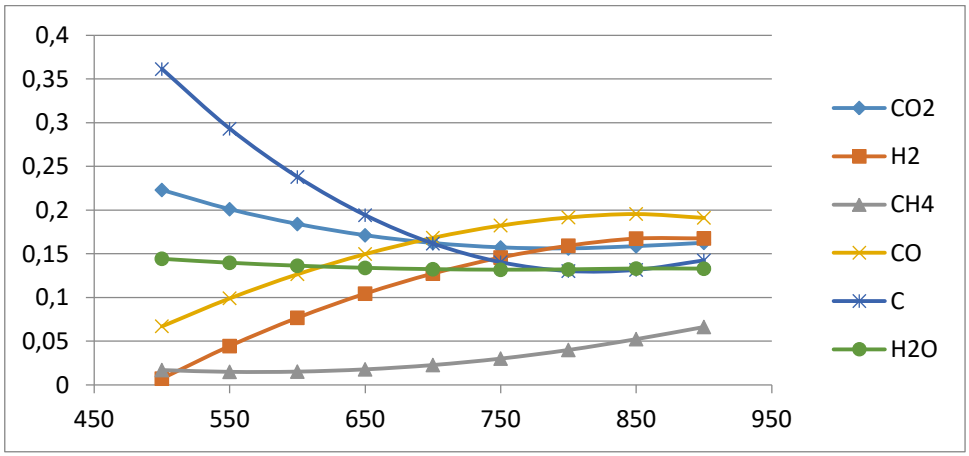

Fig.41 – Variation of the Chemical Species

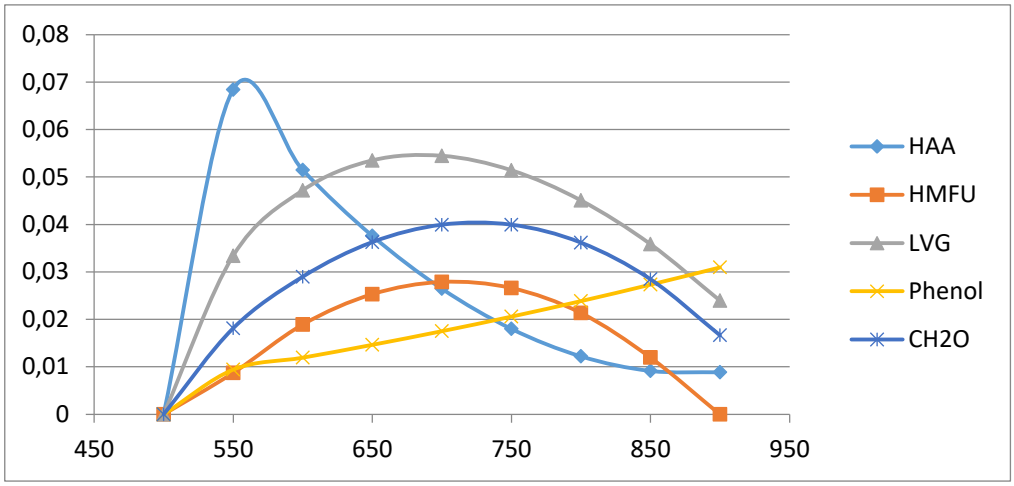

Fig.42 – Variation of Chemical Species

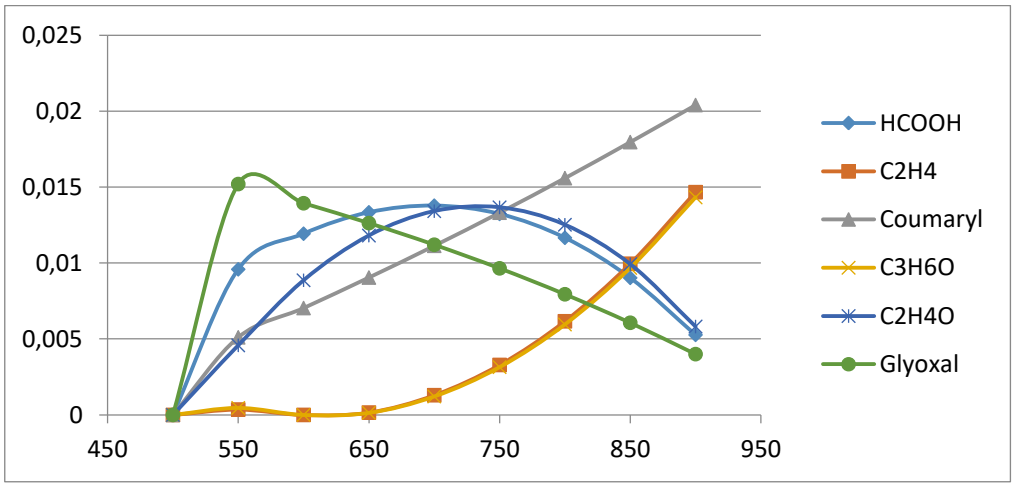

Fig.43 – Variation of Chemical Species

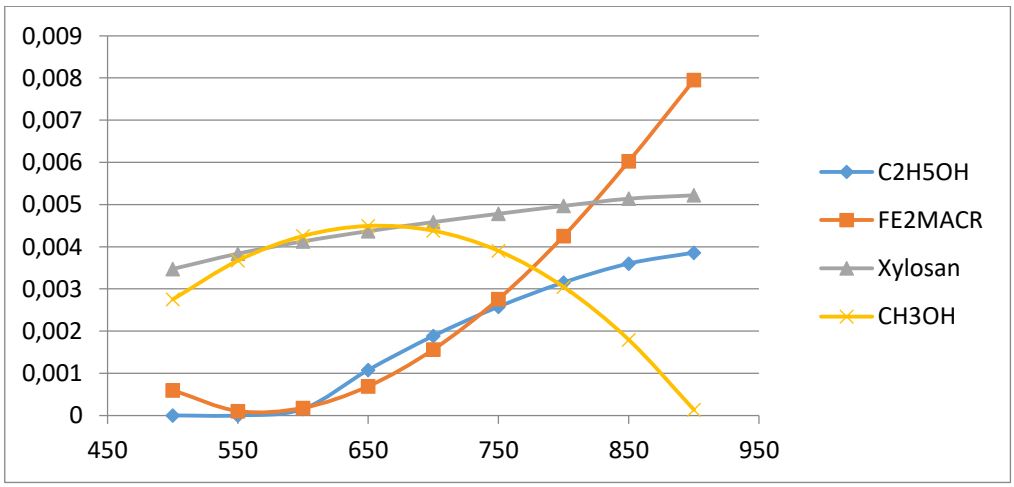

Fig.44 – Variation of Chemical Species

According to the obtained results, two different case studies, respectively at 600°C and 800°C, both with an energy recovery-line, are analyzed. According to the power obtained

from the exploitation of the produced gas, the most suitable solution is a Micro-CHP system, that is a cogeneration system with an electrical output power up to 100 kW_e. [118]

The calculation to estimate the possibility of electrical power production and the thermal power recycling are based on the *REC2-40G* proposed by Enerblu Industry[149], that is able to work with an output electrical power between 43 kW_e in full-load and 22 kW_e in half-load. Equipment specification will be showed in the specific paragraph in accordance with load needed for the recycling.

7.2 Case Study –pyrolysis at 600°C with energy recovery

The process developed at 600°C analyze the effective energetic production derived from the exploitation of biomass in the reactor and investigated the possibility to recover the heat generated from the combustion of the gaseous fraction in a CHP system to feed the process.

Composition of S4, obtained from Reactor Calculator Block using formula (59) for each product at considered temperature, is:

Compound	**kmol/h**	**%mol**	**kg/h**	**%wt**
CO_2	0.113002	4.933739	4.973201	16.57734
HCOOH	0.007832	0.34196	0.360484	1.201614
HAA	0.016926	0.739008	1.016463	3.38821
H_2	1.029328	44.94107	2.075002	6.916674
CH_4	0.025708	1.122422	0.412427	1.374757
HMFU	0.005422	0.236741	0.683818	2.279393
LVG	8.92E-03	0.389237	1.44551	4.818367
C_2H_5OH	9.08E-05	0.003966	4.19E-03	0.013951
C_2H_4	0.00015	0.006556	0.004212	0.014041
Coumaryl	1.63E-03	0.071083	0.244502	0.815008
FE2MACR	2.31E-05	0.00101	4.81E-03	0.016048
Phenol	0.004208	0.183739	0.39606	1.320201
Xylosan	8.44E-04	0.03686	1.12E-01	0.371795
CH_3OH	0.00359	0.156746	0.115035	0.383449
CH_2O	0.032636	1.424916	0.979944	3.266479

C_3H_6O	6.40E-05	0.002795	3.72E-03	0.012394
C_2H_4O	0.007244	0.316258	0.319102	1.063672
Glyoxal	0.005881	0.256759	0.341302	1.137673
CO	0.122239	5.337023	3.423961	11.4132
Char	0.535123	23.36381	6.427367	21.42456
H_2O	0.369539	16.1343	6.657352	22.19117
Total flow	2.290395	100	30	100

Tab.28 – S4 Composition

The cyclone separates ≈96% of char, corresponding at 6.19 kg/h, so the remaining fraction (23.81 kg/h) is the gas mixing flow that overcomes the cyclone and moves towards the scrubber.

The H_2O-calculator firstly defines the $c_{p,g}$ of total gas as:

$$c_{p,g} = \sum_{n=1}^{21} y_n \cdot c_{p,n} = 2.464 \left[\frac{kJ}{kg \cdot K}\right] \quad (62)$$

Then, the quantity of water needed for the gas mixture cooling in order to separate the condensable fraction from permanent gas is calculated as:

$$\dot{m}_w = \frac{23.81 \cdot 2.464 \cdot (350-100)}{4.205 \cdot (100-25)} = 46.5 \left[\frac{kg}{h}\right] \quad (63)$$

Distribution of product obtained at the end of the cycle, are showed in fig.45:

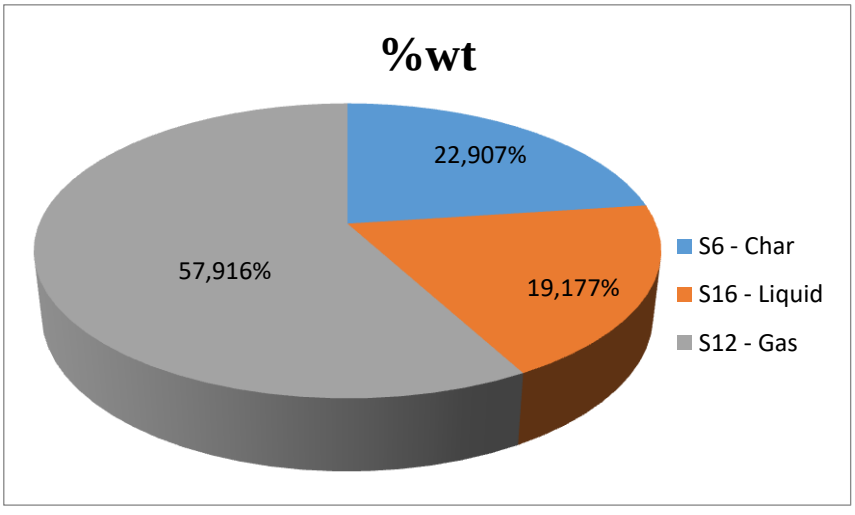

Fig.45 – Product Distribution

Instead composition of each product is reassumed in tab.29, tab.30 and tab.31:

Species	kmol/h	kg/h
Char	0.515457	6.191154
T [°C]	600	

Tab.29 – Char production (S6)

Species	kmol/h	%mol	kg/h	%wt
CO_2	8.56E-05	0.077119	3.77E-03	0.072681714
HCOOH	2.64E-03	2.376491	0.1214	2.342335503
HAA	0.016511	14.87621	0.99153	19.13099371
H_2	1.00E-05	0.009018	2.02E-05	0.000389319
CH_4	5.59E-06	0.005039	8.97E-05	0.001730995
HMFU	5.42E-03	4.885436	6.84E-01	13.19387333
LVG	8.92E-03	8.032371	1.45E+00	27.89028459
C_2H_5OH	1.47E-05	0.013229	6.76E-04	0.013051463
C_2H_4	1.25E-07	0.000113	3.50E-06	6.76227E-05
Coumaryl	1.63E-03	1.464907	2.44E-01	4.711137169
FE2MACR	2.31E-05	0.020833	4.81E-03	0.092893203
Phenol	0.004185	3.770842	3.94E-01	7.599778886
Xylosan	8.44E-04	0.760656	1.12E-01	2.152071246
CH_3OH	3.30E-04	0.29713	0.010567	0.203882262
CH_2O	2.37E-04	0.213858	0.007127	0.137511754
C_3H_6O	2.48E-06	2.24E-03	1.44E-04	0.00278324
C_2H_4O	1.70E-04	0.152927	0.007477	0.144269434
Glyoxal	3.43E-04	0.30943	0.019932	0.384570695
CO	1.26E-05	0.011311	3.52E-04	6.78E-03
Char	0.019666	17.71919	0.236214	4.557607569
H_2O	0.049947	45.00165	0.899809	17.36130131
Tot.	0.11099	100	5.182844	100
T [°C]	65			

Tab.30 – Liquid production (S16)

Species	kmol/h	%mol	kg/h	%wt
CO_2	1,13E-01	7,533247	4,969434	31,74797
HCOOH	0,005195	0,346558	0,239085	1,527428
HAA	0,000415	0,0277	0,024933	0,159291
H_2	1,03E+00	68,67116	2,074982	13,25633
CH_4	2,57E-02	1,714741	0,412337	2,634279
HMFU	1,11E-09	7,39E-08	1,40E-07	8,93E-07
C_2H_5OH	7,62E-05	0,005081	0,003509	0,022417
C_2H_4	1,50E-04	0,010009	0,004209	0,026889
Coumaryl	2,21E-06	0,000147	3,31E-04	0,002118
FE2MACR	4,91E-11	3,28E-09	1,02E-08	6,53E-08
Phenol	2,31E-05	0,001542	2,18E-03	0,013899
CH_3OH	0,00326	0,217513	0,104468	0,667407
CH_2O	0,032399	2,161492	0,972817	6,214984
C_3H_6O	6,15E-05	0,004105	0,003574	0,022832
C_2H_4O	0,007074	0,471932	3,12E-01	1,990859
Glyoxal	0,005537	0,369426	3,21E-01	2,053121
CO	1,22E-01	8,154359	3,42361	21,87224
H_2O	0,154552	10,31099	2,784303	17,78793
Tot.	1.49891	100	15.65276	100
T [°C]	65			

Tab.31 – Gas production (S12)

7.2.1 Characterization of syngas

Before investigating the possibility to recover thermal energy from combustion, it is important to analyze both the physical property and the energy content of the obtained gaseous fraction.

Starting from the molar fraction of each compound, and utilizing the following steps, already seen in chapter 4.5, by formula (16) is possible to find the partial pressure of each compound.

Moreover, according to formula (64), the value of the total density of permanent gas (ρ_{pg}) is calculated by summation of all the partial density:

$$\rho_{pg} = \sum_{n=1}^{17} \rho_{p,n} = 0.376 \left[\frac{kg}{m^3}\right] \quad (64)$$

The same method used to calculate the $c_{p,g}$ of gas mixture before the condensation, is now utilized to obtain the specific heat of permanent gas ($c_{p,pg}$). The only difference is the number of species involved during the calculation, that is reduced at n=17. Anyway, by the summation of each mass fraction (y_n) times $c_{p,n}$ of all the species, is possible to obtain the total specific heat for permanent gas ($c_{p,pg}$).

$$c_{p,pg} = \sum_{n=1}^{17} y_n \cdot c_{p,n} = 2.972 \left[\frac{kJ}{kg \cdot K}\right] \quad (65)$$

To calculate both net and gross calorific values of gas, the procedure showed in paragraph 4.5 is used. Formulas used during the calculations are:

$$HHV = 0.303\,(C) + 1.423\,(H) \quad (66)$$

$$HHV = 0.305\,(C) + 1.423\,(H) - 0.154\,(O) \quad (67)$$

$$LHV = HHV - h_v \cdot ((9H/100) + (M/100)) \quad (68)$$

In which:

h_v = 0.0408 [MJ/mol] = 2.26 [MJ/kg] is the heat of vaporization of water;
M is the moisture content of gas and is considered as fraction of H_2O in the mixture.
Table 32 resumes all the calculation developed to obtain these properties:

Compound	**wt%**	**HHV_i [MJ/kg]**	**HHV*%wt**	**H wt%**	**LHV [MJ/kg]**
CO2	31.74796838			0	
HCOOH	1.527427534	3.484863	0.05322875	0.0668972	
HAA	0.159290735	13.5476	0.02158007	0.0106939	
H2	13.25633119	141.7	18.7842213	13.255805	
CH4	2.634278821	58.44511	1.53960718	0.6620032	
HMFU	8.92705E-07	18.39106	1.6418E-07	4.281E-08	
C2H5OH	0.022416555	29.23453	0.00655338	0.0029426	
C2H4	0.026888992	46.39468	0.01247506	0.0038642	
Coumaryl	0.002117773	28.22306	0.0005977	0.0001421	
Phenol	0.01389908	29.88074	0.00415315	0.0008931	

CH3OH	0.667407442	21.64749	0.14447695	0.0839744	
CH2O	6.214984207	13.5476	0.84198099	0.41724	
C3H6O	0.022832456	29.49608	0.00673468	0.0023774	
C2H4O	1.990859477	24.0609	0.47901868	0.1821969	
Glyoxal	2.053120692	9.075631	0.18633367	0.0713115	
CO	21.87224179	10.1	2.20909642	0	
H2O	17.78793392			1.9903614	
Mixture			**24.2900581**	**16.750703**	**20.48096**

Tab.32 – Calorific Values of Permanent Gas

Definitively, all gas properties are resumed in tab.33

Compound	**kmol/h**	**kg/h**	**Vol [m^3]**	**ρ_{pg}**	**$c_{p,pg}$**	**HHV**	**LHV**
S12 – Gas	1.5	15.65	41.59	0.376	2.972	24.29	20.48

Tab.33 – Properties of Produced gas

7.2.2 Energy Recovery

Available power of obtained gas is the product between the mass flow and the LHV:[150]

$$P_g = 15.65 \cdot 20.48 = 320.512[\frac{MJ}{h}] = 89.03\ [kW] \quad (69)$$

According to this value, the REC2-40G works at 53.75% of load and, in accordance with efficiencies specified in data sheet[149], electrical and thermal power should be:

Initial Power	**Efficincy**	**Final Power**
P_g = 89.03 [kW]	η_{el} = 26.3%	P_{el} = 23.42 [KW_{el}]
P_g = 89.03 [kW]	η_{th} = 58,5%	P_{th} = 52.04 [KW_{th}]

Tab.34 – Theoretical Production

Balances used for power generation are based on the scheme proposed in fig.46. [151]

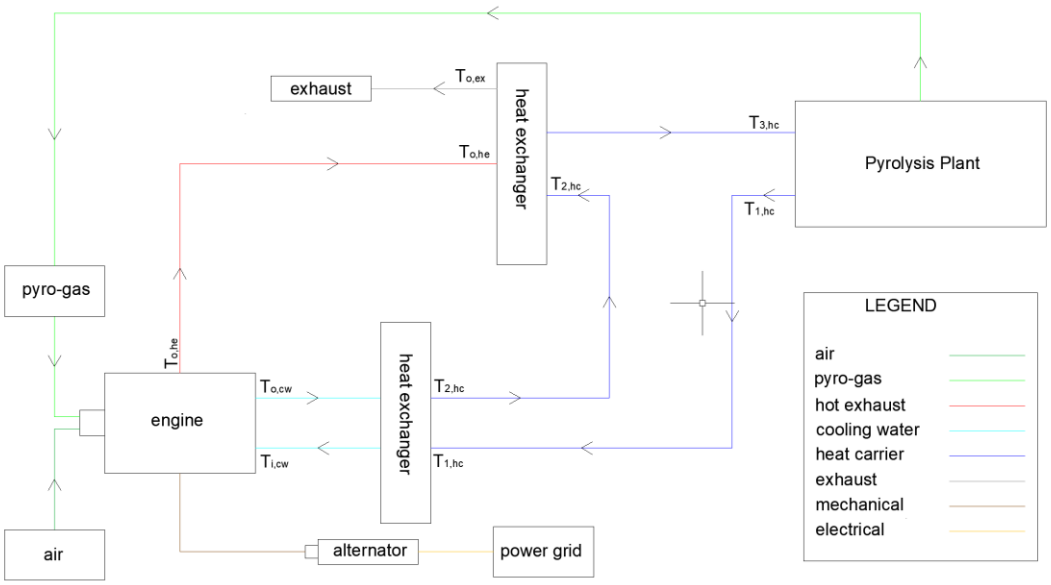

Fig.46 – CHP system cycle

At first, the right A/F ratio is investigated. The mass of oxygen necessary for a complete combustion of pyro-gas is calculated as:[115]

$$m_{O2} = \left(0.4647 \cdot \left(\frac{2 \cdot 15.9994}{12.0107}\right)\right) + \left(\frac{0.1383}{4} \cdot \left(\frac{2 \cdot 15.9994}{1.0079}\right)\right) - 0.397 = 1.9392 \left[\frac{\mathrm{kg_{O2}}}{\mathrm{kg_{pyro}}}\right] \quad (70)$$

And consequently, stoichiometric air, necessary for the combustion, is obtained:

$$m_{air,stoich} = 4.774 \cdot 1.9392 = 9.258 \left[\frac{\mathrm{kg_{air}}}{\mathrm{kg_{pyro}}}\right] \quad (71)$$

According to literature studies, Excess Air Coefficient (λ) for this application can vary between 1.5 and 2.5. In this study the value 1.8 is assumed, so the definitive A/F ratio is: [20-116-152]

$$m_{air} = 9.258 \cdot 1.8 = 16.6644 \left[\frac{\mathrm{kg_{air}}}{\mathrm{kg_{pyro}}}\right] \quad (72)$$

By pyro-gas combustion, CHP-system can produce mechanical power that is converted to electrical power by an electric generator. Mechanical power is obtained by the difference between energy content of pyro-gas, thermal power produced and the losses occurred during the cycle.[118]

Power lost (P_l) due to mechanical friction, heat dispersed during the heat exchange, oil lubrication, and alternator efficiency is assumed as the 13% of total quantity, so is:

$$P_l = 89.03 \cdot 0.13 = 11.574\ [kW] \quad (73)$$

Thermal power is distributed between the exhaust gasses and the cooling water of engine. It is recovered and re-directed to pyrolysis plant by the two heat exchangers showed in fig.46.

Values of recovered thermal power are obtained from balances between cooling water and heat carrier and between exhaust gasses and heat carrier, respectively in formulas (74) and (75):

$$m_{cw} \cdot c_{p,cw} \cdot (T_{o,cw} - T_{i,cw}) = m_{hc} \cdot c_{p,hc1} \cdot (T_{2,hc} - T_{1,hc}) = 36.41\ [kW_{th}] \quad (74)$$

$$m_{he} \cdot c_{p,he} \cdot (T_{o,he} - T_{ex}) = m_{hc} \cdot c_{p,hc2} \cdot (T_{3,hc} - T_{2,hc}) = 15.56\ [kW_{th}] \quad (75)$$

Considering:

m_{cw} = 3384 [kg/h] = mass of cooling water;

$c_{p,cw}$ = 3.873 [kJ/kgK] = 1.076*10^{-3} [kWh/kgK];

$T_{0,cw}$ = 90 [°C] = cooling water temperature at the outlet of the engine;

$T_{i,cw}$ = 80 [°C] = cooling water temperature at the inlet of the engine;

$m_{he} = m_g + m_{air}$ = 276.45 kg/h = mass of exhaust gasses;

$c_{p,he}$ = 0.45 [kJ/kgK] = 1.25*10^{-4} [kWh/kgK];

$T_{0,he}$ = 550 [°C] = temperature of the hot exhaust at the outlet of the engine;

T_{ex} = 100 [°C] = temperature of the exhaust after heat exchanger;

m_{hc} = 5640 [kg/h] = mass of heat carrier;

$c_{p,hc1}$ = 3.873 [kJ/kgK] = 1.076*10^{-3} [kWh/kgK] = specific heat of heat carrier in first exchanger;

$c_{p,hc2}$ = 3.82 [kJ/kgK] = 1.061*10^{-3} [kWh/kgK] = specific heat of heat carrier in first exchanger;

$T_{1,hc}$ = 80 [°C] = temperature of the heat carrier entering in the first heat exchanger;

$T_{2,hcw}$ = 86 [°C] = temperature of the heat carrier after the heat exchange with cooling water;

$T_{3,hcw}$ = 88.6 [°C] = temperature of the heat carrier re-directed to the plant.

Once calculated all these values, it is possible to obtain mechanical power by formula (35):

$$P_{mec} = 89.03 - 36.41 - 15.56 - 11.57 = 25.49\ [kW] \quad (76)$$

The data sheet assumes that the efficiency of alternator as 91.2%, so electrical power produced is:

$$P_{el} = 25.49 \cdot 0.912 = 23.25\ [kW_{el}] \quad (77)$$

Established a negligible difference with the theoretical values showed in specs of equipment, the calculated results are considered to be reliable.

The Sankey diagram in Fig.47 illustrates the input and the output of energy flux for different thermal energy subsystems, normalized to 100%, coming from the combustion of the syngas in the micro-CHP system.

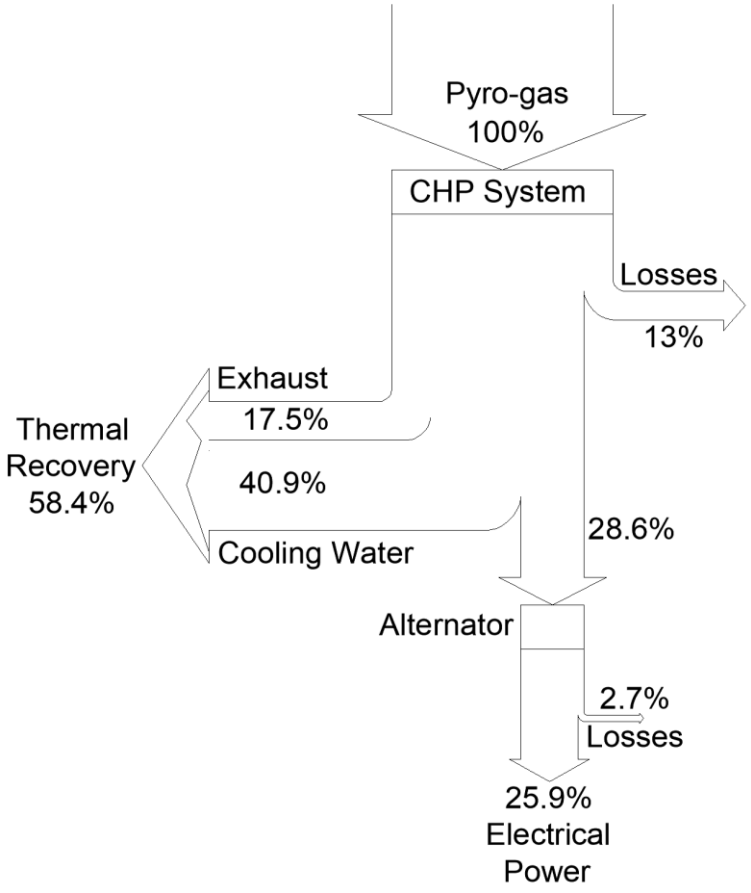

Fig.47 – Sankey diagram for case study at 600°C

7.3 Case Study –pyrolysis at 800°C with energy recovery

The process developed at 800°C analyze the effective energetic production derived from the exploitation of biomass in the reactor and investigated the possibility to recovery the heat generated from the combustion of the gaseous fraction in a CHP system to feed the process.

Composition of S4, obtained from Reactor Calculator Block using formula (59) for each product at considered temperature, is:

Compound	kmol/h	%mol	kg/h	%wt
CO2	0.097393	2.99871	4.286245	14.28748
HCOOH	0.005385	0.1658	0.247844	0.826146
HAA	0.004189	0.128977	0.251558	0.838526
H2	2.16926	66.79113	4.372967	14.57656
CH4	0.068515	2.109562	1.09917	3.6639
HMFU	0.002608	0.08029	0.328859	1.096196
LVG	6.07E-03	0.187036	0.984952	3.283173
C2H5OH	0.001879	0.057842	0.086546	0.288487
C2H4	0.009743	0.299986	0.273329	0.911095
Coumaryl	0.003285	0.101144	0.493327	1.644425
FE2MACR	5.61E-04	0.017274	1.17E-01	0.38937
Phenol	0.007979	0.245676	0.75094	2.503134
Xylosan	1.03E-03	0.031813	1.37E-01	0.455022
CH3OH	0.002612	0.08041	0.083681	0.278936
CH2O	0.026043	0.80185	0.781966	2.606554
C3H6O	0.004576	0.140909	2.66E-01	0.886008
C2H4O	0.006188	0.190543	0.272622	0.908741
Glyoxal	0.002871	0.088397	0.166622	0.555405
CO	0.187901	5.785441	5.263186	17.54395
Char	0.297766	9.168156	3.576465	11.92155
H2O	0.341965	10.52905	6.160602	20,53534
Total flow	3.247826	100	30	100

Tab.35 – S4 Composition

The cyclone separates ≈97.47% of char, corresponding at 3.49 kg/h, so the remaining fraction (26.51 kg/h) is the gas mixing flow that overcomes the cyclone and moves towards the scrubber.

The H_2O-calculator firstly defines the $c_{p,g}$ of total gas as:

$$c_{p,g} = \sum_{n=1}^{21} y_n \cdot c_{p,n} = 3.498 \left[\frac{kJ}{kg \cdot K}\right] \quad (78)$$

Then, the quantity of water needed for the gas mixture cooling in order to separate the condensable fraction from permanent gas is calculated as:

$$\dot{m}_w = \frac{26.51 \cdot 3.498 \cdot (350-100)}{4.205 \cdot (100-25)} = 73.5 \left[\frac{kg}{h}\right] \quad (79)$$

The distributions of product obtained at the end of the cycle, are showed in fig.48:

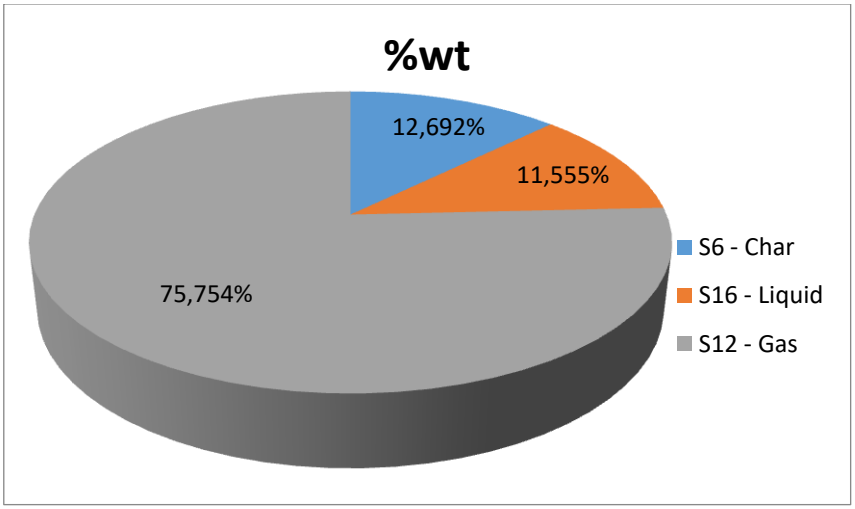

Fig.48 – Product Distribution

Instead composition of each product is reassumed in tab.36, tab.37 and tab.38:

Species	kmol/h	kg/h
Char	0.290223	3.485867
T [°C]	600	

Tab.36 – Char production (S6)

Species	kmol/h	%mol	kg/h	%wt
CO_2	8.26E-06	0.021464	3.63E-04	0.011451
HCOOH	2.45E-04	0.636238	0.011265	0.354976
HAA	0.00324	8.421775	0.194564	6.130782
H_2	2.44E-06	0.00635	4.92E-06	0.000155
CH_4	1.70E-06	0.004406	2.72E-05	0.000857
HMFU	2.61E-03	6.778361	3.29E-01	10.36242
LVG	6.07E-03	15.7903	9.85E-01	31.03614
C_2H_5OH	3.50E-05	0.091078	0.001614	0.050863

C_2H_4	9.12E-07	0.002372	2.56E-05	0.000807
Coumaryl	0.003232	8.400642	4.85E-01	15.29314
FE2MACR	5.61E-04	1.458262	1.17E-01	3.680663
Phenol	0.007489	19.46657	0.704802	22.20854
Xylosan	1.03E-03	2.685771	1.37E-01	4.301363
CH_3OH	2.66E-05	0.069131	0.000852	0.026852
CH_2O	2.10E-05	0.054619	0.000631	0.019881
C_3H_6O	1.96E-05	0.050866	1.14E-03	0.035813
C_2H_4O	1.60E-05	0.041485	0.000703	0.022154
Glyoxal	1.84E-05	0.047958	0.001071	0.03374
CO	2.21E-06	0.005735	6.18E-05	0.001947
Char	0.007543	19.60691	0.090598	2.854756
H_2O	0.006294	16.3597	0.113382	3.572702
Tot.	0.038471	100	3.173564	100
T [°C]	65			

Tab.37 – Liquid production (S16)

Species	**kmol/h**	**%mol**	**kg/h**	**%wt**
CO_2	9.74E-02	3.505002	4.285882	20.59914194
HCOOH	0.00514	0.185	0.236579	1.137062126
HAA	0.000949	0.034158	0.056993	0.273925665
H_2	2.17E+00	78.07438	4.372962	21.01767266
CH_4	6.85E-02	2.465883	1.099142	5.282782416
HMFU	5.64E-09	2.03E-07	7.12E-07	3.42072E-06
C_2H_5OH	0.001844	0.066353	0.084932	0.408206834
C_2H_4	9.74E-03	0.350632	0.273303	1.313570296
Coumaryl	5.32E-05	0.001915	0.00799	0.038401491
FE2MACR	1.30E-08	4.67E-07	2.70E-06	1.29981E-05
Phenol	0.00049	0.017644	4.61E-02	0.221752071

CH_3OH	0.002585	0.093037	0.082829	0.398096828
CH_2O	0.026022	0.936555	0.781335	3.755314949
C_3H_6O	4.56E-03	0.164009	0.264666	1.27205847
C_2H_4O	0.006173	0.222157	2.72E-01	1.306919849
Glyoxal	0.002853	0.102666	1.66E-01	0.795683709
CO	1.88E-01	6.762725	5.263124	25.29603902
H_2O	0.194988	7.017886	3.512771	16.88335526
Tot.	2.778449	100	20.80612	100
T [°C]	65			

Tab.38 – Gas production (S12)

7.3.1 Characterization of syngas

Before investigating the possibility to recover thermal energy from combustion, it is important to analyze both the physical property and the energy content of the obtained gaseous fraction.

Starting from the molar fraction of each compound, and utilizing the following steps already seen in chapter 4.5, by formula (16) is possible to find the partial pressure of each compound.

Moreover, according to formula (80), the value of the total density of permanent gas (ρ_{pg}) is calculated by summation of all the partial density:

$$\rho_{pg} = \sum_{n=1}^{17} \rho_{p,n} = 0.270 \left[\frac{kg}{m^3}\right] \quad (80)$$

The same method used to calculate the $c_{p,g}$ of gas mixture before the condensation, is now utilized to obtain the specific heat of permanent gas ($c_{p,pg}$). The only difference is the number of species involved during the calculation, that is reduced at n=17. Anyway, by the summation of each mass fraction (y_n) times $c_{p,n}$ of all the species, it is possible to obtain the total specific heat for permanent gas ($c_{p,pg}$).

$$c_{p,pg} = \sum_{n=1}^{17} y_n \cdot c_{p,n} = 4.060 \left[\frac{kJ}{kg \cdot K}\right] \quad (81)$$

To calculate both net and gross calorific values of gas, the procedure showed in paragraph 4.5 is used. Formulas used during the calculations are:

$$HHV = 0.303\,(C) + 1.423\,(H) \quad (82)$$

$$HHV = 0.305\,(C) + 1.423\,(H) - 0.154\,(O) \quad (83)$$

$$LHV = HHV - h_v \cdot ((9H/100) + (M/100)) \quad (84)$$

In which:

h_v = 0.0408 [MJ/mol] = 2.26 [MJ/kg] is the heat of vaporization of water;

M is the moisture content of gas and is considered as fraction of H_2O in the mixture.

Table 39 resumes all the calculation developed to obtain these properties:

Compound	**wt%**	**HHV_i [MJ/kg]**	**HHV*%wt**	**H wt%**	**LHV [MJ/kg]**
CO2	20,59914				
HCOOH	1,137062	3,484863	0,03962505	0,0498002	
HAA	0,273926	13,5476	0,03711034	0,0183899	
H2	21,01767	141,7	29,7820422	21,016839	
CH4	5,282782	58,44511	3,08752805	1,3275811	
HMFU	3,42E-06	18,39106	6,2911E-07	1,64E-07	
C2H5OH	0,408207	29,23453	0,11933737	0,0535846	
C2H4	1,31357	46,39468	0,60942668	0,1887729	
Coumaryl	0,038401	28,22306	0,01083807	0,0025773	
Phenol	0,221752	29,88074	0,06626116	0,0142494	
CH3OH	0,398097	21,64749	0,08617796	0,0500892	
CH2O	3,755315	13,5476	0,50875492	0,2521113	
C3H6O	1,272058	29,49608	0,37520734	0,1324491	
C2H4O	1,30692	24,0609	0,31445666	0,119605	
Glyoxal	0,795684	9,075631	0,07221332	0,0276366	
CO	25,29604	10,1	2,55489994		
H2O	16,88336			1,8891445	
Mixture			**37,6638797**	**23,253685**	**32,55252**

Tab.39 – Calorific Values of Permanent Gas

From a comparison with literature/empirical results, the obtained HHV and LHV are not considered to be reliable, so their values are estimated respectively 29.04 [MJ/kg] and 23.92 [MJ/kg]. Definitively, all gas properties are resumed in tab.40

Compound	kmol/h	kg/h	Vol [m^3]	ρ_{pg}	$c_{p,pg}$	HHV	LHV
S12 – Gas	2.78	20.81	77.10	0.270	4.060	29.04	23.92

Tab.40 – Properties of Produced gas

7.3.2 Energy Recovery

Available power of obtained gas is the product between the mass flow and the LHV:[150]

$$P_g = 20.81 \cdot 23.92 = 477.775[\frac{MJ}{h}] = 138.271\ [kW] \quad (85)$$

According to this value, the REC2-40G works at 95.73% of load and, in accordance with efficiencies specified in data sheet[149], electrical and thermal power should be:

Initial Power	Efficincy	Final Power
P_g = 138.271 [kW]	η_{el} = 29.5%	P_{el} = 40.79 [KW_{el}]
P_g = 138.271 [kW]	η_{th} = 62.5%	P_{th} = 86.42 [KW_{th}]

Tab.41 – Theoretical Production

Balances used for power generation are based on the scheme proposed in fig.49. [151]

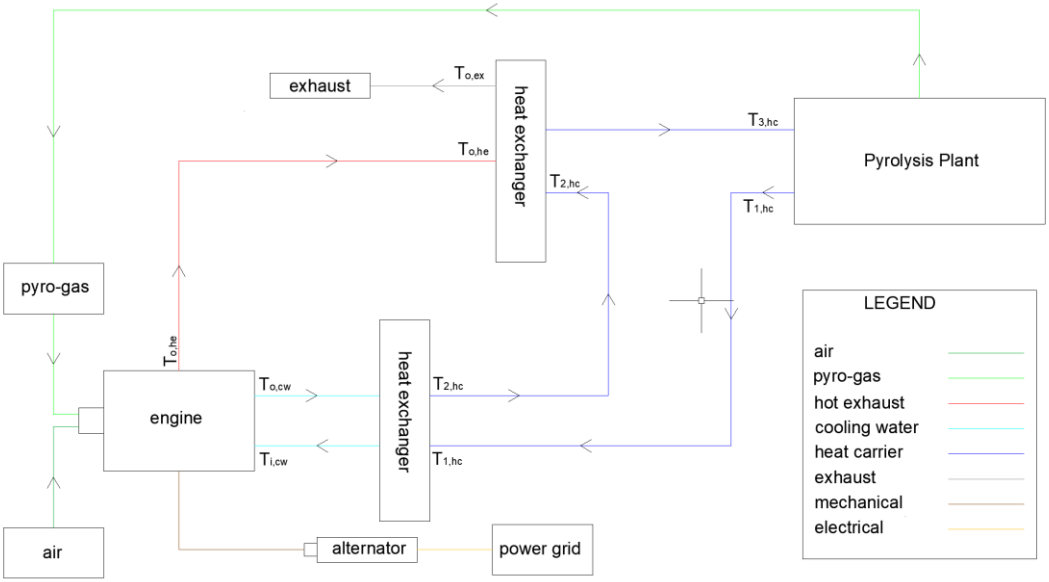

Fig.49 – CHP system cycle

At first, the right A/F ratio is investigated. The mass of oxygen necessary for a complete combustion of pyro-gas is calculated as:[115]

$$m_{O2} = \left(0.4647 \cdot \left(\frac{2 \cdot 15.9994}{12.0107}\right)\right) + \left(\frac{0.1383}{4} \cdot \left(\frac{2 \cdot 15.9994}{1.0079}\right)\right) - 0.397 = 1.9392\ \left[\frac{kg_{O2}}{kg_{pyro}}\right] \quad (86)$$

And consequently, stoichiometric air, necessary for the combustion, is obtained:

$$m_{air,stoich} = 4.774 \cdot 1.9392 = 9.258 \left[\frac{\mathrm{kg_{air}}}{\mathrm{kg_{pyro}}}\right] \quad (87)$$

According to literature studies, Excess Air Coefficient (λ) for this application can vary between 1.5 and 2.5. In this study the value 1.8 is assumed, so the definitive A/F ratio is: [20-116-152]

$$m_{air} = 9.258 \cdot 1.8 = 16.6644 \left[\frac{\mathrm{kg_{air}}}{\mathrm{kg_{pyro}}}\right] \quad (88)$$

By pyro-gas combustion, CHP-system can produce mechanical power that is converted to electrical power by an electric generator. Mechanical power is obtained by the difference between energy content of pyro-gas, thermal power produced and the losses occurred during the cycle.[118]

Power lost (P_l) due to mechanical friction, heat dispersed during the heat exchange, oil lubrication, and alternator efficiency is assumed as the 5% of total quantity, so is:

$$P_l = 138.271 \cdot 0.05 = 6.913\ [kW] \quad (89)$$

Thermal power is distributed between the exhaust gasses and the cooling water of engine. It is recovered and re-directed to pyrolysis plant by the two heat exchangers showed in fig.49.

Values of recovered thermal power are obtained from balances between cooling water and heat carrier and between exhaust gasses and heat carrier, respectively in formulas (90) and (91):

$$m_{cw} \cdot c_{p,cw} \cdot \left(T_{o,cw} - T_{i,cw}\right) = m_{hc} \cdot c_{p,hc1} \cdot \left(T_{2,hc} - T_{1,hc}\right) = 60.68\ [kW_{th}] \quad (90)$$

$$m_{he} \cdot c_{p,he} \cdot \left(T_{o,he} - T_{ex}\right) = m_{hc} \cdot c_{p,hc2} \cdot \left(T_{3,hc} - T_{2,hc}\right) = 25.94\ [kW_{th}] \quad (91)$$

Considering:

m_{cw} = 5640 [kg/h] = mass of cooling water;

$c_{p,cw}$ = 3.873 [kJ/kgK] = 1.076*10^{-3} [kWh/kgK];

$T_{0,cw}$ = 90 [°C] = cooling water temperature at the outlet of the engine;

$T_{i,cw}$ = 80 [°C] = cooling water temperature at the inlet of the engine;

$m_{he} = m_g + m_{air}$ = 367.60 kg/h = mass of exhaust gasses;

$c_{p,he}$ = 0.565 [kJ/kgK] = 1.57*10^{-4} [kWh/kgK];

$T_{0,he}$ = 550 [°C] = temperature of the hot exhaust at the outlet of the engine;

T_{ex} = 100 [°C] = temperature of the exhaust after heat exchanger;

m_{hc} = 9400 [kg/h] = mass of heat carrier;

$c_{p,hc1}$ = 3.873 [kJ/kgK] = 1.076*10^{-3} [kWh/kgK] = specific heat of heat carrier in first exchanger;

$c_{p,hc2}$ = 3.82 [kJ/kgK] = 1.061*10^{-3} [kWh/kgK] = specific heat of heat carrier in first exchanger;

$T_{1,hc}$ = 80 [°C] = temperature of the heat carrier entering in the first heat exchanger;

$T_{2,hcw}$ = 86 [°C] = temperature of the heat carrier after the heat exchange with cooling water;

$T_{3,hcw}$ = 88.6 [°C] = temperature of the heat carrier re-directed to the plant.

Once calculated all these values, it is possible to obtain mechanical power by formula (35):

$$P_{mec} = 138.27 - 60.68 - 25.94 - 6.92 = 44.74\ [kW] \quad (92)$$

The data sheet assumes that the efficiency of alternator as 91.2%, so electrical power produced is:

$$P_{el} = 44.74\ \cdot 0.912 = 40.80\ [kW_{el}] \quad (93)$$

Established a negligible difference with the theoretical values showed in specs of equipment, the calculated results are considered to be reliable.

The Sankey diagram in Fig.50 illustrates the input and the output of energy flux for different thermal energy subsystems, normalized to 100%, coming from the combustion of the syngas in the micro-CHP system.

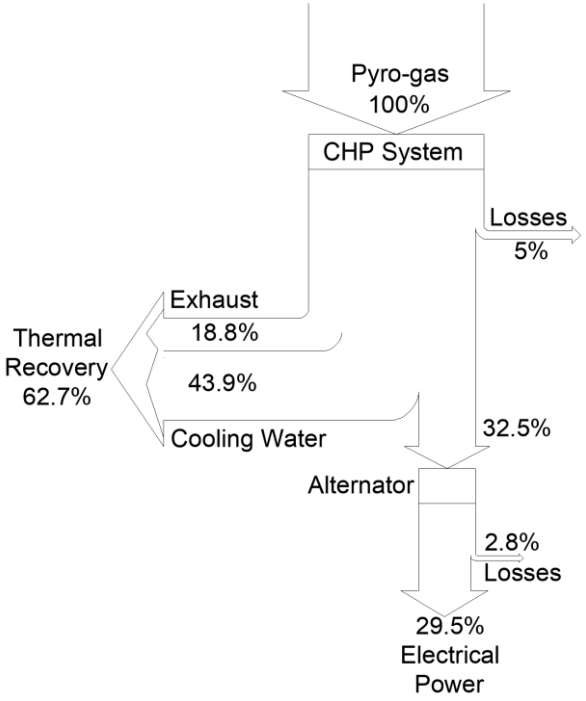

Fig.50 – Sankey diagram for case study at 800°C

7.4 Discussion

The proposed mathematical model causes a significant change in products yield and gas composition between 600°C and 800°C.

The char and oil fraction are reduced respectively from 23% and 20% to 13% and 12%, instead permanent gas reaches a 75% production rate.

Moreover, in the gaseous fraction, the distribution of the main compounds is very different between the two temperatures.

At 600°C, the predominant component is the CO_2 (over 30%) followed by CO with the 22% and H_2 is just the 13%.

At 800°C, CO becomes the component with the highest fraction (26%). Instead percentage of CO_2 decreases and H_2 increases, reaching both the ≈21%. The new component distribution results also in an increasing of calorific values of mixtures.

These changes positively affect the performances of the recycling system. Because of the increasing of quantity and energetic content of gas, the micro-CHP works near the full load that, in accordance with technical specifications, results in an increasing of overall efficiency. Indeed, thermal recovery and electric generation efficiencies vary respectively from 58.4% and 25.9 (η_{tot} = 84.3%) at 600°C to 62.7 and 29.5 (η_{tot} = 92.2%) at 800°C.

8) Economic Analysis

In order to assess the profitability of this process, an economic analysis was performed. However, the pilot-plant utilized as model in this work is designed only for research purposes, so it would be more appropriate and suitable carrying out this analysis basing it on a commercial-scale plant. During this study, all the technologies, the capital and operating costs and the obtained products have been adapted at the new scale.

To perform this analysis, a commercial-plant of 2 [MW_e] that works 7200 [h/y] was considered.

Moreover it must be considered that the lifetime of the plant must be taken into account when performing the calculations of the payback as part of the analysis for the determination of the convenience of the system. For a Biomass power plant with CHP system, a lifetime in a range between 30 and 45 years is estimated. [153]

8.1 Economic Balance

8.1.1 Capital Costs

The estimation of capital costs depends on the technology used during the process. A range of prices , expressed in [€/kW], can be used to assess the final cost, which is strictly connected to the plant size.

For thermo-chemical process with CHP system, an average price of 6,000 [€/kW] is considered.[154] So, the estimated capital costs of the plant is 12,000,000 €.

8.1.2 Operating Costs

Because of the lack of practical data regarding operating costs, this part of the analysis was based on a literature source. [155]

The original pilot-plant is fed by 30kh/h of agricultural residue. Adapting this value to the new plants ad considering a utilization factor of 7,200 h/year, the yearly feedstock used for the plant results 5,295 [t/year]. Assuming an average price of 20 [€/t], the yearly expenses for the feedstock result ≈106,000 €/y.

As regard personnel, four employees, with a 30,000 €/y salary per person are considered.

Other elements considered to calculate the O&M costs are the water treatment, the waste disposal and a 10% of capital cost for the general maintenance. All these values are resumed in tab.42:

Element	**Cost [€/y]**
Feedstock	106,000
Personnel	120,000
Water treatment	182,000
Waste Disposal	171,5000
Maintenance	60,000
Total	639,500

Tab. 42 – Operating Cost

Electrical consumption of the plant derives from the dryer, the reactor and the chiller, for a total amount of 756 [MWh/y]. Assuming an unitary cost of electrical energy of 170 [€/MWh] and considering the 7,200 h/y of utilization, the theoretical price for electricity should be 128,500 €/y. However, this amount is totally covered by the energy recovery system, so it can be considered as an avoided cost.

8.1.3 Revenues

An incoming is obtained from the sale of the pyrolysis oil produced during the pyrolysis stage. Scaling-up the value of the pilot plant in a commercial scale, the quantity of oil yearly produced is 659 t/y. Considering the energetic values of this product and a literature value of the selling price[156], yearly revenue derived from its sale is estimated 287,930 €/y.

The cogeneration system utilized for a commercial scale has different efficiency compared to the one showed in Chapter 7 and used for the pilot plant. For this reason, a different CHP system with a load power of 2.0 MW_{el} was chosen. To allow a proper comparison, also this model, named "REC2 2000 G", was chosen from EnerBlu catalogue. Moreover, using this model is possible to recover up to 2.1 MW_{th}.[157] Complete characteristics of this equipment are listed in the data-sheet, showed in details in the Appendix-D.

Considering the 7,200 working hours of the pant, total electrical and thermal power recovered are respectively 14,400 MWh_{el} and 15,120 MWh_{th}.

Part of the recovery energy is employed to feed the equipment of the plant, particularly: the heating zone (dryer and reactor) consumes approximately 540 [MWh/y] that can be supported by thermal recovery, instead the chiller, adapted to the new scale-plant, consumes

216 [MWh/y] hat can be supported by the electrical recovery. Definitively, the net power obtained from recovery system are 14,184 [MWh_{el}/y] and 14,580 [MWh_{th}/y]. The sale of the electrical energy remaining from the CHP production represent the main incoming of the plant. The sale cost depends of the Italian power exchange price and, to calculate the revenue, was assumed the average value between January and October 2019 [158]:

$$14{,}184\ \left[\frac{MWh_{el}}{y}\right] \cdot 65.32\ \left[\frac{€}{MWh}\right] = 926{,}500\ [\frac{€}{y}] \qquad (94)$$

Eventually, Italian D.M. 05/09/2011 decree establishes a form of incentives for high efficiency CHP-plant.[159] The amount of the revenue derived from primary energy saving expressed in tons of equivalent oil (toe) originated by the system. Each toe grants a White Certificate, that can be sold in the environmental market. According to literature data [137], this kind of plant can save 9,650 [MWh/y], which is equivalent to 1,161 toe/y and the actual value of a White Certificate is 276 €/toe. So, the final incoming obtained from the incentives is 320,436 €/y.

Considering the three revenues obtained, the total incoming per year are estimated:

$$287{,}930 + 926{,}500 + 320{,}436 = 1{,}534{,}866\ [\frac{€}{y}] \qquad (95)$$

8.2 Levelized Cost Of Electrcity (LCOE)

To calculate the LCOE, the lifetime period of the plant was generally considered between 15 and 20 ears. So, considering the capital costs of 12,000,000 € and a lifetime period of 20 years, the capital cost per year is 600,000 [€/y]. Definitively, considering the Net Electric Production per year and assuming the discount rate r=5 %, in accordance with formula (96) showed in paragraph 4.8, results:

$$LCOE = 87.4\ [\frac{€}{MWh_{el}}] \qquad (96)$$

8.3 Conclusions

Considering the capital investment as the starting point, the economic balance may consider just the operating costs and the total revenues during the years. From this analysis, the calculated payback time is between 14 and 15 years. Since the estimated lifetime for the plant is between 30 and 45 years[153], it can be consider an acceptable period for an industry. Figure 51 shows the economical trend and the accumulated profit of the plant in a period of 20 years.

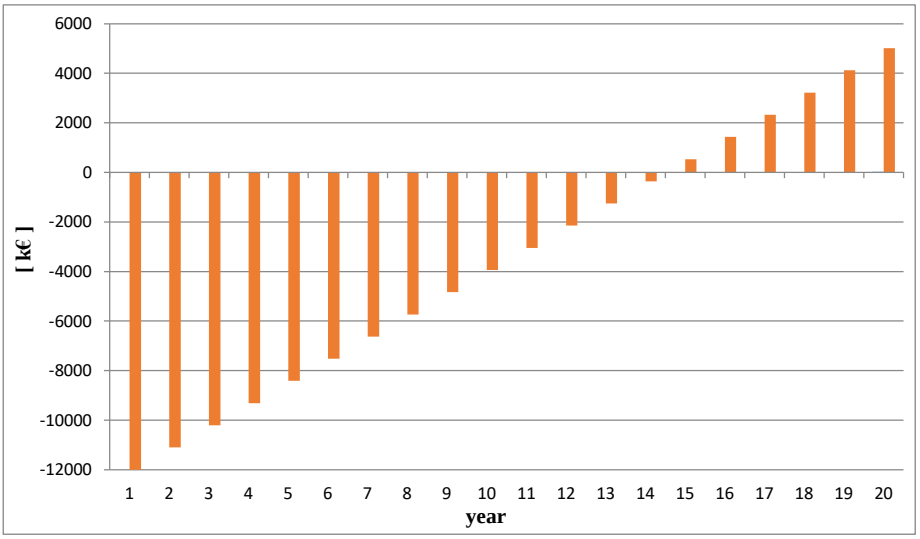

Fig.51 – Economical Trend

The results of LCOE are in line with literature values regarding Biomass plants [160], so it can be consider acceptable too.

Definitively, the economic evaluation of a Biomass pyrolysis plant supported by a CHP, scales-up to a commercial plants, results a profitable system for a lifetime longer than 15 – 20 years.

9) Conclusions

The main aim of this thesis is the develop of an accurate simulation model for describing the pyrolysis process of a biomass. The simulation should be able to predict the production yield and composition of products and to estimate the possibility to exploit them for energetic production.

9.1 Overall Observations

The layout and characteristics of simulations are based on a pilot plant fed by 30 kg/h of olive pits and some determined agricultural residues.
Feedstock and reactions used for first Chemcad simulation are based on a literature work in which the resulting oil is simulated by the n-propyl acid, instead syngas is just characterized by the most important components of the mixture. This means that a great number of compounds are not considered during the process. Moreover, the obtained results highlighted some inaccuracies:

- The independence from temperature in terms of both product yield and composition;
- An excessive out-put of carbonaceous product;
- Too low production of liquid obtained from gas condensation.

To solve these problems, other preliminary simulations were developed by Aspen software. Firstly, a correct distribution of cellulose, hemicellulose and lignin in the complete biomass was investigated and the average values of the ultimate analysis of the considered materials was used to perform a new simulation.
For the first test, cellulose, hemicellulose and lignin were directly utilized to feed a CSTR. To perform the thermo-chemical process, this block was set by a group of 18 reactions of decomposition of lignocellulosic compounds and their kinetic parameters.
The three main compounds were mixed together to assemble the definitive materials, named Biomass, included in the software library as “non-conventional” component. This latter was utilized to feed the stoichiometric reactor, performing the second attempt of simulation.
Yields and composition of products resulting from both tests show an independence from temperature. This gives rise to a limited possibility for the user to manage and check possible lacks found during the simulations.

To overcome these issues, a conclusive simulation, modeled by an Yield Reactor supported by a calculator block , was performed.

9.2 Final Results

The choice of yield reactor coupled with calculator block allows to operate on the evolution of products with temperature, improving the possibility to evaluate and check simulation results.

Within the considered range of temperature, permanent gas grows in accordance with temperature, whereas char and pyro-oil fractions decrease rapidly.

Moreover, a fast increasing of H_2 component, combined with the increasing of CO and CH_4 and a consequently drop of CO_2, significantly change composition and properties of pyro-gas.

Temperature has a positive effect also in cyclone efficiency: working at 800°C its efficiency increase of 1.5%, allowing a better separation of solid particles and a cleaner liquid product.

The observations about the micro-CHP section are more complicated. Efficiency of the system increases with load. It means that working near the full load results in a better conversion in terms of generated electric power and heat recovery.

The two analyzed study cases work respectively near the 50% and the 100% of load, for this reason there is a substantial difference in CHP performance. It should be interesting to evaluate the 600°C case coupled with a system able to work near the full load with the considered input. On the other hand, this system should not be able to work with a greater input as the one of 800°C, fixing some limitation in working condition of the overall process.

In conclusion, the choice of right CHP-system depends on the operative parameter of the plant: if it works every time at the same predetermined and standard temperature, it is possible to choose a suitable and matching system, otherwise a system able to work in a wide range of input values, even with reduced efficiencies, is the most suitable option.

9.3 Possible improvements

The proposed mathematical model is based on theoretical consideration. Empirical results obtained by experimental test could supply some information to improve the model by a dependence on other parameters such as heating rate, dimension of particles or residence time in the reactor.

Empirical results could also take some advantages for the distribution and the characterization of products, resulting in a most accurate simulation and prevision.

A further improvement could be obtained by the valorization of char product. It is mainly composed by carbon, so a combustion system might be considered in order to obtain thermal power able to support the process. It is also useful to minimizing the waste product of pyrolysis through their complete exploitation for energetic production.

References

[1] https://ec.europa.eu/clima/policies/strategies_en.

[2] https://ec.europa.eu/energy/en/topics/energy-strategy-and-energy-union/2050-energy-strategy.

[3] United Nation – Adoption of the Paris Agreement Proposed by the President, Conference of Parties, XXI Session, Paris, 12 December 2015.

[4] https://ec.europa.eu/clima/policies/ets_en.

[5] https://ec.europa.eu/clima/policies/strategies/2020_en.

[6] Communication from the Commission to the European Parliament, the Council, the European Economic and Social Committee and the Committee of the Regions, Energy 2020 – A Strategy for Competitive, Sustainable and Secure Energy, European Commission, Brussels, 10 November 2010.

[7] European Commission – Factsheet: Horizon 2020 budget, https://ec.europa.eu/programmes/horizon2020/sites/horizon2020/files/Factsheet_budget_H2020_0.pdf.

[8] Blesi, M., Kober, T., Bruchof, D., Kuder, R., "Effects of climate and energy policy related measures and targets on the future structure of the European energy system in 2020 and beyond", Energy Policy 38, 6278–6292, 22 July 2010.

[9] https://ec.europa.eu/clima/policies/strategies/2030_en#tab-0-1.

[10] European Council 23/24 October 2014 – Conclusions, Brussels, 24 October 2014.

[11] European Commission, Directorate-General for Energy in collaboration with Climate Action DG and Mobility and Transport, EU Energy and Trends to 2030 – update 2009, Luxembourg, Belgium, 04 August 2010, ISBN 978-92-79-16191-9.

[12] Buck, M., Graf, A., Graichen, P., “European Energy Transition 2030: The Big Picture – Ten Priorities for the next European Commission to meet the EU’s 2030 target and accelerate towards 2050”, Agora Energiwende, March 2019.

[13] European Commission, Communication from the Commission to the Council, the European Parliament, the European Economic and Social Committee and Committee of the Regions, Energy Roadmap to 2050 – Impact assessment and scenario analysis, Commission Staff Working Paper, Brussels 15 December 2011.

[14] European Commission, Directorate-General for Energy, Directorate-General for Climate Action and Directorate-General for Mobility and Transport, EU Energy, Transport and GHS Emission – Trends to 2050 – EU Reference Scenario 2016, 20 July 2016.

[15] Employment Effects of selected scenarios from the Energy roadmap 2050 – Final report for the European Commission (DG Energy), Cambridge Econometrics, Cambridge, UK, October 2013.

[16] Saxena, R.,C., Adhikari,D.,K., Goyal, H.,B., “Biomass-based Energy fuel through biochemical routes: A review”, Renewable and Sustainable Energy Reviews (13) 167-178, 2009.

[17] Basu, P., “Biomass Gasification, Pyrolysis and Torrefaction – Practical Design and Theory”, Elsevier, 2013.

[18] Vassilev, S.,V., Baxter, D., Andersen, L.,K., Vassileva, C.,G., “An overview of the chemical composition of biomass”, Fuel (89), 913-933, 2010.

[19] Shinya, Y., Yukihiko, M., “The Asian Biomass Handbook – A Guide For Biomass Production and Utilization – Support Project fro Building Asian-Partnership for Environmentally Conscious Agriculture, Entrusted by Ministry of Agriculture, Forestry, and Fisheries”, The Japan Institute of Energy, 2008.

[20] Quaak, P., Knoef, H., Stansen, H., “Energy from Biomass – A Review of Combustion and Gasification Technologies”, World Bank Technical Paper n°. 422, Energy Series, 1999.

[21] Ptasinski, K.,J., “Efficiency of Biomass Energy – An Exergy Approach to Biofuels, Power, and Biorefineries”, John Wiley & Sons, 2016.

[22] Wang, S., Luo, Z., “Pyrolysis of Biomass – Green Alternative Energy Resources – Volme 1”, De Gruyter, Science Press Bejing, 2017.

[23] Jawaid, M., Md Tahir, P., Saba, N., “Lignocellulosic Fibre and Biomass-Based Composite Materials – Processing, Properties and Applications”, Woodhead Publishing Series in Composites Science and Engineering, Elsevier, 2017.

[24] Wang, S., Dai, G., Yang, H., Luo, Z., “Lignocellulosic biomass pyrolysis mechanism: A state-of-the-art review”, Progress in Energy and Combustion Science (92), 33-86, 2017.

[25] Vyazovkin, S., “Thermogravimetric Analysis” in “Characterization of Materials”, Kufmann,E.,N., doi:10.1002/0471266965.com029.pub2 , October 2012.

[26] Carrier M., Loppinet-Serani, A., Denux, D., Lasnier, J.-M., Ham-Pichavant, F., Cansell, F., Aymonier, C., “Thermogravimetric analysis as a new method to determine the lignocellulosic composition of biomass”, Biomass and Bioenergy, 298-307, 2011.

[27] Dahlquist, E., “Technologies for Converting Biomass to Useful Energy – Combustion, Gasification, Pyrolysis, Torrefaction and Fermentation” in “Technologies for Converting Biomass to Useful Energy”, CRC Press, Taylor & Francis Group, 2013.

[28] Zhang, L., Xu, C.,C., Champagne, P., “Overview of recent advances in thermo-chemical conversion of biomass”, Energy Conversion and Management (51) 969-982, 2010.

[29] Wampler, T., P., “Applied Pyrolysis Handbook – Second Edition”, CRC Press, Taylor & Francis Group, 2007.

[30] Basu, P., “Biomass Gasification and Pyrolysis – Practical Design and Theory”, Elsevier, 2010.

[31] Zhou,C.,H., Xia, X., Lin, C.,X., Tong, D.,S., Beltramin, J., “Catalytic conversion of lignocellulosic biomass to fine chemicals and fuels”, Chem. Soc. Rev. (40) 5588-5617, 2011.

[32] Yin, W., Venderbosch, R.,H., Heeres, H.,J., " 8 – Recent developments in the catalytic hydrotreatment of pyrolysis liquids", Chapter 8 in "Direct Thermochemical Liquefaction for Energy Applycation", edited by Lasse Rosendahl, Woodhead Publishing Series in Energy (WP), Elsavier, Pages 249-292, 2018.

[33] Bridgwater, A.,V., "Review of fast pyrolysis of biomass and product upgrading", Biomass and Bioenergy (38) 68-94, 2012.

[34] Roy, P., Dias, G., "Prospects for pyrolysis technologies in the bioenergy sector: A review", Renewable and Sustainable Energy Reviews 77, 59-69, 2017.

[35] Bilbao, R., Millera, A., Aruzo, J., "Product distribution on the flash pyrolysis of lignocellulosic materials in a fluidized bed" Fuel (67) 1586-1588, November 1988.

[36] Debdoubi, A., El Amarti, A., Colacio, E., Blesa, M.J., Hajjaj, L.H., "*The effect of heating rate on yields and composition of oil products from esparto pyrolysis*", International Journal of Energy Research 30, 1243-1250, 2006.

[37] Blanco Lòpez, M.C., Blanco, C.G., Martìnez-Alonso, A., Tascòn, J.M.D., *"Composition of gases released during olive stones pyrolysis"*, Journal of Analytical and Applied Pyrolysis (65) 313-322, 2002.

[38] Uzun, B.,B., Pütün, A., E., Pütün, E., "Composition of products obtained via fast pyrolysis of olive-oil residue: Effect of pyrolysis temperature", Journal of Analytical and Applied Pyrolysis (79) 147-153, 2007.

[39] Yue, Y., Lin, Q., Irfan, M., Chen, Q., Zhao, X, "Characteristics and potential of bio-oil and biochar derived from Salsola collina Pall. in a fixed bed slow pyrolysis system", Bioresource Technology (220) 378-383, 2016.

[40] Kim, S.,J., Jung, S.,H., Kim, J.,S., "Fast pyrolysis of palm kernel shells: Influence of operation parameter on the bio-oil yield of phenol and phenolic compounds" Bioresource Technology (101) 9294-9300, 2010.

[41] Irfan, M., Chen, Q., Yue, Y., Pang, R., Lin, Q., Zhao, X., Chen, H., "Co-production of biochar, bio-oil and syngas from halophyte grass (Achnatherum splendens L.) under three different pyrolysis temperatures", Bioresource Technology (211) 457-463, 2016.

[42] Sánchez, M.E., Lindao, E., Margaleff, O., Martínez, O., Morán, A., *"Pyrolysis of agricultural residues from rape and sunflowers: Production and characterization of bio-fuels and biochar soil management"*, J. Anal. Appl. Pyrolysis 85, 142-144, November 2008.

[43] Tsai, W.T., Lee, M.K., Chang, Y.M., *"Fast pyrolysis of rise husk: Product yields and composition"*, Bioresource Technology 98, 22-28, January 2006.

[44] Mohammed, I.Y., Abakr, Y.A., Kazi, F.K., Yosuf, S., Alshareef, I., Chin, S.A., *"Pyrolysis of Napier Grass in a Fixed Bed Reactor: Effect of Operating Conditions on Product Yields and Characteristics"*, Peer-Reviewed Article, BioResource 10(4), 6457-6478, 2015.

[45] Duman, G., Okutucu, C., Ucar, S., Stahl, R., Yanik, J., "The slow and fast pyrolysis of cherry seed", Bioresource Technology (102), 1869-1878, 2011.

[46] Atreya, A., Chen, Y., Baum, H.,R., "The effect of size, shape and pyrolysis conditions on the thermal decomposition of wood particles and firebrands" International Journal of Heat and Mass Transfer (107) 319-328, April 2017.

[47] Borwn, R.,C., Wang, K., "Fast Pyrolysis of Biomass – Advances in Science and Technology", Royal Society of Chemistry, Green Chemistry Series No.50, 2017.

[48] Lede, J., Panagopoulos, J., Zhi Li, H., Vollermaux, J., "Fast Pyrolysis of wood: direct measurement and study of ablation rate", Fuel (64) 1514-1520, November 1985.

[49] Diebold, J. P., and Scahill, J., "Ablative Pyrolysis in Biomass in the Entrained Flow Cyclonic Reactor at SERI.", Annual report October 1981–November 1982, SERI/PR-234–1883, UC Category: 61a.

[50] Strezov, V., Evans, T., J., "Biomass Processing Technologies", CRC Press, Teylor &Frances Group, LLC, 2015.

[51] Ringer, M., Putsche, V., Scahill, J., "Large-Scale Pirolysis Oil Production: A Technology Assessment and Economic Analysis", Technocal Report NREL/TP-510-37779, November 2006.

[52] Venderbosh, R.H., Prince, W., “Fast Pyrolysis Technology Development”, Biofuels, Bioproducts and Biorefining (4), March 2010.

[53] Johnson,D.,A., Maclean, D., Feller, J., Diebold, J., Chum, H.,L., “Developments in the scale-up of the vortex-pyrolysis system”, Biomass and Bioenergy (7) 259-266, 1994.

[54] Bridgwater, A., V., Peacocke G., V., C., “Fast Pyrolysys Processes for Biomass” Renewable & Sustainable Energy Review (4) 1-73, 2000.

[55] Peacocke G., V., C., Bridgwater, A., V., “Ablative Pyrolysis of Biomass For Liquids”, Biomass and Bioenergy (7) 147-154, 1994.

[56] Uddin, Md., S., Joardder M., U., H., Islam, M., N., “Design and construction of fixed bed pyrolysis system and plum seed pyrolysis for bio-oil production”, International journal of advanced renewable energy research(1) 405-409, August 2012.

[57] Brech, Y.,L., Jia, L.,Cissé, S., Mauviel, G., Brosse, N., Dufur, A., “Mechanism of biomass pyrolysis studied by combining a fixed bed reactor with advanced gas analysis”, Journal of analytical and applied pyrolysis(117) 334-346, 2016.

[58] Aziz, M., A., Al-Khulaidi, R., A., Rashid, MM., Islam, M.R., Rashid, M., “Design and fabrication of fixed-bed batch type pyrolysis reactor for pilot scale pyrolytic oil production in Bangladesh”, Materials science and Engineering(184), 2017.

[59] Aysu, T., Küçük, M.,M., “Biomass pyrolysis in a fixed-bed reactor: Effects of pyrolysis parameter on product yields and characterization of products”, Energy(64) 1002-1025, 2014.

[60] Dhanavath, K.,N., Shah, K., Bankupalli, S., Bhargava, S.,K., Parthasarathy,R., “Derivation of optimum operating conditions for the slow pyrolysis of Mahua press seed cake in a fixed bed batch reactor for bio-oil production”, Journal of environmental and chemical engineering(5) 4051-4063, 2007.

[61] Ringer, M., Putsche, V., Schahil, J., “Large-scale Pyrolysis oil production: A technology assessment and Economic Analysis”, National Renewable Energy Laboratory, Technical Report NREL/TP-510-37779, November 2006.

[62] Moraes, M.,S.,A., Tomasini, D., da Silva, J.,M., Machado, M.,E., Krause, L.,C., Zini, C.,A.,Jacques, R.,A., Caramão,E.,B., "Chromatographic methods applied to the characterization of bio-oil from pyrolysis of agro-industrial biomasses", INTECH, 2017.

[63] Leonardini, L., "Analisi Sperimentale di un impianto di pirolisi per biomasse agricole e caratterizzazione dei prodotti di conversion (impianto di pirolisi della Italenergie di Sulmona in Abruzzo Italia", Commissione delle Comunità Europee, Rapporto EUR 10386 IT, 1986.

[64] Sadaka, S., Boateng, A.,A., "Pyrolysis and Bio-oil", Agriculture and natural resource FSA1052, 2017.

[65] Garia-Nunez,J.A., Pelaz-Samaniego,M.,R., Garcia-Perez,M.,E., Fonts, I., Abrego, J., Westerhof,R.,J.,M., Garcia-Perez, M., "Historical developments of pyrolysis reactors: a review", Energy & Fuels.

[66] Meier,D., Faix, O., "State of art of applied fast pyrolysis of lignocellulosic materials – a review" Bioresource Technology(68) 71-77, 1999.

[67] Crocker, M., "Thermochemical conversion of biomass to liquid fuels and chemicals", RSC Energy and Environment Series(1), 2010. Treedet, W., Suntivarakorn, R., "Fast Pyrolysis of Sugarcane Bagasse in Circulating Fluidized Bed Reactor - Part A: Effect of Hydrodynamics Performance to Bio-Oil Production", Energy Procedia(138) 801-805, 2017.

[68] Treedet, W., Suntivarakorn, R., "Fast Pyrolysis of Sugarcane Bagasse in Circulating Fluidized Bed Reactor - Part A: Effect of Hydrodynamics Performance to Bio-Oil Production", Energy Procedia(138) 801-805, 2017.

[69] Van de Velden, M., Ingram, a., Fan, X., Baeyens, J., "Fast Pyrolysis of Biomass in a circulating fluidized bed", The 12th International Conference on Fluidization – New Horizons in Fluidization Engineering, Engineering Conferences International, 2017.

[70] Jahirul, M.I., Rasul, M.,G., Chowdhury,A.,A., Ashwath,N., "Biofuel Production through Biomass Pyrolysis – a technological Review" Energies(5)4952-5001, 2012.

[71] Dhyani, V., Bhasker, T., “A cormprehensive review on the pyrolysis of lignocellulosic biomass”, Renewable Energy (xxx) 1-22, 2017.

[72] Guda, V.,K., Steele, P.,H., Penmetsa, V.,K., Li, Q., “Fast pyrolysis of biomass: recent avances in fast pyrolysis technology”, Elsavier, B.V. 177-211, 2015.

[73] Trebbi, G., Rossi, C., Pedrelli, G., “Plans for the production nd Utilization of Bio-Oil biomass fast pysolysis”, 10.1007/978-94-009-1559-6_30, 1997.

[74] Sadhukhan, J., Ng, K.,S., Elias Martinez, H., “Biorefineries and Chemical Processes: Design, Integration and Sustainability Analysis”, John Wiley & Sons, Ltd, 2014.

[75] Pandey, A., Bhaskar, T., Stöcker, M., Sukumaran, R., “Recent Advances in thermochemical conversion of biomass”, Elsavier, 2015.

[76] Kapoor, L., Mekala, A., Bose, D., “Auger Reactor for Biomass Fast Pyrolysis: Design and Operation”, 2016 1st Century Energy Needs – Materials, Systems and Applications (ICTFCEN), Kharagpur, 2016.

[77] Badger, P.,C., Fransham, P., “Use of mobile fast pyrolysis plants to densify biomass and reduce biomass handling costs – A preliminary assessment”, Biomass and Bioenergy (30) 321-325, 2006.

[78] Funke, A., Richter, D., Niebel, A., Dahmen, N., Sauer, J., “Fast pyrolysis of biomass residue in a twin-screw mixing reactor”, Journal of Visualized Experiments (115): 54395, 2016.

[79] Hornung, A., “Transormation of Biomass – Theory to Practice”, John Wiley & Sons, Ltd, 2014.

[80] Westerhout, R.,W., Waanders, J., Kuiper, J.,A.,M., Van Swaaij, W.,P.,M., “Development of Continuous Rotating Cone Reactor Pilot Plant for the Pyrolysis of Polyethene and Polypropene”, Ind Eng. Chem. Res.(37) 2316-2322, 1998.

[81] Bridgwater, A.,V., “Progress in Thermochemical Biomass Conversion”, Blackwell Science Ltd, 2011.

[82] Gupta, V.,K., Tuohy, M.,G., Kubicek, C.,P., Saddler, J., Xu, F., “Bioenergy Research: Advances and Application”, Elsavier, B.V., 2014.

[83] Butler, E., Devlin, G., Meier, D., McDonnell, K., “A review of recent laboratory research and commercial developments in fast pyrolysis and upgrading”, Renewable and Sustainable Energy Reviews(15) 4171-4186, 2011.

[84] https://www.btg-btl.com/en/company/projects/empyro.

[85] Meier, D., Faix, O., “State of art of applied pyrolysis of lignocellulosic materials – a review”, Bioresource Technology (68) 71-77, 1999.

[86] Cao, N., Darmstadt, H., Soutric, F., Roy, C., “Thermogrvimetric study on the steam activation of charcoals obtained by vacuum and atmospheric pyrolysis of softwood bark residues”, Carbon (49) 471-479, 2002.

[87] Final report of Project: "PON02_00667 – PON02_00451_3362376. Valorizzazione Biomolecolare ed Energetica di biomasse residuali del settore Agroindustriale ed Ittico (BIO4BIO)”.

[88] Czernik, S., Bridgwater, A.,V., “Overview of Applications of Biomass Fast Pyrolysis Oil”, Energy & Fuels (18) 590-598, 2004.

[89] Van Paasen, S.,V.,B., Boerrigter, H., Kuipers, J., Stokes, A.,M.,V., Struiijk, F., Scheffer,A., “Tar dewpoin analyser – For application in biomass gasification product gases”, ECN Energy innovation, ECN-C--05-026, May 2005.

[90] Rabou, L.,P.,M., Zwart, R.,W.,R., Vreugdenhil, B.,J., Bos, L., “Tar in Biomass Producer Gas, the Energy research Center of the Netherlands (ECN) Experience: An En Enduring Challenge”, Energy & Fuels (23), 6189-6198, 2009.

[91] Carrier, M., Loppinet-Serani, A., Denux, D., Lasnier, J.-M., Ham-Pichavant, F., Cancell, F., Aymonier, C., “Thermogravimetric analysis as a new method to determine the lignocellulosic composition of biomass”, Biomass and Bioenergy (35) 298-307, 2011.

[92] Ranzi, E., Corbetta, M., Manenti, F., Perucci, S., “Kinetic modelling of the thermal degradation and combustion of biomass”, Chemical Engineering Science (110), 2013.

[93] Chen, T., Wu, J., Zhang, J., Wu, J., Sun, L., “Gasification kinetic analysis of three peseudocomponents of biomass-cellulose, semicellulose and lignin”, Bioresource Technology (153) 223-229, 2014.

[94] Pang, C.,H., Gaddipatti, S., Tucker, G., Lester, E., Wu, T., “Relationship between thermal behaviour of lignocellulosic components and properties of biomass”, Bioresource Technology (172) 312-320, 2014.

[95] Ranzi, E., Cuoci, A., Faravelli, T., Frassoldti, A., Migliavacca, G., Pierucci, S., Sommariva, S., “Chemical Kinetics of Biomass Pyrolysis”, Energy & Fuels (22) 4292-4300, 2008.

[96] Gorensek, M.,B., Shukre, R., Chen,C.-C., “Development of a Thermophysical Properties Model for Flowsheet Simulation of Biomass Pyrolysis Process”, ACS Sustainable Chemistry & Engineerin (7) 9017-9027, 2019.

[97] Hosoya, T., Kawamoto, H., Saka, S., “Cellulose-hemicellulose and cellulose-lignin interactions in wood pyrolysis at gasification temperature”, Journal of Analytical and Applied Pyrolysis (80) 118-125, 2007.

[98] Lee, Yuri, and Hang Seok Choi. "Study on the Process Analysis of Fast Pyrolysis System for Various Waste Biomass." *한국폐기물자원순환학회 3RINCs 초록집* 2015 (2015): 639-642.

[99] Gagliano, A., Nocera, F., Patania, F., Buno, M., Castaldo, D.,G., “A robust numerical model for characterizing the syngas composition in a dowdraft gasification process”, Comptes Rendus Chimie (19) 441-449, April 2016.

[100] Gagliano, A., Nocera, F., Patania, F., Detommaso, M., Buno, M., Aneli, S., Agrifoglio, A., “Small-Scale Biomass Gasification and Micro-CHP Plant for the Agroindustrial Sector”, 9^{o} Congresso Internazionale AIGE – Catania, 17-18 Settembre 2015.

[101] https://phyllis.nl/Browse/Standard/ECN-Phyllis.

[102] Vargas-Moreno, J.,M., Callejón-Ferre, A.,J., Pérez-Alonso, J., Velázquez-Martí, B., “A review of the mathematical model for predicting the heating value of

biomass materials", Renewable and Sustainable Energy Reviews (16) 3065-3083, 2012.

[103] Zaror, C.,A., Pyle, L., "The pyrolysis of biomass: A general review", Proceedings of the Indian Academy of Sciences Section C: Engineering Sciences (5) 269-285, 1982.

[104] Di Blasi, C., "Analysis of Conventional and Secondary Reaction Effects Within Porous Solid Fuels Undergoing Pyrolysis", Combustion Science and Technology (90) 315-340, 1993.

[105] Park, W.,C., Atreya, A., Baum, H.,R., "Experimental and Theoretical Investigation of Heat and Mass Transfer Processes during Wood Pyrolysis", Combuation and Flame (157) 481-494, 2010.

[106] Wang, L., Parnel, C.,B., Shaw, B.,W., Lacey, R.,E., "Analysis of Cyclone Collection Efficiency", The Society for Engineering in agricultural, food and biological systems, 2003 ASAE Annual International Meeting, 27-30 July 2003.

[107] Bashir, K., "Design and fabrication of cyclone separator", PhD Thesis, August 2015.

[108] Schifftner, K.,C., Hesketh, H., E., "Wet Scrubbers – Second Edition", CRC Press, Taylor & Francis Group, 1996.

[109] Spellman, F.,R., Whiting, N.,E., "Handbook of Mathematics and Statistics for the Environment", CRC Press, Taylor & Francis Group, 2014.

[110] "Natural gas – Calculation of calorific values, density, relative density and Wobbe index from composition", SIS – Standardiseringen Sverige Swedish Standards Institution, Allmänna Standardiseringsgruppen, STG, 1996.

[111] McBride, B.,J., Gordon, S., Reno, M.,A., "Coefficients for Calculating Thermodynamic and Transport Properties of Individual Species", NASA Technical Memorandum 4513, 1993.

[112] Marzouk O,.A,. "Assessment of Three Databases for NASA Seven-Coefficient Polynomial Fits for Calculating Thermodynamic Properties of Individual Species",

International Journal of Aeronautical Science & Aerospace Research (IJASAR) (1) 150-163, 2018.

[113] Demibras, A., Ak, N., Aslan, A., Sen, N., "Calculation of higher heating values of hydrocarbon compounds and fatty acids", Petroleum Science and Technology (0) 1-6, 2018.

[114] Beckman,D., Elliot, D.,C., Gervert, B., Hoernell, C., Kjellstoem, B., Oestman, A., Solantausta, Y. and Tulenheimo, V., "Techno-economic assessment of selected biomass liquefaction process", VTT research report 697, Espoo: VTT Technical Research Center of Finland, 1990.

[115] Dion, L.,M., Lefsrud, M., Orsat, V., Cimon, C., "Biomass Gasification and Syngas Combustion for Greenhouse CO_2 Enrichment", Bioresource (8) 1520-1538, 2013.

[116] Heywood, J.,B., "Internal Combustion Engine Fundamentals", McGraw-Hill, 1988.

[117] Balli, O., & Aras, H. (2007). Energetic Analyses of the Combined Heat and Power (CHP) System. Energy Exploration & Exploitation, 25(1), 39–62. https://doi.org/10.1260/014459807781036412.

[118] Gagliano, A., Nocera, F., Patania, F., Detommaso, M., Buno, M., "Evaluation of Performance of a Small Biomass Gasifier and Micro-CHP Plant for Agro-Industrial Firms", International Journal of Heat and Technology (33) 145-154, 2015.

[119] "Chemcad Verion 6 – User Guide", Chemstations Inc., 2010.

[120] "Aspen Plus – Getting Started Building and Running a Process Model", Aspentech., Aspen Technology, Inc., Version Number: V8.4, November 2013.

[121] "Aspen Plus – Aspen Plus User Guide", Aspen Technology, Inc., Version 10.2, February 2000.

[122] "Aspen Physical Property System – Physical Property Methods and Models 11.1", Aspentech process, to the power of e., Aspen Technology. Inc., September 2001.

[123] “Aspen Plus – Getting Started Customizing Unit Operation Model”, Aspentech., Aspen Technology, Inc., Version Number: V8.0, December 2012.

[124] “Chemcad Physical Properties – Version 5.6 User’s Guide and Tutorial”, Chemstations, Inc.

[125] “Aspen Physical Property System – Physical Property Data 11.1”, Aspentech process, to the power of e., Aspen Technology. Inc., September 2001.

[126] “Aspen Plus – User Models”, Aspentech, Aspen Technology, Inc., Version Number: V7.0, 2008

[127] Benanti, E., Freda, C., Lorefice, V., Braccio, G., Sharma, V.K., “Simulation of Olive Pits Pyrolysis in a Rotary Kiln Plant”, Thermal Science 45, 145-158, 2011.

[128] Fonseca, F.,G., Funke, A., Niebel, A., Dias, A.,P.,S., “Moisture content as a design and operational parameter for fast pyrolysis”, Journal of Analytical and Applied Pyrolysis 139, 73-86, 2019.

[129] Ward, J., Rasul, M.,G., Bhuiya, M.,M.,K., “Energy recovery from biomass fast pyrolysis”, 10th International Conference on Mechanical Engineering, ICME 2013, Procedia Engineering (90) 669-674, 2014.

[130] Adeniyi, A.,G., Ighalo, J.,O., Amosa, M.,K., “Modelling and Simulation of Banana (Musa spp.) Waste Pyrolysis for Bio-oil Production”, Biofuels, 2019.

[131] Kerezsi, J.,T., “Computer simulation of an industrial Ethane-Cracking Furnace Operation”, 2013 4th International Youth Conference on Energy (IYCE), June 2013.

[132] Villarini, M., Bocci, E., Di Carlo, A., Savuto, E., Pallozzi, V., “The case study o fan innovative small scale biomass waste gasification heat and power plant contextualized in a farm”, ATI 2015 – 70th Conference of the ATI Engineering Associeation, Energy Procedia (82) 335-342, 2015.

[133] Cohce, M.,K., Dincer, I., Rosen, M.,A., “Energy and Exergy analyses of a biomass-based hydrogen production system”, Bioresource Technology (102) 4866-4874, 2011.

[134] Borello, D., Pantaleo, A.,M., Caucci, M., De Caprariis, B., De Filippis, P., Shah, N., "Modeling and Experimental Study of Small Scale Olive Pomace Gasifier for Cogeneration: Energy and Profitability Analysis", Energies (10) 1930-1946, 2017.

[135] "Chemcad Suite CC-Dynamics (CC-DCOLUMN & CC-ReAcs) – User's Guide Dynamic Process Simulation – Including Continuous and Batch Distillation and Reaction", Chemstation Inc.

[136] Aspen-Plus V8.8 Help – Software Supporting Material.

[137] Abdelhady, S., Borello, D., Shaban, A., "Techno-economic assessment of biomass power plant fed with rice straw: Sensitivity and parametric analysis of the performance and the LCOE", Renewable Energy (115), 1026-1034, 2018.

[138] Wooley, R.,J., Putsche, V., "Development of an ASPEN PLUS Physical property Database for Biofuels Components", National Renewable Energy Laboratory (NREL), April 1996.

[139] Frassoldatim A., Miglivaccam G., Crippa, T., Velata, F., Faravelli, T., Ranzi, E., "Detailed Kinetic Modeling of Thermal Degradation of Biomass", 29th Meeting on Combustion, Biomass and Bioenergy (34) 290-301, March 2010.

[140] Gauthier, G., Melkior, T., Salvador, S., Corbetta, M., Frassoldati, A., Pierucci, S., Ranzi, E., Bennadji, H., Fisher, M.,E., "Pyrolysis of Thick Biomass Particles: Experimental Kinetic Modelling", Chemical Engineering Transactions (32), 2013.

[141] Bloneau, J., Jeanmart, H., "Biomass pyrolysis at high temperatures: Prediction of gaseous species yields from an anisotropic particle", Biomass and Bioenergy (41) 107-121, 2012.

[142] Wakelyn, N.,T., McLain, A.,G., "Polynomial Coefficients of Thermochemical Data for the C-H-O-N Sytem", NASA Technical Memorandum X-72657, January 1975.

[143] Gagliano, A., Nocera, F., Bruno, M., Cardillo, G., "Development of an equilibrium-based model of gasification of biomass by Aspen Plus", 8th International Conference on Suitability in Energy and Buildings, Energy Procedia (111) 1010-1019, 2017.

[144] Gagliano, A., Nocera, F., Patania, F., Bruno, M., "A numerical model to characterize the producer gas composition by the pyrolysis process", 2016 7th International Renewable Congress (IREC), Hammamet, March 2016.

[145] Figueroa, J.,E.,J., Ardila, Y.,C., Lunelli, B.,H., Filho, R.,M., Maicel, M.,R.,W., "Evaluation of Pyrolysis and Steam Gasification Processes of Sugarcane Bagasse in a Fixed Bed Reactor", Chemical Engineering Transaction (32), 2013.

[146] Brownsort, P.,A., "Biomass Pyrolysis Process: Review of Scope, Control and Variability", UKBCR Working Paper 5, December 2009.

[147] Tihay, V., Gillard, P., "Pyrolysis gases relased during the thermal decomposition of three Mediterranean Species", Journal of Analytical and Applied Pyrolysis (88) 168-174, 2010.

[148] Commandre, J.M., Lahmidi, H., Salvador, S., Dupassieux, N., "Pyrolysis of wood at high temperature: The influence of experimental parameters on gaseous products", Elsevier, Fuel Processing Technology (92) 837-844, 2011.

[149] Enerblu Cogeneration, Micro-CHP REC2 40 G Spec. Datasheet (see appendix C).

[150] Hagos, F.,Y., Rashid, A., Aziz, A., Sulaiman, S.,A., "Study of Syngas Combustion Parameters Effect on Internal Combustion Engine", Asian Journal of Scientific Research, 2013.

[151] Enerblu Cogeneration, Product Catalogue.

[152] Hagos, F.,Y., Rashid, A., Aziz, A., Sulaiman, S.,A., "Effect of Air-Fuel Ratio on the Combustion Characteristics of Syngas (H_2:CO) in Direct-Injection Spark-Ignition Engine", The 6th International Conference on Applied Energy – ICAE2014, Energy Procedia (61) 2567-2571, 2014.

[153] Tidbal, R., Bluestein, J., Rodriguez, N., Knoke, S., "Cost and Performance Assumptions for Modeling Electricity Generation Technologies", NREL – National Renewable Energy Laboratory, November 2010.

[154] IRENA – International Renewable Energy Agency, "Renewable Energy Technologies: Cost Analysis Series – Biomass for Power Generation", Volume 1: Power Sector, Issue 1/5, IRENA Working Paper, June 2012.

[155] Porcu, A., Sollai, S., Marotto, D., Mureddu, M., Ferrara, F., Pettinau, A., "Techno-Economic Analysis of a Small-Scale Biomass-to-Energy BFB Gasification-Based System", Energies (12), 2019.

[156] U.S. Department of Energy, Energy Efficiency & Renewable Energy – https://www.energy.gov/eere/office-energy-efficiency-renewable-energy.

[157] Enerblu Cogeneration, Micro-CHP REC2 2000 G Spec. Datasheet (see appendix D).

[158] Gestore Mercati Energetici – https://www.mercatoelettrico.org .

[159] Ministero dello Sviluppo Economico (Italian Ministry of Economic Development). Definizione del Nuovo Regime di Sostegno per la Cogenerazione ad Alto Rendimento (Decree 5 September 2011); Gazzetta Ufficiale della Repubblica Italiana 2011. (In Italian). Available online: http://www.gazzettaufficiale.it/eli/id/2011/09/19/11A12047/sg (accessed on 4 January 2019).

[160] Independent Statistics & Analysis, "Levelized Cost and Levelized Avoided Cost of New Generation Resources in the *Annual Energy Outlook 2019*", U.S. Energy Information Administration (EIA), February 2019.

Appendix-A – Characteristics of Literature Investigation Plants

HHV= High Heating Value; M= moisture (umidità); Cell=Cellulose; HC=Hemicellulose; Lign= Lignin; Ash= ceneri (material inerte); VM= volatile matter (materiale volatile); FC=fixed carbon (Carbonio fisso); Φ=particle size; HR= Heating Rate; rt= residence time

Ultimate Analsys						
Feedstock	**C**	**H**	**N**	**S**	**O**	**HHV**
Esparto [36]	46.94	6.44	0.86	0.0	43.56	19.1
Olive Stones [37]	51.80	6.11	0.11	0.08	43.40	–
Olive Oil [38]	49.08	5.59	1.14	0.0	44.19	16.40
Salsola-Collina [39]	42.41	5.67	2.76	0.0	33.58	17.01
Palm Kernel Shell [40]	44.56	5.22	0.4	0.05	49.77	15.6
Halophyte Grass [41]	–	–	–	–	–	–
Rape [42]	44.7	5.8	0.8	0.6	48.1	15.3
Sunflowers [42]	43.6	5.8	1.0	0.3	49.3	15.7
Rise Husk [43]	45.28	5.51	0.67	0.29	48.35	–
Napier Grass [44]	48.6	6.01	0.99	0.32	44.10	18.10
Cherry Seed [45]	52.48	7.58	4.54	0.10	35.30	20.69
Cherry Seed Shell [45]	48.86	6.32	3.09	0.11	41.62	20.40

Structural Composition and Proximate Analysis							
Feedstock	**Cell**	**HC**	**Lign**	**M**	**Ash**	**VM**	**FC**
Esparto [36]	–	–	–	5.20	2.2	80.5	16.8
Olive Stones [37]	11.82	24.16	50.45	4.3	0.6	82.9	0.9
Olive Oil [38]	23.21	35.62	34.98	8.83	5.12	68.72	17.30

Salsola-Collina [39]	–	–	–	–	15.58	–	–
Palm Kernel Shell [40]	33.04	23.82	45.59	9.4	6.7	82.5	1.4
Halophyte Grass [41]	35.04	28.73	8.10	–	–	–	–
Rape [42]	–	–	–	8.8	7.3	78.7	14
Sunflowers [42]	–	–	–	8.1	8.3	74.5	17.2
Rise Husk [43]	–	–	–	6.37	11.70	81.93	
Napier Grass [44]	38.8	19.8	27	75.3	1.75	81.5	16.7
Cherry Seed [45]	32.06	28.59	29.08	5.53	1.16	77.62	15.69
Cherry Seed Shell [45]	27.19	31.93	36.9	6.08	0.78	76.12	17.02

Process Parameter				
Feedstock	**Φ [mm]**	**T [°C]**	**HR [°C/min]**	**rt [min]**
Esparto [36]	<1	400 - 700	50-150-250	–
Olive Stones [37]	2-4	600	5	15
Olive Oil [38]	–	400 - 700	300	5
Salsola-Collina [39]	–	300 - 700	10	120
Palm Kernel Shell [40]	–	435 - 530	10-15-20	–
Halophyte Grass [41]	<20	300 - 700	10	120
Rape [42]	2-3	550	30	1
Sunflowers [42]	1-3	550	30	1
Rise Husk [43]	<50	400-800	100	1-8
Napier Grass [44]	0.2-2	450-650	30	15(±2)
Cherry Seed [45]	<2	400 - 600	5	60
Cherry Seed Shell [45]	<2	400 - 600	5	60

Appendix-B –Nasa Coefficients of Compounds[111-142]

NASA COEFFICIENTS					
Compound	**a_1**	**a_2**	**a_3**	**a_4**	**a_5**
CO2	2,356774	0,008985	-7,1E-06	2,46E-09	-1,4E-13
H2O	4,198641	-0,00204	6,52E-06	-5,5E-09	1,77E-12
HCOOH	3,232625	0,002811	2,44E-05	-3,2E-08	1,21E-11
Char	2,55424	-0,00032	7,34E-07	-7,3E-10	2,67E-13
HAA	2,789368	0,01	3,43E-05	-5,1E-08	2,06E-11
CO	3,579533	-0,00061	1,02E-06	9,07E-10	-9E-13
H2	2,344331	0,007981	-1,9E-05	2,02E-08	-7,4E-12
Glyoxal	4,728073	0,019672	-2,9E-05	3,05E-08	-1,3E-11
CH4	5	0	4,92E-05	-4,8E-08	1,67E-11
C2H4O	3,759049	-0,00944	8,03E-05	-1E-07	4E-11
HMFU	9,11271	0,013497	3,32E-05	-4,2E-08	1,51E-11
C3H6O	3,568511	0,005027	6,42E-05	-8,9E-08	3,62E-11
LVG	7,867179	0,02837	8,64E-06	-2E-08	4,99E-12
CH2O	4,793723	-0,00991	3,73E-05	-3,8E-08	1,32E-11
C2H5OH	4,858682	-0,00374	6,96E-05	-8,9E-08	3,52E-11
CH3OH	5,7154	-0,01523	6,52E-05	-7,1E-08	2,61E-11
C2H4	3,959201	-0,00757	5,71E-05	-6,9E-08	2,7E-11
Xylosan	2,896873	0,002198	1,64E-04	-1,9E-07	6,87E-11
Coumaryl	5,843177	0,017489	0,000121	-1,8E-07	7,54E-11
Phenol	-0,29105	0,040857	2,43E-05	-7,1E-08	3,46E-11
FE2MACR	1,99E-01	0,055779	8,87E-05	-2E-07	7,6E-11

Appendix-C – Micro-CHP Specifications[149]

Micro CHP

REC2 40 G

Features 100% load	
Net electrical base load power	43 kW
Total Heating capacity (water 70-80 °C in / 80-90 °C out)	90 kW
Fuel power	142 kw
Gas consumption	14,8 Sm3/h
Electrical efficiency	30 %
Thermal efficiency	63 %
Global efficiency	93,7 %
Features 75% load	
Total Heating capacity (water 70-80 °C in / 80-90 °C out)	71 kw
Fuel power	117 kw
Gas consumption	12,2 Sm3/h
Electrical efficiency	28 %
Thermal efficiency	61 %
Global efficiency	88,1 %
Features 50% load	
Net electrical base load power	22 kw
Total Heating capacity (water 70-80 °C in / 80-90 °C out)	47 kw
Fuel power	82 kw
Gas consumption	8,5 Sm3/h
Electrical efficiency	26 %
Thermal efficiency	58 %
Global efficiency	84,2 %
Engine Specs	
Cycle	Otto 4 tempi tipo
Running speed	1500 rpm
Number of cylinders and total displacement	8V / 5,7 n° / dm3
Bore and stroke	101,6 / 91,4 mm
Ignition	elettronica tipo
Air intake system	naturale tipo
Mechanical power at the flyweel	45 kw
Speed stability at constant load	0,25 %
Luboil consumption	0,03 Kg/h
Combustion air flow	142 mc/h
PPM emissions	< 20 ppm/Nmc
NOx emissions at 5% O2 without catalizer (*)	< 500 mg/Nmc
CO emissions at 5% O2 senza catalizzatore (*)	< 650 mg/Nmc
Alternator Specs	
Generator rated power in continous duty	45 kw
Rated voltage	400 tipo
Pole number	4 p

Frequency	50 Hz
Full load generator efficiency	91,2 %
Isolation class	H cl.
Isp	7
Heat recovery Specs	
Thermal power recovery from water and lub oil	63 kw
Thermal power recovery from exhaust	27 kw
Exhaust gas flow	188 kg/h
Maximum Exhaust gas temperature	1200 °C
Water pressure drop (70°/80°)	< 60 mmca
Minimum flow of water users	5.160 l/h
Max water flow user	15.480 l/h
Dimensions, Weights, Connections, Noise	
Width	1200 mm
Depth	2850 mm
Height	2330 mm
Operation weight	2140 Kg
Shipping weight	2000 Kg
Degree of machine protection	44 IP
Exhaust connection	G 3 DN
External water circuit connection	G 2 DN
External connection condensation drain	G 1/2 POLLICI
Gas pipeline connection	G 1 1/4 POLLICI/DN
Noise level at 1 m Engine with canopy and silencer	< 58 dB(A)
Noise level at 7 m Engine with canopy and silencer	< 53 dB(A)
Maintenance's Space	
Width right and left side	800 mm
Depth right and left side	1000 mm
Height	800 mm
Natural gas	
Minimum flow pressure of gas supply to the machine	0,028 mbar
Minimum temperature gas supply	15 °C
Terms and tolerances	
Maximum outdoor temperature without derating	25 °C
Maximum altitude work without derating	100 m.s.l.m.
Maximum water outlet temperature	92 °C
Minimum water outlet temperature	92 °C
Thermal power tolerance	10 % ±
Sound Pressure Level tolerance [dB(A)]	3 ±

Appendix-D – Commercial-CHP Specifications[157]

Big CHP

REC2 2000 G

Features 100% load	
Net electrical base load power	2000 kW
Total Heating capacity (water 70-80 °C in / 80-90 °C out)	2102 kW
Fuel power	4721 kw
Gas consumption	492,6 Sm3/h
Electrical efficiency	42,4 %
Thermal efficiency	44,5 %
Global efficiency	86,9 %
Total Heating capacity	2102 kw
Features 75% load	
Net electrical base load power	1500 kw
Total Heating capacity (water 70-80 °C in / 80-90 °C out)	1670 kw
Fuel power	3647 kw
Gas consumption	388,9 Sm3/h
Electrical efficiency	41,1 %
Thermal efficiency	45,8 %
Global efficiency	86,9 %
Features 50% load	
Net electrical base load power	1000 kw
Total Heating capacity (water 70-80 °C in / 80-90 °C out)	1226 kw
Fuel power	2563 kw
Gas consumption	259,3 Sm3/h
Electrical efficiency	39,0 %
Thermal efficiency	47,8 %
Global efficiency	86,9 %
Engine Specs	
Cycle	otto 4 tempi tipo
Running speed	1500 rpm
Number of cylinders and total displacement	20V / 53,1 n° / dm3
Bore and stroke	171 / 195 mm
Ignition	elettronica tipo
Air intake system	forzata con intercooler tipo
Engine jacket water flow (min / max)	60 / 85 m3/h
Mechanical power at the flyweel	2055 kw
Speed stability at constant load	0,25 %
Average lub oil consumption	0,240 Kg/h
Oil filling system and tank capacity	AUTO 600 tipe/l
Combustion air flow	10485 kg/h
Exhaust mass flow	10741 kg/h
NOx emissions at 5% O2 wit catalizer	500 mg/Nmc

CO emissions at 5% O2	650 mg/Nmc
Alternator Specs	
Generator rated power in continous duty	2300 kw
Rated voltage	400 tipo
Pole number	4 p
Frequency	50 Hz
Power factor	1 PF
Full load generator efficiency	97,3 %
Voltage precision	+/- 5% %
Isolation class	H cl.
Heat recovery Specs	
Thermal power recovery from water and lub oil	1055 kw
Thermal power recovery from intercooler	178 kw
Thermal power recovery from exhaust	1047 kw
Exhaust gas flow	11104 kg/h
Maximum Exhaust gas temperature	420 °C
Max exhaust back pressure after silencer	5000 Pa
Water flow (70°/80°)	181,03 mc/h
Water pressure drop (70°/80°)	< 70 mmca
Water pressure drop	< 50 mmca
Dimensions, Weights, Connections, Noise	
Width	3000 mm
Depth	13500 mm
Height	3000 mm
Operation weight	nd Kg
Shipping weight	27000 Kg
Degree of machine protection	44 IP
Exhaust connection	450 DN
External water circuit connection	125 DN
External connection condensation drain	1 POLLICI
Gas pipeline connection	65 POLLICI/DN
Noise level at 7 m Engine with canopy and silencer	< 65 dB(A)
Maintenance's Space	
Width right and left side	1000 mm
Depth right and left side	1000 mm
Height	1000 mm
Natural gas	
Minimum flow pressure of gas supply to the machine	100 mbar
Minimum temperature gas supply	15 °C
Terms and tolerances	
Maximum outdoor temperature without derating	20 / 25 °C
Maximum altitude work without derating	100 m.s.l.m.
Maximum relative humidity	30 %
Maximum water inlet temperature	70 °C
Maximum water outlet temperature	90 °C
Maximum Delta T ° water users	13 °C
Minimum Delta T ° water users	6 °C
Lower calorific value of supply gas	34500 kJ/Sm3
Electrical power and consumption tolerance	5 % ±
Thermal power tolerance	10 % ±
Sound Pressure Level tolerance [dB(A)]	3 ±